UNIVERSIDADE FEDERAL DE MINAS GERAIS
Escola de Engenharia
Programa de Pós-Graduação em Engenharia de Estruturas

Túlio Antunes Pinto Coelho

RELIABILITY AND LIFE-CYCLE COSTS OF REINFORCED CONCRETE BEAMS UNDER FIRE

Belo Horizonte
2025

Túlio Antunes Pinto Coelho

RELIABILITY AND LIFE-CYCLE COSTS OF REINFORCED CONCRETE BEAMS UNDER FIRE

Tese apresentada ao Programa de Pós-Graduação em Engenharia de Estruturas da Universidade Federal de Minas Gerais, como requisito parcial para a obtenção do título de Doutor em Engenharia de Estruturas.

Orientadora: Profª Sofia Maria Carrato Diniz

Coorientador: Prof. Francisco Carlos Rodrigues

Belo Horizonte

2025

Coelho, Túlio Antunes Pinto.
C672r Reliability and life-cycle costs of reinforced concrete beams under fire [recurso eletrônico] / Túlio Antunes Pinto Coelho. – 2025.
1 recurso online (208 f. : il., color.) : pdf.

Orientadora: Sofia Maria Carrato Diniz.
Coorientador: Francisco Carlos Rodrigues.

Tese (doutorado) – Universidade Federal de Minas Gerais, Escola de Engenharia.

Anexos: f. 196-208.

Bibliografia: f. 188-195.

1. Engenharia de estruturas – Teses. 2. Resistência de materiais – Normas – Teses. 3. Incêndios – Medidas de segurança – Normas – Teses. 4. Concreto armado – Resistência – Teses. I. Diniz, Sofia Maria Carrato. II. Rodrigues, Francisco Carlos. III. Universidade Federal de Minas Gerais. Escola de Engenharia. IV. Título.

CDU: 624(043)

Ficha catalográfica elaborada pelo bibliotecário Marcio A. A. Gomes CRB/6 2812
Biblioteca Prof. Mário Werneck, Escola de Engenharia da UFMG

UNIVERSIDADE FEDERAL DE MINAS GERAIS

PROPEEs PROGRAMA DE PÓS-GRADUAÇÃO EM ENGENHARIA DE ESTRUTURAS UFMG

ATA DA DEFESA DE TESE DE DOUTORADO EM ENGENHARIA DE ESTRUTURAS Nº 108 DO ALUNO TÚLIO ANTUNES PINTO COELHO

Às **14:00** horas do dia **23** de **janeiro** de 2025, reuniu-se em ambiente virtual, na Escola de Engenharia da Universidade Federal de Minas Gerais - UFMG, a Comissão Examinadora indicada pelo Colegiado do Programa em 08 de novembro de 2024 para julgar a defesa da Tese de Doutorado intitulada: **"Reliability and Life-Cycle Costs of Reinforced Concrete Beams under Fire"**, cuja aprovação é um dos requisitos para a obtenção do Grau de DOUTOR EM ENGENHARIA DE ESTRUTURAS na área de ESTRUTURAS.

Abrindo a Sessão, a Presidente da Comissão, Profa. Dra. Sofia Maria Carrato Diniz, após dar conhecimento aos presentes do teor das Normas Regulamentares, passou a palavra ao aluno para apresentação de seu trabalho. Finalizada a apresentação, seguiu-se para a fase de arguição pelos examinadores, com as respectivas respostas do aluno. Logo após a fase de arguição, a Comissão se reuniu, sem a presença do aluno e do público, para julgamento e expedição do resultado final, a saber:

(**X**) Aprovado

(   ) Reprovado

O resultado final foi comunicado publicamente ao aluno pela Presidente da Comissão.

Nada mais havendo a tratar, a Presidente encerrou a reunião e lavrou a presente ata, que será assinada por todos os membros participantes da Comissão Examinadora e pelo aluno.

Comissão Examinadora:

Profa. Dra. Sofia Maria Carrato Diniz - DEES - UFMG (Orientadora)

Prof. Dr. Marcilio Sousa da Rocha Freitas - UFOP

Prof. Dr. José Márcio Fonseca Calixto - DEES - UFMG

Prof. Dr. Mauro de Vasconcellos Real - FURG

Prof. Dr. Christopher Eamon - Wayne State University - EUA

A aprovação do aluno na Defesa de Tese de Doutorado não significa que o mesmo tenha cumprido todos os requisitos necessários para obtenção do DIPLOMA de Doutor em Engenharia de Estruturas.

Para ciência do aluno:

1. Atesto que as alterações solicitadas pela Comissão Examinadora serão cumpridas no prazo de ATÉ 60 dias corridos.

2. Atesto estar ciente que a versão corrigida da dissertação deverá ser entregue ao Repositório Institucional da UFMG, conforme orientações disponíveis em: https://repositorio.ufmg.br/custom/instructions.jsp

Ciente:	**Túlio Antunes Pinto Coelho**
	Aluno

Belo Horizonte, 23 de janeiro de 2025.

Este documento não terá validade sem a assinatura do Coordenador do Programa de Pós-Graduação.

Após a Homologação da Defesa pelo Colegiado do Programa, este documento será assinado pela Coordenação e disponibilizado ao aluno.

Documento assinado eletronicamente por **Sofia Maria Carrato Diniz**, **Membro de comissão**, em 23/01/2025, às 17:58, conforme horário oficial de Brasília, com fundamento no art. 5º do Decreto nº 10.543, de 13 de novembro de 2020.

Documento assinado eletronicamente por **Túlio Antunes Pinto Coelho**, **Usuário Externo**, em 24/01/2025, às 10:29, conforme horário oficial de Brasília, com fundamento no art. 5º do Decreto nº 10.543, de 13 de novembro de 2020.

Documento assinado eletronicamente por **José Marcio Fonseca Calixto**, **Usuário Externo**, em 27/01/2025, às 09:50, conforme horário oficial de Brasília, com fundamento no art. 5º do Decreto nº 10.543, de 13 de novembro de 2020.

Documento assinado eletronicamente por **Mauro de Vasconcellos Real**, **Usuário Externo**, em 27/01/2025, às 10:40, conforme horário oficial de Brasília, com fundamento no art. 5º do Decreto nº 10.543, de 13 de novembro de 2020.

Documento assinado eletronicamente por **Marcilio Sousa da Rocha Freitas**, **Usuário Externo**, em 27/01/2025, às 13:40, conforme horário oficial de Brasília, com fundamento no art. 5º do Decreto nº 10.543, de 13 de novembro de 2020.

Documento assinado eletronicamente por **Chris Eamon**, **Usuário Externo**, em 04/02/2025, às 09:33, conforme horário oficial de Brasília, com fundamento no art. 5º do Decreto nº 10.543, de 13 de novembro de 2020.

Documento assinado eletronicamente por **Leandro Lopes da Silva**, **Coordenador(a)**, em 13/02/2025, às 13:27, conforme horário oficial de Brasília, com fundamento no art. 5º do Decreto nº 10.543, de 13 de novembro de 2020.

A autenticidade deste documento pode ser conferida no site https://sei.ufmg.br/sei/controlador_externo.php?acao=documento_conferir&id_orgao_acesso_externo=0, informando o código verificador **3889713** e o código CRC **51F0B243**.

Referência: Processo nº 23072.203327/2025-50 SEI nº 3889713

RESUMO

As normas e especificações atuais para o projeto de estruturas de concreto armado (CA) baseiam-se predominantemente nos Métodos de Estado Limite, que são semi-probabilísticos por natureza. Nas últimas décadas, avanços significativos foram feitos na avaliação da confiabilidade de componentes estruturais de CA, como lajes, vigas e colunas, com ênfase na calibração de fatores parciais. A avaliação de confiabilidade é crucial para o "projeto baseado em desempenho" (PBD), pois leva em conta as incertezas relacionadas às variáveis de projeto. No entanto, os estudos sobre a confiabilidade de componentes de CA expostos ao fogo ainda são limitados. Dada a natureza imprevisível dos incêndios e as incertezas associadas (como as propriedades mecânicas dos materiais a altas temperaturas, as dimensões das estruturas e os modelos matemáticos utilizados), entender o desempenho dos elementos estruturais de CA sob condições de incêndio, assim como a caracterização probabilística desse desempenho, é de extrema importância. Esta pesquisa aborda a avaliação de confiabilidade de estruturas de CA expostas ao fogo, enfocando os conceitos-chave, métodos e descrições probabilísticas das variáveis subjacentes, juntamente com a definição e quantificação do desempenho estrutural. Especificamente, o estudo analisa vigas de CA projetadas de acordo com a ABNT NBR 15200. Identificam-se lacunas tanto no estado da prática quanto no estado da arte quanto ao comportamento das vigas de CA sob condições de incêndio, destacando as limitações das normas atuais e a escassez de pesquisas na área. A pesquisa investiga três aspectos principais do desempenho de segurança e econômico das vigas de CA em situação de incêndio: (i) avaliação probabilística da resistência à flexão para incêndios padrão e paramétricos, (ii) avaliação das probabilidades de falha de vigas projetadas conforme a ABNT NBR 15200, e (iii) avaliação dos níveis de segurança alvo, incorporando os custos ao longo do ciclo de vida. Os resultados obtidos destacam a importância de equilibrar segurança e economia, especialmente quando se consideram sistemas ativos de supressão de incêndio, que podem reduzir as probabilidades de falha e permitir escolhas de projeto mais econômicas. Além disso, a pesquisa enfatiza a necessidade de um referencial probabilístico na evolução futura da ABNT NBR 15200, integrando custos do ciclo de vida e princípios de gerenciamento de risco. Esta abordagem oferece uma metodologia mais abrangente, baseada no desempenho, para o projeto de estruturas de CA resistentes ao fogo, garantindo tanto a segurança quanto a viabilidade econômica diante de riscos de incêndio.

Palavras-chave: concreto armado; confiabilidade; fogo; incertezas; vigas; níveis de segurança alvo; custos ao longo do ciclo de vida; projeto contra incêndio.

ABSTRACT

Current standards and specifications for the design of reinforced concrete (RC) structures predominantly rely on Limit State Methods, which are semi-probabilistic in nature. Over the last few decades, significant advancements have been made in the reliability assessment of RC structural components, including slabs, beams, and columns, with an emphasis on calibrating partial factors in these semi-probabilistic methods. Reliability assessment is crucial for performance-based design (PBD), as it accounts for uncertainties related to design variables. However, studies on the reliability of RC components under fire exposure remain limited. Given the unpredictable nature of fires and the associated uncertainties (e.g., mechanical properties of materials at high temperatures, structural dimensions, and the mathematical models used), understanding the performance of RC structural elements under fire, as well as the probabilistic characterization of this performance, is paramount. This research addresses the reliability assessment of RC structures exposed to fire, focusing on the key concepts, methods, and probabilistic descriptions of the underlying variables, alongside the definition and quantification of structural performance. Specifically, the study examines RC beams designed in accordance with ABNT NBR 15200. It identifies gaps in both the state-of-the-practice and the state-of-the-art regarding RC beam behavior under fire conditions, highlighting the limitations of current standards and the scarcity of research in this area. The research investigates three primary aspects of the safety and economic performance of RC beams under fire: (i) probabilistic evaluation of bending capacity for both standard and parametric fires, (ii) assessment of failure probabilities for beams designed according to ABNT NBR 15200, and (iii) evaluation of target safety levels, incorporating life-cycle costs. Insights gained from the study underscore the importance of balancing safety and costs, particularly when considering active fire suppression systems, which can reduce failure probabilities and allow for more cost-effective design choices. Additionally, the research emphasizes the need for a probabilistic framework in the future evolution of ABNT NBR 15200, integrating life-cycle costs and risk management principles. This approach offers a more comprehensive, performance-based methodology for designing fire-resistant RC structures, ensuring both safety and economic feasibility in the face of fire hazards.

Keywords: reinforced concrete; reliability; fire; uncertainties; beams; target safety levels; life-cycle costs; fire design.

LIST OF FIGURES

LIST OF TABLES

LIST OF SYMBOLS

A - Obsolescence cost

$A_{S,req}(X)$ – Minimum area of compression reinforcement in section x

$A_{S,req}(0)$ – Compression reinforcement section area required for support

A_s – Total cross-sectional area of steel bars

a – Concrete cover according to Eurocode

a_{eff}– Effective concrete cover according to Eurocode

$a(T_c)$ - Depth of the compressive stress block

b – Beam width

b_{min} – Minimum beam width

B – Random variable that represents the width of the beam

C - Total building construction and maintenance cost

c_1 – Distance from the axis of the bar to the concrete surface of the tension reinforcements

c_p - Specific heat capacity

d_{ef} – Effective beam height

d' – Distance between the concrete fibers in tension and the axis of the steel rebar (tensile reinforcement)

D' - Random variable that represents the distance between the concrete fibers in tension and the axis of the steel rebar (tensile reinforcement)

D_L - Fire-induced loss to human life and limb

D_M - Fire-induced material damage

D_R - Reconstruction cost after fire-induced failure

d – Distance between the axis of the tensile steel rebar to the most compressed fiber

e - Life expectancy

E – Young's modulus

$E_{c,\theta}$ – Young's modulus of concrete at temperature θ

E_{ck} – Young's modulus of concrete at room temperature

E_S – Young's modulus of steel under normal conditions

$E_{S,\theta}$ – Young's modulus of steel at temperature θ

F_{gk} – Characteristic value of the permanent action

$F_X(x)$ - Cumulative distribution function (CDF)

f – Limit state function

$f_{y,k}$ – Characteristic yield strength of steel in normal situation

$f_{y,\theta}$ – Characteristic yield strength of steel as a function of temperature θ

$f_{c,\theta}$ – Compressive strength of concrete at temperature θ

f_{ck} – Characteristic compressive strength of concrete in normal situation

F_y – Random variable that represents the yield strength of steel

F_c – Random variable that represents the compressive strength of concrete

g - Annual GDP per capita

h – Beam height

H - Random variable that represents the beam height

$k_{c,\theta}$ – Strength reduction factor of concrete at temperature θ

$k_{cE,\theta}$ – Strength reduction factor of the Young's modulus of concrete at temperature θ

$k_{S,\theta}$ – Strength reduction factor of steel resistance at temperature θ

$k_{SE,\theta}$ – Reduction factor of the Young's modulus of steel at temperature θ

k - Thermal conductivity

$M_n\ (T)$ - Resisting moment of the beam

M_{sd} – Design moment

M_g – Moment due to dead loads

M_q – Moment due to live loads

P_f – Probability of Failure

P_l - Acceptable probability of loss of life for a given reference period

P_a - Probability of occurrence of serious fires within the considered reference period

P(fire) - Probability of an (initial) fire outbreak

p - Probability of occurrence of fire per m^2/year

q -Trade-off between work and leisure

r - Steel yield strength reduction factor

R (**X**) – Function of random variables that represent the element's resisting moment

$R_{d,fi}$ – Resistance in a fire situation

S (**X**) – Function of random variables that represent the element's bending moment

$S_{d,fi}$ – Load effects in a fire situation

x_{500} - Position of the 500 ºC isotherm in the section is needed

V_c - Shear capacity

X – Vector of random variables

Y - Life-cycle cost

α- Thermal diffusivity

β – Reliability index

γ - Societal discount rate

γ_g – Weighting coefficient of permanent actions

γ_q – Weighting coefficient of variable actions

γ_s – Partial safety factor for steel

γ_c – Partial safety factor for concrete

ε_{res} – Resulting emissivity

n_w - Ratio of the beam surface temperature rise and that of the fire temperature

n_x - Ratio between the temperature rise on the surface (x) to that of an interior point in the section

n_y - Ratio between the temperature rise on the surface (y) to that of an interior point in the section

θ_a – Steel surface temperature

θ_R – Uncertainties in the resistance model

θ_S – Uncertainties in the load action model

λ – Thermal conductivity of the material

λ_{fi} - Rate of fully developed fire

φ_{2j} – Reduction factor for combined effects

φ_v - Shear strength reduction factor

ρ – Density

μ_x – Mean of random variable X

μ_M- Average failure cost

μ_L - LQI-based valuation of risk to human lives.

σ_X – Standard deviation of random variable X

$\Phi(x)$ – Cumulative distribution of the standard normal variable

ω - Obsolescence rate

SUMMARY

1

INTRODUCTION

1.1 Research Significance

Structural stability and integrity during a fire event are paramount for ensuring the overall safety of a building. The fundamental principle guiding fire safety design is that a building should withstand fire without collapsing, thereby protecting occupants and firefighters. The structure must allow sufficient time for occupants to evacuate or be rescued, and ideally, it should be able to endure a complete burnout (Bailey and Khoury, 2011).

Reinforced concrete (RC) structures exhibit robust performance in fire situations due to the inherent properties of concrete. As a non-combustible material with relatively low thermal conductivity, concrete transfers heat slowly, resulting in a delayed thermal response. This means that the internal sections of concrete elements remain relatively cool for extended durations of fire exposure, which protects the embedded reinforcing steel from rapid temperature-induced degradation. Such delayed failure modes, often manifesting during the cooling phase, highlight the resilience of concrete under extreme conditions (Gernay, 2019).

However, exposure to high temperatures triggers a series of physical and chemical transformations in concrete, including water evaporation, disintegration of hydration products and aggregates, coarsening of microstructure, and increased porosity (Ma et al., 2015). These changes significantly diminish the mechanical properties of concrete at elevated temperatures, complicating the evaluation of structural integrity during fire events.

Designing structures for fire performance is one of the most challenging tasks faced by engineers (Fitzgerald, 1997). This complexity arises from the unpredictable nature of fire behavior and the intricate response of structural elements when subjected to fire. Furthermore, the modeling required to accurately simulate these conditions introduces a high degree of uncertainty (Achenbach et al., 2019). Effective structural fire performance must therefore account for various uncertainties, including fire exposure duration, mechanical properties of materials, thermal responses, and loading conditions. A thorough understanding of these uncertainties in performance evaluation is essential for ensuring safety, shifting the focus from trial-and-error methods to explicit reliability-based design (Van Coile et al., 2019A).

Modern design specifications strive to achieve an acceptable level of fire performance by defining minimum design requirements that ensure occupant safety during specific design events. Compliance with prescriptive criteria related to materials, structural configuration, detailing, strength, and stiffness is often regarded as sufficient evidence of achieving the desired performance (Szoke, 2015). However, traditional prescriptive fire safety recommendations often lack clarity regarding the underlying target safety levels and the associated balance between risk and investment costs, highlighting the necessity for performance-based design (PBD) (Hopkin et al., 2020).

PBD operates on the premise that structural systems must meet explicit performance objectives. It establishes specific performance expectations for the completed design and outlines processes in minimal terms (Szoke, 2015). This approach effectively reverses the conventional design process by beginning with the desired end goals. The subsequent steps involve identifying optimal solutions for multiple, sometimes competing, objectives. The design process culminates in demonstrating compliance with performance standards through analysis, simulation, testing, or a combination of these methods (Szoke, 2015).

The advantages of PBD include economic benefits over simplistic approximations, fostering innovation suitable for complex buildings, providing a better understanding of structural behavior in fire, and identifying critical vulnerabilities in fire situations (O'Connor, 2019). PBD procedures are underpinned by reliability-based design principles, which have evolved considerably over recent decades. A common simplification in this approach involves applying the concept of limit states alongside partial safety factors.

In a reliability-based design framework, it is crucial to statistically characterize the stochastic variables involved in the problem. A target safety level should be established based on the class of structure and materials utilized. An initial proposal for partial safety factors can then be evaluated for appropriateness using reliability methods such as First Order Reliability Method

(FORM) and Monte Carlo simulations (MCS) during the code calibration process (Nowak and Szerszen, 2003; Szerszen and Nowak, 2003). This calibration process typically formulates a minimization problem, where the objective is to minimize the discrepancy between computed reliability and the target reliability index (Faber and Sørensen, 2002).

Given this context, it becomes evident that the performance of structural elements designed using traditional prescriptive approaches may not be adequate. In some instances, these approaches lead to excessive investment, while in others, they result in inadequate safety measures. Importantly, the uncertainty surrounding structural performance during real fire incidents implies a certain probability of failure when subjected to severe fire conditions. Only by considering these uncertainties can the costs and benefits of fire safety investments be assessed rationally. Consequently, design methodologies should be rooted in a solid understanding of reliability. The International Forum of Fire Research Directors (FORUM) has identified the need for research into estimating uncertainty and incorporating it into structural risk analyses concerning fires as crucial for enabling the application of PBD in fire code applications (Croce et al., 2008).

Furthermore, the partial safety factors currently employed in structural fire engineering design warrant scrutiny. For example, the American Society of Civil Engineers (ASCE) recommends coefficients of 1,2 for permanent loads and 0,5 for live loads, while the American Concrete Institute (ACI) sets these coefficients at 1,0 for both permanent and live loads. The EUROCODE defines these factors as 1,0 for permanent loads and 0.3 for live loads (EUROCODE 1992–1–2, 2002). In the Brazilian standard ABNT NBR 8681:2004, the coefficients are 1,2 for permanent loads and 0,28 for live loads in the context of commercial buildings. These discrepancies underscore the absence of a systematic, probabilistically calibrated approach for addressing fire safety across the diverse standards used for RC member design worldwide.

In the context of structural design, critical components that determine fire performance, such as beams, columns, walls, and slabs, must be designed for adequate fire resistance. The significance of these design considerations lies in ensuring that fire resistance is sufficient to withstand the worst expected fire severity within the building.

Typically, design projects operate on implicit reliability levels deemed acceptable, as derived from the application of partial safety factors outlined in technical standards. For ultimate limit states (ULS) under normal temperature conditions, adjustments to these factors have been made through the calibration of technical standards, employing concepts and methods from structural reliability. For instance, the calibration of the US standard ACI 318 has been documented by Szerszen and Nowak (2003). However, studies focusing on ULS in fire conditions for RC structures remain scarce.

In this context, the reliability of RC structures during fire events warrants thorough investigation. Among the various elements of RC construction, beams are the central focus of this research, building on previous studies conducted by the author (Coelho, 2018). Despite this focus, there remains a limited body of research on fundamental parameters critical to the development of PBD, including target safety levels, parametric fire considerations, and life-cycle cost analysis. While further investigations into other load-bearing RC elements, such as columns and slabs, are recommended, they fall outside the current scope of this study.

1.2 Objectives

Considering the gaps in the literature, the research presented herein focuses on three key topics related to RC beams:

- Probabilistic evaluation of bending capacity under both standard and parametric fire exposures;
- Assessment of failure probability;
- Evaluation of target safety levels and their associated costs.

As explored in this research, most existing studies primarily focus on standard fire exposure, often disregarding the uncertainties associated with real fire scenarios. By addressing these uncertainties, this study contributes to a more realistic perspective on the reliability of RC beams, especially under parametric fire conditions, which better reflect the complexity of fire behavior in actual buildings. Incorporating parametric fire exposure into reliability assessments provides a more accurate understanding of structural performance, filling a significant gap in current fire engineering literature.

Moreover, once a probabilistic framework is established, target safety levels can be determined. These safety levels can serve as benchmarks for code calibration and design applications, facilitating the adoption of a reliability-based design approach in structural fire safety. In this context, life-cycle costs become a crucial tool for identifying optimal safety levels that balance reliability and cost-effectiveness. While there are published studies on steel structures (Hopkin et al., 2020) and RC slabs (Van Coile et al., 2014), no published research specifically targets the reliability analysis of RC beams under fire exposure.

In summary, the primary objective of this research is to develop and apply a comprehensive theoretical framework for the reliability analysis of RC beams exposed to fire. This framework aims to address the following gaps:

- The inclusion of parametric fire scenarios in bending capacity evaluations;
- The exploration of methodologies for defining acceptable reliability indices for RC beams, with attention to the corresponding costs, to inform both design practices and code development.

1.3 Thesis Organization

To achieve these objectives, the research will first review current structural fire design methodologies (Chapter 2). The review will provide input for the establishment of deterministic models for the bending capacity of concrete beams exposed to fire (Chapter 3). The thesis will subsequently move into the field of uncertainty and reliability analyses (Chapter 4). A review of the main studies about the theme are then presented and serves as a basis for this study (Chapter 5). The most appropriate reliability analysis tool (e.g. MCS) will then be utilized for studies involving the performance of beams under fire situation at the flexural ultimate limit state. The results of the case studies will function as input for a life-cycle costs analysis (Chapter 6). The possible implications of the life-cycle costs result on the codes, standards, or even the field of fire engineering, in order to achieve the target probability of failure and reliability index, will be discussed (Chapter 7 and Chapter 8).

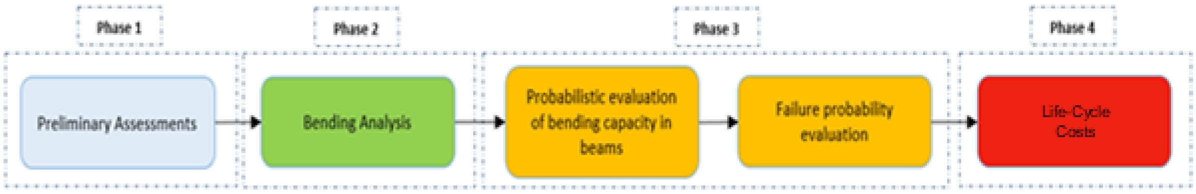

Figure 1.1- Flowchart of the research phases

Phase 1: Preliminary Assessments

In this phase, first an introduction of fire engineering applied to RC structures is presented, involving the concepts of fire severity (real and standardized fire) and fire resistance (e.g. properties of materials in a fire situation). The same is done for the assessment methodologies of an RC beam.

Phase 2: Bending Analysis

Based on the studies previously presented in the literature, the bending assessment methodology is expanded to the fire situations. The main objective of this phase is to create/choose a deterministic model for bending capacity of beams in a fire situation (real and standardized fire).

Phase 3: Probabilistic Evaluation of Bending

In this phase, the concepts of reliability and uncertainties are first introduced. Following that, the statistical description of the random variables relevant to the problem is provided. Additionally, a performance function for the ultimate limit state of beams subjected to bending in a fire scenario is presented.

The choice of the most adequate methodology for the problem at hand for reliability analysis is made (e.g. MCS), some case studies are presented and discussed.

Phase 4: Life-cycle Cost

In this phase, in possession of the results obtained previously, an analysis of the target safety levels can be done taking the discussion to the level of PBD and life-cycle cost in RC beams. A base/support for this study can be obtained from the research of Van Coile and Hopkin (2018), where target safety levels for insulated steel beams exposed to fire are presented.

This thesis is divided in eight chapters and three annexes, as follows:

- Chapter 1 – This chapter introduces the research by providing an overview of its relevance, the justification for its pursuit, and the main objectives. The significance of the topic in the context of structural fire engineering is highlighted, laying the groundwork for the subsequent chapters.

- Chapter 2 – This chapter delves into the foundational principles of fire engineering, covering key concepts such as fire severity, fire resistance, and the criteria that guided the development of this research. It also explores various fire protection systems and their importance in safeguarding structures, establishing a theoretical framework for the study.
- Chapter 3 – In this chapter, the design concepts for RC beams under fire conditions are examined. A thorough review of the design methodologies specified in the Brazilian standard ABNT NBR 15200:2024 is conducted, with emphasis on fire resistance criteria and structural performance during fire events.
- Chapter 4 – This chapter addresses the inherent uncertainties in the fire design of RC structures. It presents strategies for managing these uncertainties, focusing on probabilistic methods such as reliability analysis. The MCS, a key tool for evaluating the reliability of fire-exposed structures, is introduced and discussed in detail.
- Chapter 5 – In this chapter, a comprehensive reliability assessment of concrete beams subjected to fire exposure is conducted. The chapter reviews relevant literature and previously published research on the topic. The results of the reliability evaluation are presented, and the data is systematically compared with findings from other studies to draw meaningful conclusions.
- Chapter 6 – This chapter describes the beams analyzed in the research, providing a detailed account of the characteristics and equations that represent the key variables of interest. Statistical analyses are performed to assess the behavior of these variables under fire conditions. A performance equation is developed, and the MCS is applied to evaluate the failure probability of the beams.
- Chapter 7 – This chapter explores methodologies for defining acceptable failure probabilities based on life-cycle costs techniques. The proposed methodologies are then applied to the case study, allowing for a critical assessment of the outcomes. The chapter concludes by discussing how these methods can inform practical design guidelines for fire safety in RC structures.
- Chapter 8 – This chapter provides a comprehensive summary of the research conducted throughout the study. It synthesizes the key findings from the various analyses and case studies, highlighting the main conclusions drawn from the investigation of RC beams under fire conditions. The chapter emphasizes the contributions of the research to the field of structural fire engineering and the reliability assessment of RC structures.

Furthermore, based on the insights gained, recommendations for future work are proposed. These suggestions aim to address remaining challenges, explore potential improvements in design methodologies, and expand the scope of fire safety in structural engineering.

- Annex A - Application of the detailed methodology in one of the case studies.
- Annex B – MATLAB code used for the reliability analysis
- Annex C – List of publications

2

BASIC PRINCIPLES OF FIRE ENGINEERING APPLIED TO RC STRUCTURES

2.1 Introduction

Until the 1940's, studies related to structural elements in a fire situation were especially focused on steel structures, due to the large steel constructions of that time. Since the 1950's, the thermal effects on the degradation of the strength of ordinary concrete have been studied by several researchers, using more refined experimental procedures. These studies served as the basis for the first recommendations on this topic, which were proposed in North American and European design codes (Costa, 2008).

The topic began to be developed in Brazilian Structural Engineering about 45-50 years ago, with the publication of the standard NB 503 (1977) - *"Particular requirements of reinforced and prestressed concrete in relation to fire resistance",* to complement design in concrete structures (Bacarji, 1993).

Through the evolution of the RC construction method, the interest in understanding the behavior of this material and the phenomena of fire propagation also began to emerge. Conceptually, it is defined that fire is a combustion characterized by the appearance and spread of the flame, the release of heat, the emission of gases, the production of smoke and the formation of various products from carbon. In short, a fire can only exist when there is a fuel, an oxidizer and a heat source.

Numerous fires have occurred across the world and also in Brazil, normally caused by problems in the electrical system of buildings. Some took on greater proportions, caused immeasurable material losses or significant cultural losses, as in the case of the Portuguese Language Museum, in São Paulo. But there are those that, in addition to financial and cultural losses, have led to human losses. Some of the most significant cases of fires in Brazil are briefly mentioned below, based on news from the media:

- **Andraus Building (1972), in São Paulo (SP):** The fire occurred in 1972 at the Andraus building in downtown São Paulo. It was ignited by a sign displaying advertisements. The incident resulted in 330 injuries and 16 fatalities (Figure 2.1).
- **Joelma Building (1974), in São Paulo (SP):** In 1974, the 25-story Joelma Building became the site of another tragedy. A short circuit in an air conditioner sparked a fire that raged for over 8 hours. The incident left 345 people injured and claimed 188 lives (Figure 2.2).
- **Renner Store (1976), Porto Alegre (RS):** The store's fire occurred on April 27, 1976, caused by a short circuit in the appliance sector, killing about 41 people.
- **Grande Avenida Building (1981), São Paulo (SP):** On February 14, 1981, Paulista avenue stopped with the fire at the Grande Avenida building, where the Record TV transmission tower was located. There were dozens of injuries and 17 were killed.
- **Andorinha Building (1986), Rio de Janeiro (RJ):** In 1986, in Rio de Janeiro, the Andorinha Building was destroyed by fire. The most likely cause is that the fire started on the 9th floor in an outlet that was live loaded by several electrical devices. It is estimated 23 dead and more than 40 injured.
- **Canecão Mineiro (2001), Belo Horizonte (MG):** In 2001, in a concert hall in Belo Horizonte, Minas Gerais, an accident with fireworks on stage caused the flames to spread, leaving 7 dead and more than 300 injured.
- **Kiss Nightclub (2013), Santa Maria (RS):** The fire started on the stage of the nightclub, on January 27, 2013, with a flag launched by a member of the band that played in the house. There were 242 fatalities and countless injuries.
- **Wilton Paes Building (2018), São Paulo (SP):** On May 1, 2018, the building in which several families lived irregularly collapsed after an alleged explosion of a pressure cooker or gas cylinder. At least 317 families lived irregularly in the property and the collapse left 7 dead and 455 people homeless.
- **National Museum (2018), Rio de Janeiro (RJ):** On September 3, 2018, the UFRJ national museum, the oldest in the country, is set on fire, the result of neglect and poor conservation of its facilities. Such a fire resulted in irreparable losses for Brazilian culture.

- **Flamengo Accommodation (2019), Rio de Janeiro (RJ):** The fire started at 5 am due to a short circuit in an air conditioning unit in one of the rooms. Construction was not authorized by law. There were 10 deaths, all teenagers aspiring to be professional soccer players, who were between 14 and 17 years old.
- **Badim Hospital (2019), Rio de Janeiro (RJ):** The suspicion is that flames started after a short circuit in a generator, but the hypothesis has not been confirmed yet. Resulted in the death of 11 patients.
- **Bonsucesso Hospital (2020), Rio de Janeiro (RJ):** The fire that hit the Federal Hospital of Bonsucesso caused the death of three patients who were hospitalized in the health unit - the largest in the public network of Rio de Janeiro. Reports issued by public authorities (firefighters) indicated that the building had several problems that could turn into a major fire.

Figure 2.1: Fire in Andraus Building (Negrisolo, 2011)

Figure 2.2: Fire in Joelma Building (Negrisolo, 2011)

Considering the relevance of this phenomenon and the importance of a better understanding of its influence on structures, this chapter presents the basic principles of fire engineering applied to RC structures, the object of this study. Therefore, the introduction of two concepts is fundamental: (i) fire severity and (ii) fire resistance.

2.2 Fire Severity

The fire severity is a measure of the destructive potential of a fire. For a given severity, a structural component with relatively less fire resistance will be "destroyed" or lose the function for which it was designed before a component with relatively greater fire resistance. Fire severity is usually defined in terms of a standard fire exposure time period. However, "real" fires have standard fire characteristics, which results in several methods for determining "equivalence" to standard fire exposure. Reis (2011) lists some of the fire models used in the last century to analyze fire compartments.

Table 2.1 - Analytical models (simplified methods) (Reis, 2011; adapted)

Nominal Fire Curves	ISO 834 standard fire curve
	ASTM E119 fire curve
	Hydrocarbon fire curve
	Fire curve for exterior elements
Parametric Fire Curves	Swedish fire curves
	EUROCODE 1
	Babrauskas
	Law
	Lie
	Ma and Mäkeläinen
	BFD Curves
	iBMB Curves

Considering the scope of this research, the real fire curve, the standard fire curve, the ASTM E119 curve, and the parametric fire model proposed in EUROCODE 1 are discussed in detail below.

2.2.1 Real Fire

In a real fire situation, three products are generated: heat, smoke, and flames. The fire can be influenced by various factors, such as the geometric shape and dimensions of the space, the specific surface of the combustible materials, the location of the fire's origin, climatic conditions, ventilation openings, preventive measures, and the availability of protection systems. Therefore, each fire is unique (Seito et al., 2008).

It can be said that the phases of a real fire are related to its risk categories; with that the evolution of the fire is characterized by five phases, namely (Costa, 2008):

1. The initial phase (first phase), or ignition: This phase consists of two stages—abrasion and flare. Abrasion begins with slow combustion, without flames, producing minimal heat and potentially releasing toxic gases. Flaming involves combustion with flames and smoke, marked by a gradual rise in temperature. During this stage, there is still no immediate risk to life or threat of structural collapse.
2. The phase between ignition and flashover is called the pre-flashover stage and is one of the key stages of a real fire. During this phase, the compartment begins to heat up, marked by a rapid increase in temperature. The spread of the fire still depends on the characteristics of the compartment, such as fuel and ventilation.
3. The phase of generalized inflammation or flashover (third phase) is the point from which the fire will spread and burn the combustible materials in it more quickly. Hot gases and smoke can be transferred through the openings to other compartments. It is the moment when the situation is no longer controllable, and all compartments are filled with flames;
4. The post-generalized inflammation phase (fourth phase) is a stage characterized by an intense increase in the temperature of the gases. It is the stage in which the whole compartment is on fire and moves towards the peak of maximum temperature of the fire, which corresponds to the maximum temperature of the gases in the environment.
5. The extinction phase (fifth phase), or what is called the cooling phase, is the stage in which the intensity and severity of the fire will decrease due to the gradual reduction of the temperature of the gases in the compartment after the complete extinction of the present combustible material.

Figure 2.3 shows the phases described above in a time-temperature diagram.

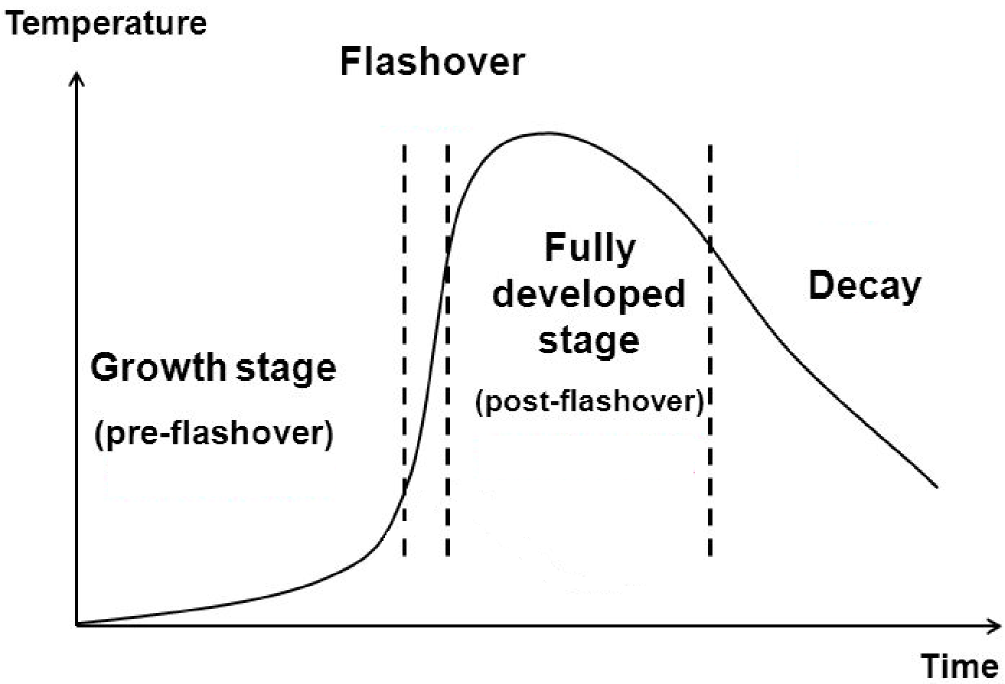

Figure 2.3: Main phases of a real fire (Costa, 2008; adapted)

2.2.2 Standard Fire

Derived from these studies on the types of fires and their characteristics, internationally known curves have emerged to standardize fires for easier study. An example is ISO 834, the 'standard curve' or 'standard fire,' which, in its current form, consists of a series of 14 parts (standards and technical reports). This curve does not depend on the dimensions, purpose of the compartment, or the thermal characteristics of the materials (Costa & Rita, 2004). It is important to note that any conclusions about a standard fire and a real fire must be carefully analyzed, as the behavior of the standard curve does not accurately represent that of a real fire (Costa & Silva, 2003).

The ISO 834:1975 curve is the result of the standardization of two traditional standard curves: the American ASTM E-119 (1918) and the British BS 476 (1932), both similar and of the same origin. This curve is used in several countries to simulate the standardized thermal process to which construction elements or systems are subjected during tests and is also used in the evaluation of materials according to fire resistance classes (Costa, 2008).

To facilitate the testing procedures and design of structures, the fire was standardized by nominal curves, which are represented by equations and applied to any compartment. These standard curves represent the conventional evolution of fire in a compartment from the stage of generalized inflammation.

The ISO 834:1975 standard fire curve is characterized by having a branch with upward development, assuming that the temperature of the gases is always increasing over time, and is expressed by Equation 2.1 (Costa, 2008):

$$\theta_g = \mathrm{T}_0 + 345\log(8t + 1) \tag{2.1}$$

where, θ_g is the temperature of the hot gases from the burning compartment (ºC), t is time (minutes) and T_0 is the ambient temperature, usually taken as 20 ºC.

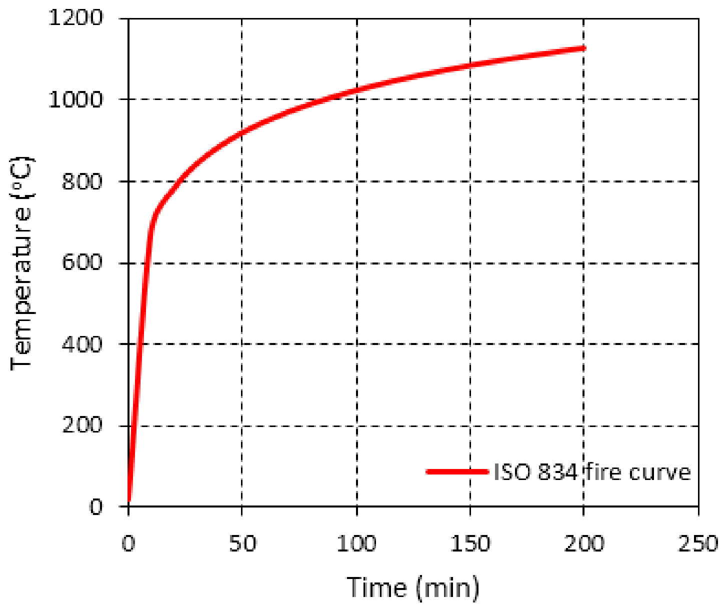

Figure 2.4: Fire curve standardized according to ISO 834:1975 (Costa, 2008; adapted)

As shown in the graph in Figure 2.4, the ISO 834 standard fire curve has characteristics that are far from comparable to a real fire (Figure 2.3). This occurs mainly due to the fact that characteristics of the compartment, such as ventilation, type and quantity of fuel, are not being considered (Inácio, 2011).

The ISO 834 curve, although it does not manifest the physical reality of a fire in a compartment, has merit in its use for the simple fact of being standardized, unifying the tests and allowing the comparison of the results obtained in different laboratories around the world.

2.2.1 ASTM E119 Fire

Another standardized fire is the ASTM E-119. In this case the mean value of fire temperature ($\bar{T}$) can be described using Equation 2.2.

$$\bar{T}\ (°C) = 750\left(1 - e^{-3,79553\sqrt{t}}\right) + 170,41\sqrt{t} + T_0 \tag{2.2}$$

where t is time (hours) and T_0 is the ambient temperature, usually taken as 20 ºC. A comparison between the real fire in a parametrized form, the ISO curve and the ASTM curve can be seen in Figure 2.5.

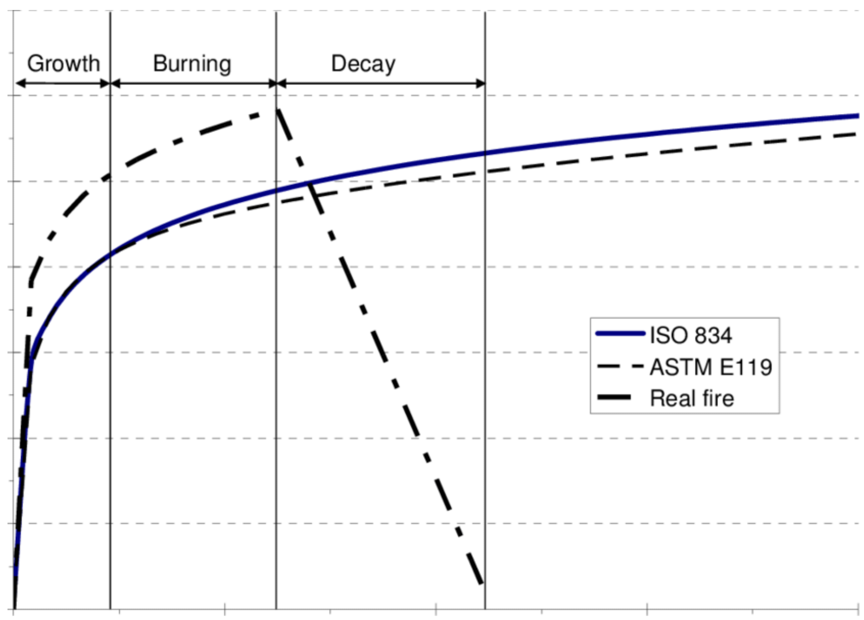

Figure 2.5: Comparison between ISO 834, ASTM E-119 and real fire (Green et al. 2007)

2.2.2 Parametric Fire

The great advantage of parametric curves is that they can be standardized or parameterized by the specific characteristics of the place of fire. These parametric fire curves allow taking into account the compartment geometry, fire load density and ventilation characteristics, while at the same time maintaining the simplicity of a straightforward analytical formula (Van Coile, 2016).

The parametric curves presented by Eurocode 1 (2002), for example, are based on a natural fire model and are valid for compartments up to 500 m² in floor area and 4m height, without horizontal openings (in the ceiling). In this model, it is considered that all flammable material participates in the combustion process.

The formulation for gas temperature in the heating phase, the ascending branch, is given by Equation 2.3 (EUROCODE 1992–1–2, 2002):

$$\theta_g = 20 + 1325(1 - 0{,}324e^{-0{,}2t^*} - 0{,}204e^{-1{,}7t^*} - 0{,}472e^{-19t^*}) \quad (2.3)$$

$$t^* = t.\Gamma \quad \text{(hours)} \quad (2.4)$$

where θ_g is the temperature of the gases inside the compartment, expressed in degrees Celsius (ºC), Γ is a time conversion fator and t is time.

This time conversion factor considers the opening factor, limiting this between 0,02 and 0,20. It also considers a thermal absorptivity factor of the surrounding surface, composed of the physical characteristics of the surrounding material, such as specific gravity, specific heat and thermal conductivity.

The critical temperature of the curve is given the instant that $t^* = t^*_{max}$, which is defined by (EUROCODE 1992–1–2, 2002):

$$t^*_{max} = t_{max}.\Gamma \quad (2.5)$$

$$t_{max} = max\left[\left(0{,}2\,.\,10^{-3}.\,q_{t,d}/O\right); t_{lim}\right] \quad (2.6)$$

In this equation, $q_{t,d}$ relates the fire loads of the compartment to the area of the pavement surface. The time limit t_{lim} varies according to the growth rate of the fire. The maximum time also varies depending on the largest energy source, whether controlled fire load or ventilation.

The curves in the cooling phase occur as a function of t^*, previously defined. They are given by the following equations:

$$\theta_g = \theta_{max} - 625(t^* - t^*_{max}\,.\,x), for\ t^*_{max} \leq 0{,}5 \quad (2.7)$$

$$\theta_g = \theta_{max} - 250(3 - t^*_{max})(t^* - t^*_{max}\,.\,x), for\ 0{,}5 \leq t^*_{max} \leq 2.0 \quad (2.8)$$

$$\theta_g = \theta_{max} - 250(t^* - t^*_{max} \, . x), for\ t^*_{max} \geq 2{,}0 \tag{2.9}$$

where x is obtained as a function of the time limit, maximum time and conversion factor of the time. Parametric curves of Eurocode, with varying opening factors, are presented in Figure 2.6.

It is important to note that the opening factor (O) is calculated using the formula O = Av / ($\sqrt{h\ *\ At}$), where Av represents the total area of openings (m²), h is the average height of the openings (m), and At is the total area of internal and external surfaces (m²). The resulting unit of measurement for the opening factor is expressed in $m^{1/2}$.

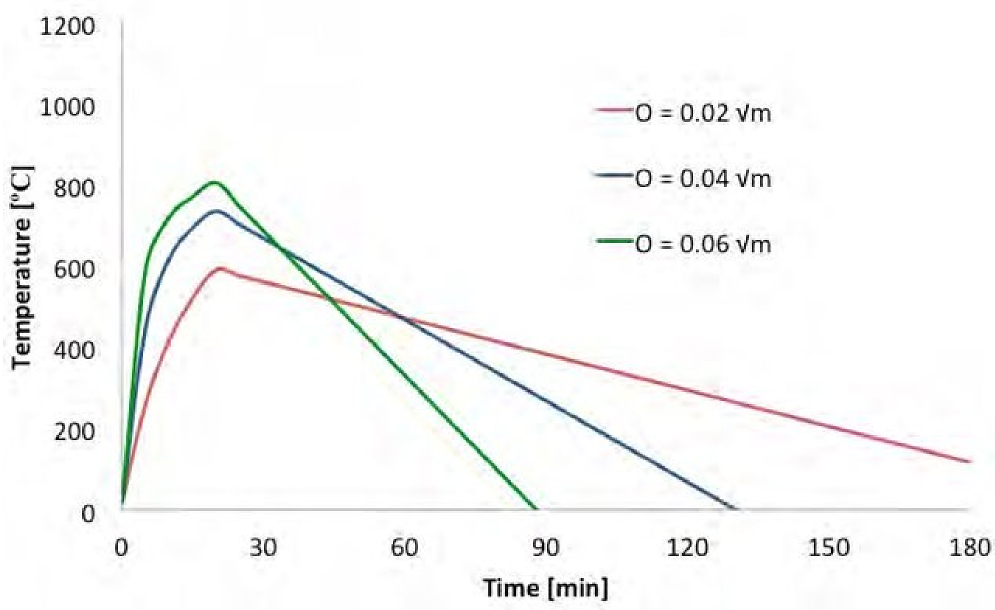

Figure 2.6: Parametric fire curves from Eurocode (Lucherini, 2016)

The use and differences between the application of these curves is extremely relevant. Considering, for example, a compartment with twelve windows, two doors and the dimensions and characteristics as shown in Figure 2.7, and a hotel occupancy, some analysis can be done.

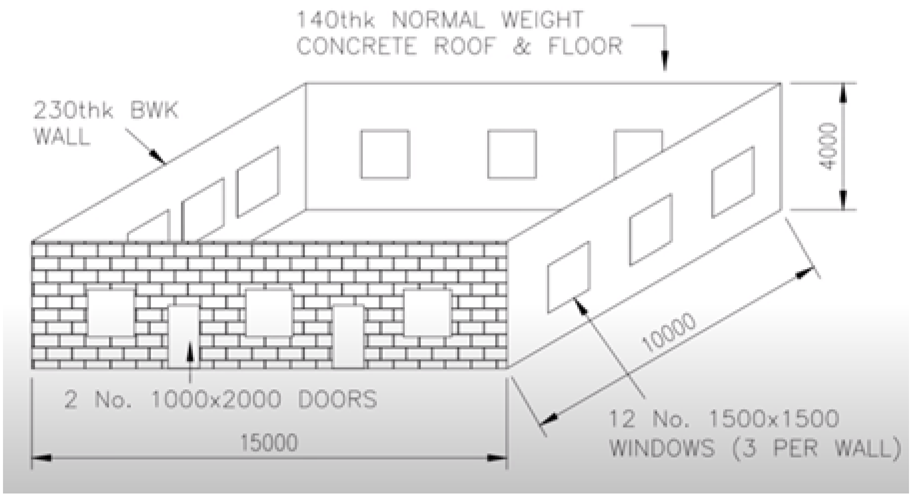

Figure 2.7: Parametric fire curves – EUROCODE example (EUROCODE 1992–1–2, 2002)

For this case, the differences in temperatures inside the compartment after 20, 30, 60, 90 and 120 minutes of fire can be seen in Figure 2.8. The large decrease in temperature after 30 minutes of fire, for this case, shows how the choice of fire model directly affects the severity of fire and, consequently, the other dependent values of this variable (e.g. resisting moment).

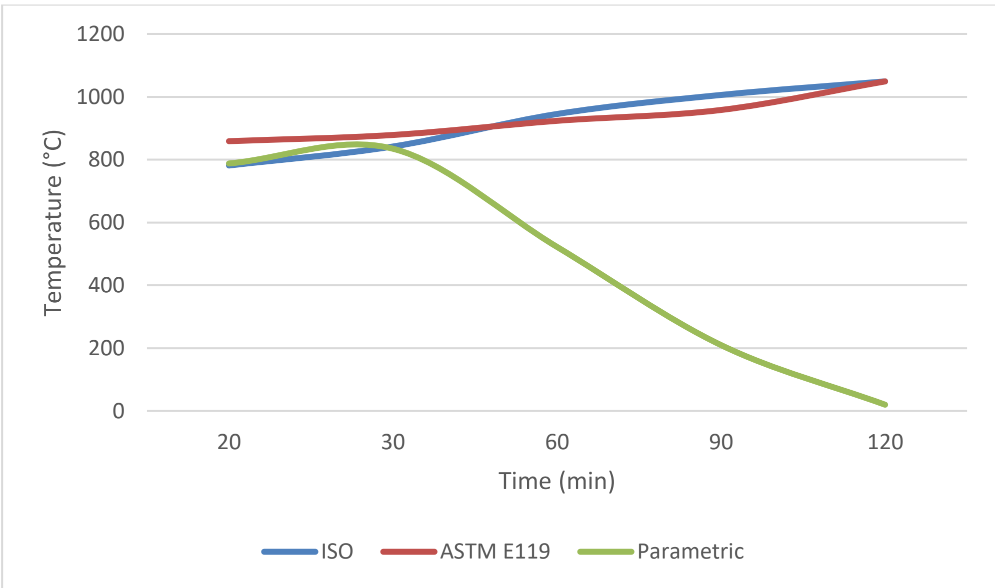

Figure 2.8: Temperature in the compartment according to different models.

2.3 Fire Resistance

Being a term that is often attributed to the behavior of structural components in a fire situation, fire resistance is a measure of the ability of a structural component to withstand a fire. More specifically, the fire resistance of a component, or set of components, is its ability to withstand exposure to fire without loss of bearing capacity, or to function as a barrier against the spread of fire - or both. It is often quantified as the expected time for the elements to meet certain criteria when exposed to a standard fire resistance test.

In most international standards (Eurocode 2 - Part 1–2 and ACI 216R – 89: Guide for Determining the Fire Endurance of Concrete Elements), these criteria are:

(I) **Stability -** resistance to structural collapse.
(II) **Integrity -** resistance to heat transfer.
(III) **Isolation -** resistance to excessive temperature on the unexposed (internal) face.

The properties of the materials vary according to the temperature of the gases to which they are submitted by the action of fire and, therefore, it is essential to know the temperatures in these structural elements. The thermal action on concrete and steel is translated in the reduction of mechanical properties, which, under high temperatures, experience a decrease in strength and Young's modulus.

2.3.1 Concrete

Reinforced and prestressed concrete structural systems are rarely externally protected, since concrete is usually made of inorganic materials with low conductivity and high thermal capacity. However, concrete gradually loses its resistance to compression under high temperatures, and it is necessary to ensure that the elements have been designed with a reserve of sufficient strength to withstand the loads applied during the expected period for exposure to fire.

Compared to steel, concrete has a slow heat transfer to its interior, as shown in Figure 2.9, for 30 minutes of ISO fire. This favors the protection of the reinforcement but makes the modeling of concrete a little more challenging.

In this case, the exposure of the elements results in a thermal gradient of 795 ºC from the exposed surface to an internal point in the concrete, while the same exposure in steel leads to a thermal gradient of only 25 ºC. This demonstrates that concrete cannot be treated as being exposed to a uniform temperature based solely on the fire temperature. In contrast, such an approximation may be reasonable for certain steel profiles, but concrete requires specific methods for its accurate thermal evaluation.

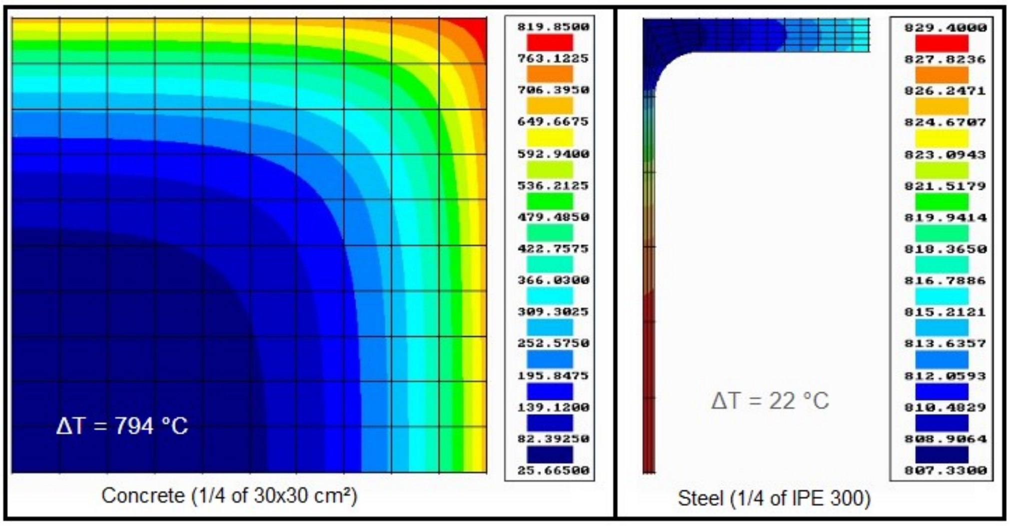

Figure 2.9: Temperature distribution calculated by finite element analysis (F.E.) after 30 minutes of exposure to ISO fire conditions (Gernay, 2018).

Another important design consideration is to ensure that the frame is sufficiently insulated as the steel loses considerable yield strength under high temperatures. The critical temperature of the steel is defined as the temperature at which only 60% of the original strength remains, at which point failure is imminent under design loads (Mehta & Monteiro, 1994). For conventional reinforcement, the critical temperature is 538 °C, while for steel bars used in prestressed structures, made of hot-rolled steel with a high carbon content, the critical temperature is significantly below 427 °C (Fitzgerald, 1997). The time needed to reach these temperatures in the concrete elements (slab, beam or column) depends on the thickness of the concrete cover that protects the steel.

The degree of restriction against thermal expansion that each concrete element undergoes as its temperature increases, and the degree of continuity provided by the structural system in its connections, also affects fire resistance (Mehta & Monteiro, 1994). Both are generally considered beneficial when it comes to concrete structures. The restriction against expansion creates additional compression stresses that, when accounted for in the design, reduce the tensile forces that are initially resisted by the steel reinforcements. Continuity allows a certain redistribution of stresses to occur before excessive deflections and rotations develop at midspan and in the connections, respectively, causing the collapse of the structure.

Concrete mixes predominantly with siliceous aggregates, containing large amounts of quartz (SiO_2) such as granite, sandstone and some shales, have a sudden volume expansion when heated to approximately 500 ºC. At 573 ºC, the quartz-α crystals become quartz-β. This phase change is followed by an expansion of around 0,85% (Mehta & Monteiro, 1994).

The concretes prepared with limestone aggregates show expansions similar to those of siliceous only after 700 ºC, due to reasons derived from decarbonation. These concretes have the advantage of presenting less difference in the coefficients of thermal expansion between the matrix and the aggregate, thus minimizing the destructive effects of the differential thermal expansion. The calcination of limestone aggregates is endothermic: heat is absorbed, delaying the rise in temperature. The calcined material has a lower specific mass, providing a form of surface insulation, but calcination also causes expansion and fragmentation of aggregates, chipping and release of carbon dioxide (Mehta & Monteiro, 1994).

Another particularly important phenomenon in concrete structures in a fire situation is spalling. It can be described as the chipping of layers or pieces of concrete on the surface of a structural element, when exposed to high temperatures and rapid growth, such as those seen in fires (Malhotra, 1984).

Theories on how and why spalling occur are based on the “movement of moisture”. As the temperature of the concrete increases, the moisture contained in it becomes steam. If it is unable to escape, there is an increase in pressure within the concrete. As this process continues, the vapor pressure increases to the point where it exceeds the concrete's tensile capacity, causing pieces of concrete to be dislodged. In addition to this conventional "moisture movement" theory, there is also a consensus that the expansion of aggregates caused by thermal stresses also directly influences explosive spalling (Zeiml et al., 2008).

According to ABNT NBR 15200:2024 - Design of concrete structures in a fire situation, the change in the strength and stiffness properties of concrete when subjected to axial compression and high temperatures can be obtained from Table 2.2.

Table 2.2 provides, for concretes prepared with siliceous and limestone aggregates, the following parameters:

- The relationship between the compressive strength of concrete subjected to different temperatures ($f_{c,\theta}$) and the characteristic compressive strength of concrete under normal conditions (f_{ck}).
- The relationship between the Young's modulus of concrete subjected to different temperatures ($E_{c,\theta}$) and the Young's modulus of concrete under normal conditions (E_{ck}).

Table 2.1: Relationship values for concretes of normal specific mass (2000 kg/m³ to 2800 kg/m³) prepared with predominantly siliceous or limestone aggregates (ABNT NBR 15200: 2012)

Concrete temperature θ °C	Siliceous aggregate		Calcareous aggregate	
	$f_{c,\theta}/f_{ck}$	$E_{c,\theta}/E_c$	$f_{c,\theta}/f_{ck}$	$E_{c,\theta}/E_c$
1	2	3	4	5
20	1,00	1,00	1,00	1,00
100	1,00	1,00	1,00	1,00
200	0,95	0,90	0,97	0,94
300	0,85	0,72	0,91	0,83
400	0,75	0,56	0,85	0,72
500	0,60	0,36	0,74	0,55
600	0,45	0,20	0,60	0,36
700	0,30	0,09	0,43	0,19
800	0,15	0,02	0,27	0,07
900	0,08	0,01	0,15	0,02
1 000	0,04	0,00	0,06	0,00
1 100	0,01	0,00	0,02	0,00
1 200	0,00	0,00	0,00	0,00

2.3.1.1 Concrete Compressive Strength at Temperature θ

The compressive strength of concrete decreases with increasing temperature, as can be seen in Table 2.2, which can be obtained by Equation 2.10 (ABNT NBR 15200: 2012).

$$f_{c,\theta} = k_{c,\theta} \cdot f_{c,k} \tag{2.10}$$

where, f_{ck} is the characteristic compressive strength of concrete under normal conditions; $k_{(c,\theta)}$ is the factor for reducing the strength of the concrete at temperature θ, obtained from the abacus in Figure 2.10, and $f_{(c,\theta)}$ is the characteristic compressive strength of the concrete as a function of temperature θ.

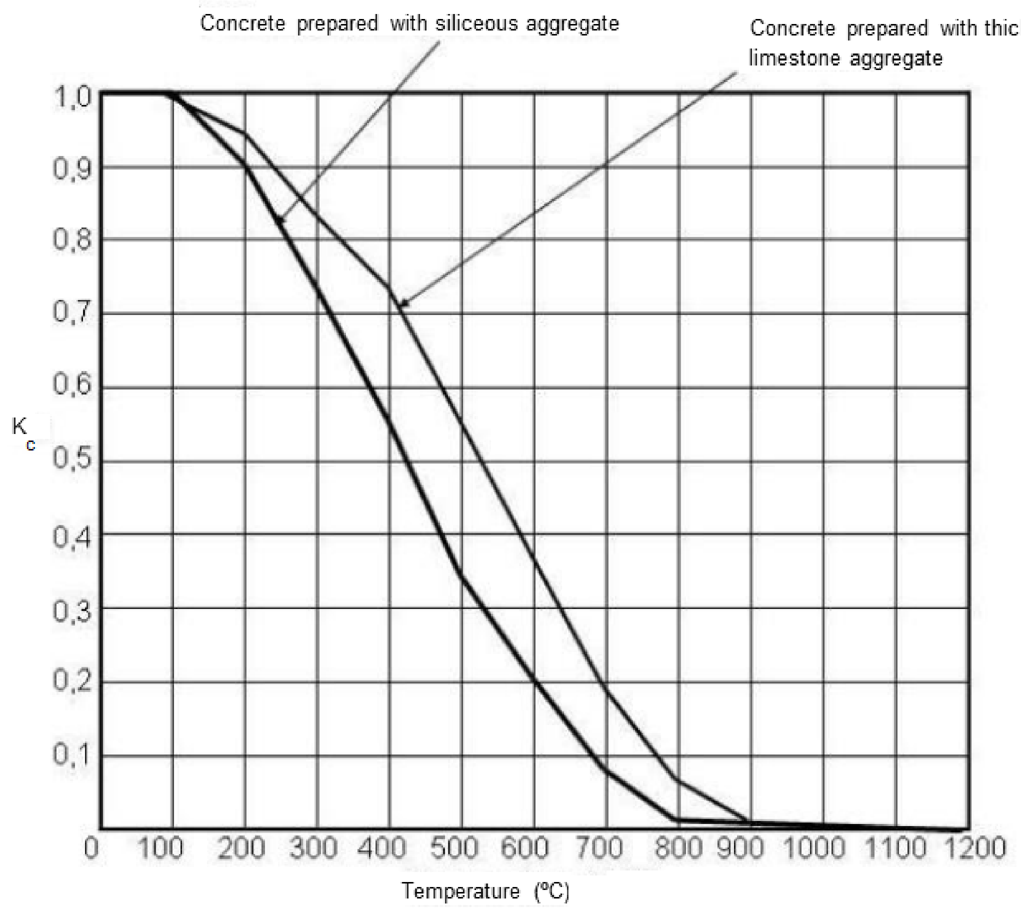

Figure 2.10: Factor of reduction of the concrete resistance in function of temperature (ABNT NBR 15200: 2012)

2.3.1.2 Young's Modulus of Concrete at Temperature θ

The Young's modulus of concrete also decreases with increasing temperature, and can be obtained by Equation 2.11 (ABNT NBR 15200: 2012):

$$E_{ci,\theta} = k_{cE,\theta} \cdot E_{ci} \tag{2.11}$$

where, E_{ci} is the initial elastic modulus of the concrete in a normal situation; $k_{(cE,\theta)}$ is the reduction factor of the concrete's elasticity modulus at temperature θ, obtained from the abacus in Figure 2.11, and $E_{(ci,\theta)}$ is the initial elasticity modulus of the concrete as a function of temperature θ.

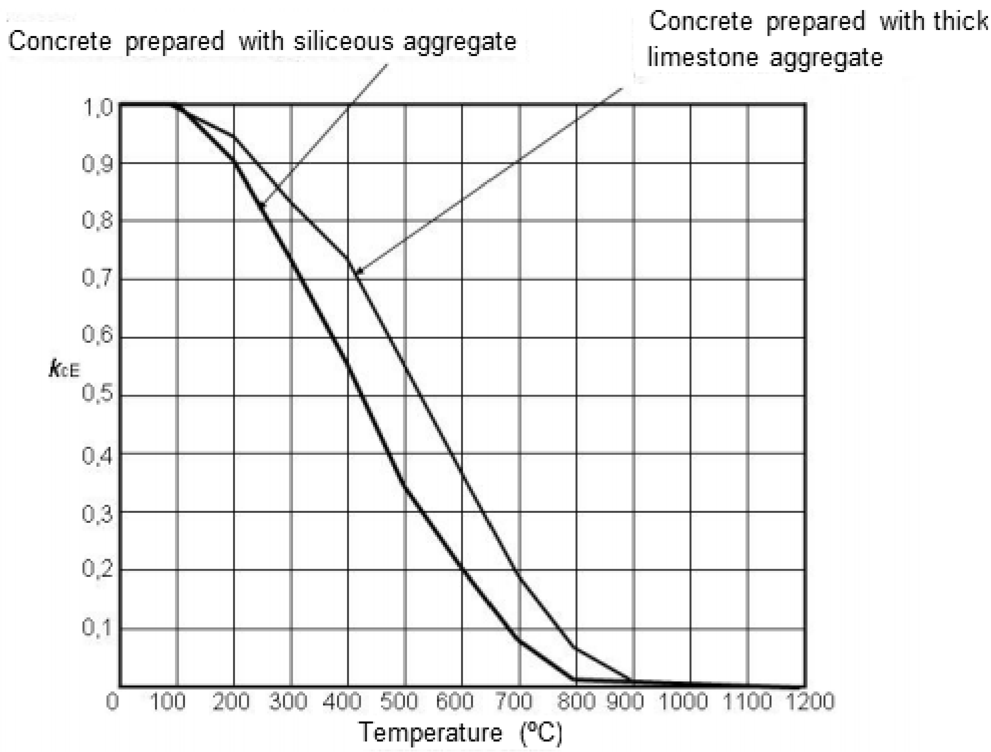

Figure 2.11: Young's modulus reduction factor of the concrete as a function of temperature (ABNT NBR 15200: 2012)

The combined effect of reducing compressive strength and Young's modulus of concrete with the increase in temperature caused by fire is a critical aspect to consider in structural fire engineering. When exposed to high temperatures, concrete undergoes thermal degradation, leading to a loss of both compressive strength and stiffness as presented in early sections.

The combined effect of these two factors can have significant implications for the structural behavior of concrete elements in fire conditions. The reduced compressive strength reduces the load-carrying capacity of the concrete, while the decreased modulus of elasticity affects the overall stiffness and deflection of the structure.

In structural fire engineering, these effects are accounted for through empirical or analytical models that consider the temperature-dependent reduction in compressive strength and modulus of elasticity. These models are typically incorporated into design codes and standards to ensure the safety and integrity of structures during fire events (Costa & Silva, 2003).

It is worth noting that the magnitude of the reduction in compressive strength and Young's modulus depends on various factors, including the concrete mix design, exposure temperature, heating rate, and duration of exposure.

2.3.2 Steel

Steel, like concrete, has the advantage of being non-combustible, but this characteristic alone does little to resist collapse. Its high thermal conductivity causes it to absorb heat much faster than other materials; thus, if the structural element has a small mass, its temperature will increase rapidly. Both the yield stress and the Young's modulus—two of the most critical material properties for determining load capacity—decrease significantly as temperature rises (DeFalco, 1974). At a temperature of 593 °C, these properties can drop by at least 40% compared to their values at ambient temperature. As a result, the strength of the steel may no longer be sufficient to support the applied loads, even with standard safety factors (De Falco, 1974).

The ratio of the heated mass perimeter to a structural steel element is a good indicator of its intrinsic fire resistance. A robust steel column can absorb considerable heat and not reach its critical temperature before 30 to 40 minutes of exposure to a fully developed fire. On the other hand, steel structures in cold formed shapes, for example, can fail within 5 to 10 minutes of exposure to the same fire (Silva, 2001).

Another important aspect to consider when using steel is its significant coefficient of linear expansion under high temperature. If the structural element is axially restricted against displacement, the expansion due to heat will be translated into thermal stress, which will increase the overall stress level in the element and cause an early collapse (Yang, 2011).

The good principles of fire protection engineering determine that thermal expansion is prevented by limiting the temperature of the steel, or that its effect on the structure is incorporated into the design.

In these terms, ABNT NBR 6118:2023 - Design of concrete structures - defines two types of reinforcement: passive and active. Passive reinforcements are those that are not used as prestressing reinforcement, that is, those that are not previously stretched. Active reinforcements, on the contrary, are designed to produce prestressing forces, that is, to which a pre-elongation is applied.

2.3.2.1 Yield Strength of Steel (Passive reinforcement) at Temperature θ

According to ABNT NBR 15200:2024, yield strength of steel (passive reinforcement) decreases with increasing temperature, which can be obtained by Equation 2.12:

$$f_{y,\theta} = k_{S,\theta} \cdot f_{y,k} \tag{2.12}$$

where, $f_{(y,k)}$ is the characteristic yield strength of steel in a normal situation; $k_{(S,\theta)}$ the reduction factor of the steel resistance at temperature θ, obtained from the graph of Figure 2.12, and $f_{(y,\theta)}$ the characteristic yield strength of steel at temperature θ.

This graph shows how much the steel's resistance factor decreases as a function of temperature θ, being:

- **Full curve:** $k_{(S,\theta)}$ applicable when $\varepsilon_{si} \geq 2\%$, usually tensioned reinforcement of beams, slabs or ties.
- **Dashed curve:** $k_{(S,\theta)}$ applicable when $\varepsilon_{si} \leq 2\%$, usually compressed reinforcement of columns, beams or slabs.

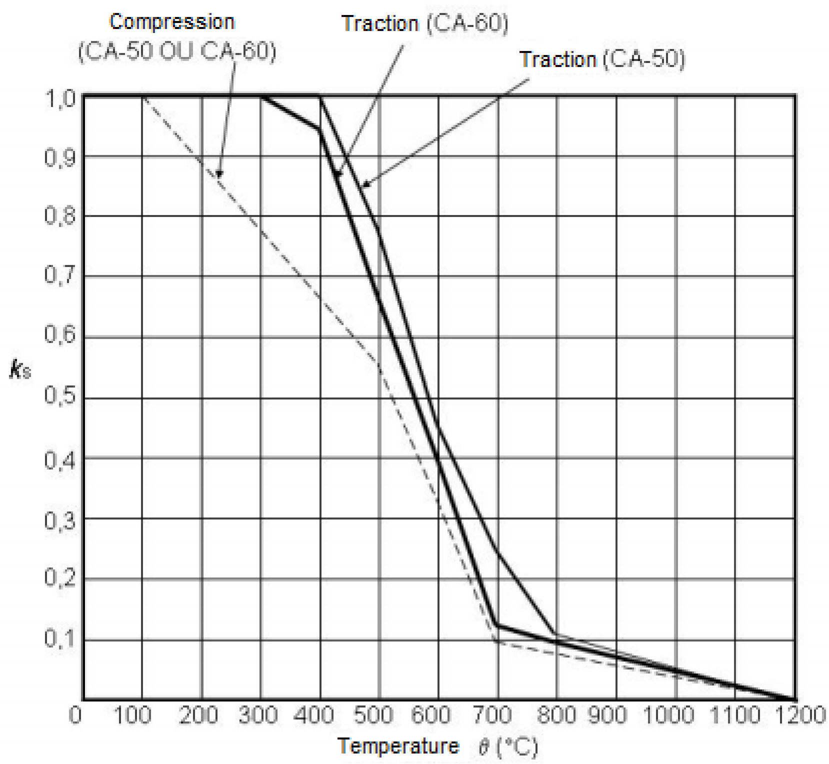

Figure 2.12: Reduction factor of the resistance of passive reinforcement steel as a function of temperature (ABNT NBR 15200: 2012)

2.3.2.2 Young's Modulus of Steel (Passive reinforcement) at Temperature θ

According to ABNT NBR 15200:2024 the Young's modulus of the passive steel reinforcement (E_S) also decreases with increasing temperature, which can be obtained by Equation 2.13:

$$E_{S,\theta} = k_{SE,\theta} \cdot E_S \tag{2.13}$$

where, $E_{(S)}$ is the Young's modulus of passive steel reinforcement under normal conditions; $k_{(SE,\theta)}$ is the reduction factor of the Young's modulus at temperature θ, obtained from the graph in Figure 2.13

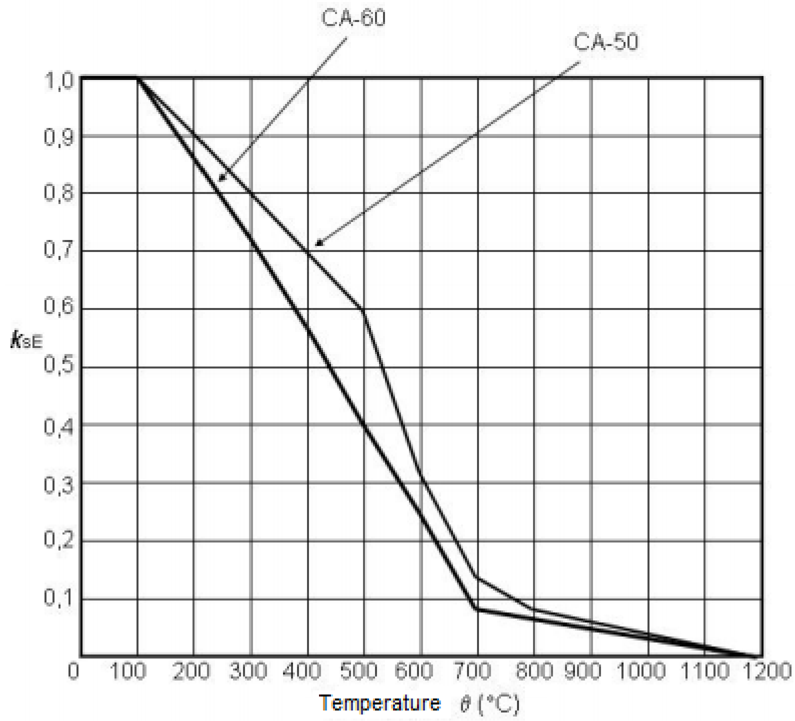

Figure 2.13: Reduction factor of the elasticity modulus of passive reinforcement steel as a function of temperature (NRB 15200:2012)

2.4 Fire Protection Systems

Fire safety conditions require the implementation of adequate fire suppression measures to prevent the structural collapse of the building, facilitate the safe evacuation of occupants, and ensure access for emergency responders to carry out firefighting and property protection operations. In the latter case, security is not limited to the property itself but extends to adjacent developments. The types of fire protection can be divided into (i) passive and (ii) active measures.

2.4.1 Passive Protection

Passive protection refers to fire safety measures that are integrated into the building's design and construction, ensuring protection against fire situations without relying on external actions (Seito et al., 2008). The fire performance of passive protection is inherent to the structure itself. The main means of passive protection include:

- Emergency exits (location, quantity).
- Proper selection of materials.
- Fire resistance of construction elements.
- Smoke control.
- Separation between buildings.
- Compartmentation.

2.4.2 Active Protection

The active protection measures complement the passive ones, being composed of equipment and building installations that will be activated in case of emergency, manually or automatically, usually not exercising any function in the normal situation of the building's use (Seito et al., 2008). Among the main active protection systems are:

- Manual or automatic fire detection and alarm.
- Manual and/or automatic fire extinguishing (Extinguishers and Sprinklers).
- Emergency lighting and signaling.
- Control of smoke occurrence.

For the design and proper installation of the active measures, a good integration between the architectural design and the project of each system is necessary, normally divided by specialty, namely: electrical, hydraulic and mechanical. It is important to be followed up by the designer so that there is compatibility between the proposed passive and active measures, aiming at the best performance of fire safety measures. In case of an accident, safety to life must be preserved by the stability of the structure until the escape of the building's occupants (Seito et al., 2008)

Figure 2.14 shows, depending on the development of the fire, the most efficient means of protection. Important to note that structural fire safety is only needed after flashover.

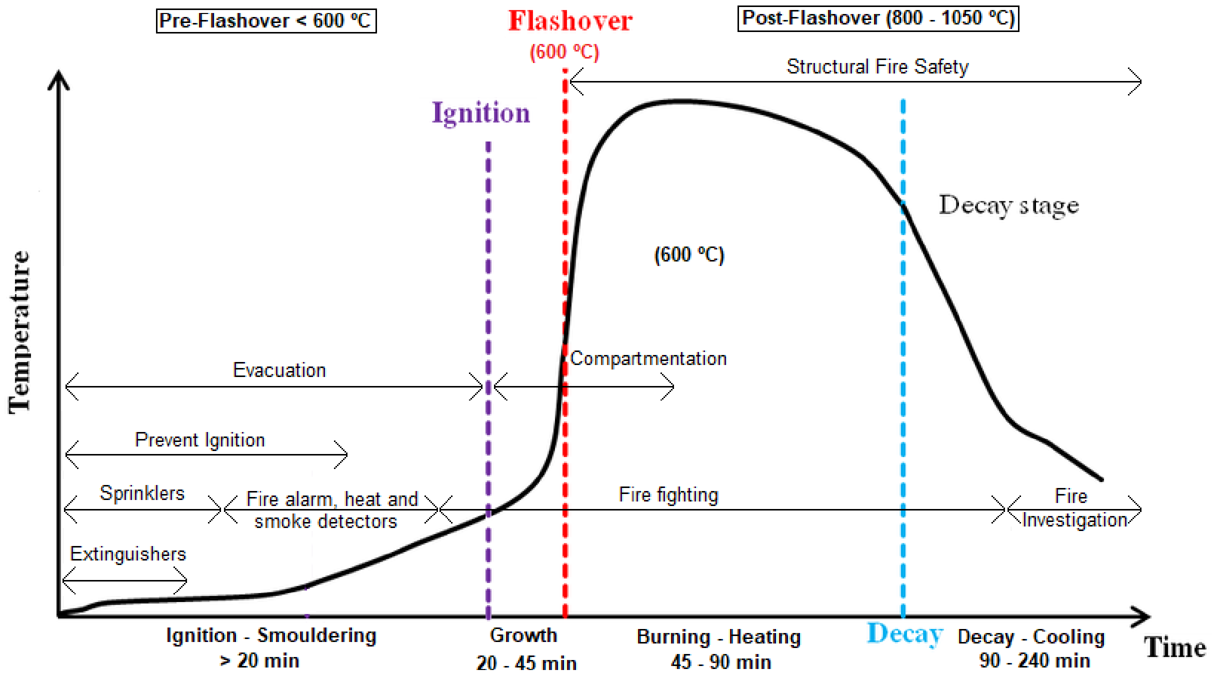

Figure 2.14: Performance of the means of protection in the behavior of the real fire (Kodur, 2014; adapted)

2.5 Summary

In this chapter, a detailed exploration of the basic principles of fire engineering applied to RC structures is provided. The chapter begins with an introduction to the fundamental concepts of fire behavior and its effects on RC structures, highlighting the importance of understanding fire severity and the impact of temperature on material properties. The concept of fire severity is thoroughly discussed, focusing on both real and standardized fires. Real fire scenarios are explored, emphasizing the complexities of modeling fire behavior in actual conditions. In contrast, standardized fires, such as the ISO 834 curve and the ASTM E119 fire test, are introduced as simplified representations of fire exposure commonly used in design codes. Furthermore, the chapter introduces the parametric fire model, which allows for a more accurate representation of fire scenarios by incorporating additional variables like ventilation, compartment geometry, and material properties.

The chapter then shifts focus to the concept of fire resistance, a key element in ensuring the structural integrity of RC elements during a fire. It delves into how concrete and steel, the primary materials used in RC structures, respond to high temperatures. The properties of concrete under fire conditions, including compressive strength and Young's modulus at elevated temperatures, are explored in depth. The reductions in these properties as a result of fire exposure are discussed in relation to the Brazilian standard ABNT NBR 15200:2024, which provides critical guidelines for assessing concrete's fire performance. Additionally, the effect of temperature on steel, particularly the yield strength and Young's modulus of passive reinforcement, is examined, with an emphasis on how these reductions influence the overall structural performance of RC beams during a fire.

Finally, the chapter introduces fire protection systems, discussing both passive and active measures to enhance the fire resistance of RC structures. Passive fire protection, such as fireproof coatings, insulation, and fire-resistant cladding, is explored for its role in delaying temperature rise within the structure, thus allowing more time for safe evacuation and reducing the likelihood of structural failure. Active fire protection systems, including sprinklers and fire suppression systems, are also addressed, with a focus on their role in controlling the fire and limiting its spread. The chapter concludes by discussing the performance of these fire protection measures in relation to fire duration, highlighting how they contribute to maintaining structural integrity over time in fire situations.

3

STATE-OF-THE-PRACTICE ON DESIGN OF RC BEAMS IN FIRE SITUATION

3.1 Introduction

In the Brazilian engineering practice, five standards make up the technical framework that involves the design of RC structures in a fire situation, they are:

- **ABNT NBR 8681:2004 -** Actions and safety of structures - Procedure: sets up the partial safety factors, depending on the type of load and structure analyzed.
- **ABNT NBR 6120:2019** – Design loads for structures: sets up the nominal values of the loads to be used in the design process of structures, depending on the materials used.
- **ABNT NBR 6118:2023** - Design of concrete structures - Procedure: sets up the basic requirements for the design of concrete structures.
- **ABNT NBR 14432:2001** - Fire resistance requirements for building construction elements - Procedure: sets up the conditions to be met by the structural and compartmental elements that integrate the buildings so that, in a fire situation, structural collapse is avoided.
- **ABNT NBR 15200:2024 -** Fire design of concrete structures: sets up the design criteria for concrete structures in a fire situation.

The flowchart of the design process is as follows:

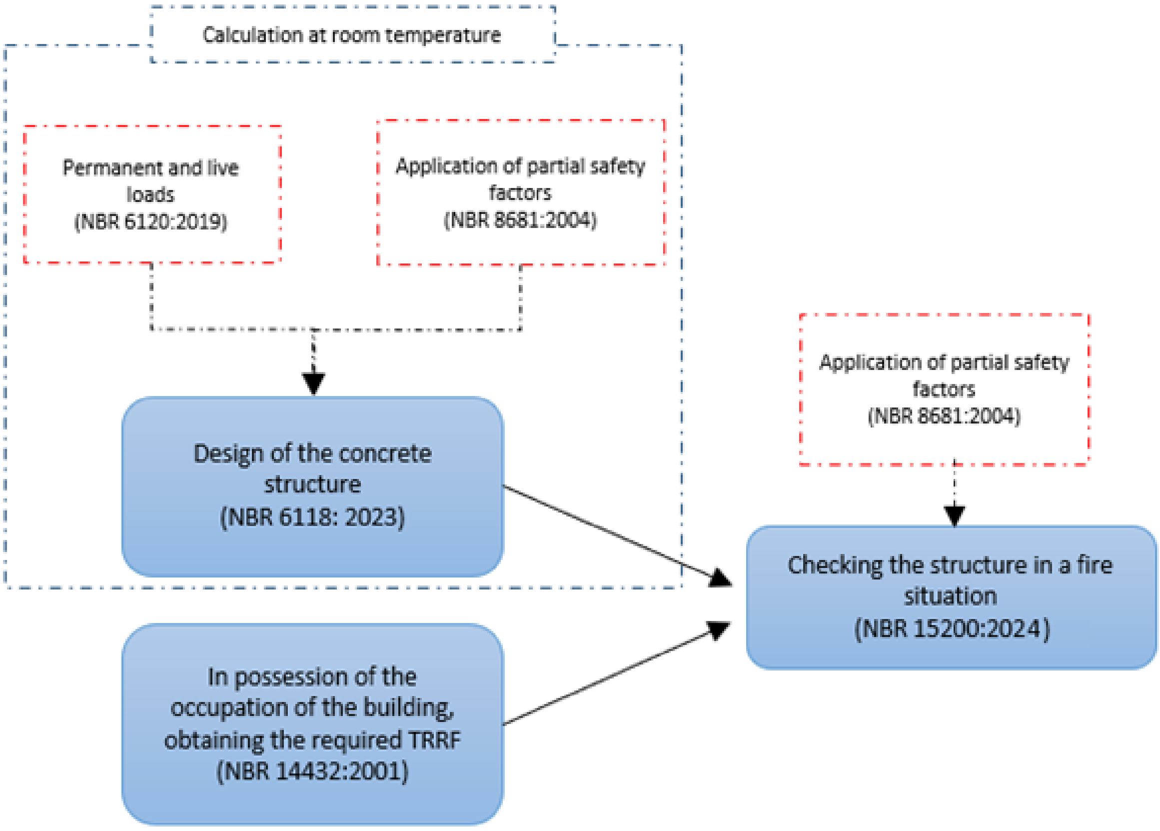

Figure 3.1: Flowchart of design of structures in fire situations.

First, the structure is designed according to ABNT NBR 6118:2023, based on the coefficients set up in ABNT NBR 6120:2019, according to the materials used. Partial safety factors are also applied, according to ABNT NBR 8681:2004, aiming to create a safety margin in relation to permanent and live loads. Then, the fire resistance rating (TRRF, in Brazil) is obtained through ABNT NBR 14432:2001, depending on the occupancy and height of the building.

With all this information, the structure is verified in a fire situation, following one of the four methods set up in ABNT NBR 15200:2024. Depending on the method used, verification requires the use of partial safety factors associated with loads, prescribed in ABNT NBR 8681:2004.

The entire structure must be checked in a fire situation. In this case, verification should only be done in the ultimate limit state (ELU), which analyzes the limit state related to the collapse of the structure or structural ruin (ABNT NBR 6118:2023). This situation differs from designing at room temperature, which involves checking not only ultimate limit states (bending, shear, etc.), but also serviceability limit states (ELS).

When designing for fire situations, all internal forces arising from deformations are neglected. This is not only because these deformations are minimal under fire conditions, but also due to the significant plastic deformations that occur during such circumstances, which are typically large and difficult to predict (ABNT NBR 15200:2023). Fire situations are considered exceptional events that can lead to substantial reductions in the strength of the materials involved. Additionally, these situations incorporate factors related to the degradation of material properties as the temperature increases (ABNT NBR 8681:2004). Therefore, as specified in ABNT NBR 15200:2023, the necessary verification process is simplified to:

$$S_{d,fi} = \gamma_g . F_{gk} + \gamma_q . \sum_2^n (\varphi_{2j} . F_{qjk}) \leq R_{d,fi} \tag{3.1}$$

where, $S_{d,fi}$ is the design load effects in a fire situation; F_{gk} is the characteristic value of the permanent action; F_{qjk} is the the characteristic value of the variable action; γ_g is the partial load factor of the permanent loads; γ_q the partial load factor of the variable loads; φ_{2j} the almost permanent combination reduction factor, and $R_{d,fi}$ the design resistance in fire situation.

When the fire action is the main one, the reduction factor (φ_{2j}) is multiplied by 0,7, according to ABNT NBR 8681:2004. As all internal forces resulting from imposed deformations are disregarded, in the fire analysis, the design loads related to live loads can be calculated assuming only 70% of the corresponding design load at room temperature (ABNT NBR 15200:2024).

ABNT NBR 15200:2024 suggests different verification processes, namely:

- Tabular method.
- General Analytical Method.
- Advanced calculation method.
- Experimental method.

A presentation of these methods is made in the following sections, together with the concept of TRRF.

3.2 Fire Resistance Rating (TRRF)

The Required Fire Resistance Time (TRRF, in Portuguese) can be defined as the minimum fire resistance time (described in minutes) that a structural element, when subjected to standard fire, must resist. In this case, "resisting" refers to integrity, impermeability and insulation, where applicable (ABNT NBR 15200:2024).

The ABNT NBR 14432:2001 - Fire resistance requirements for building construction elements - indicates the TRRF that must be respected by Brazilian buildings. These are independent of the structural material used, depending on the type of occupancy and height of the building. The standard establishes the conditions to be met by the structural and compartmentalization elements that integrate the buildings so that, in a fire situation, structural collapse is avoided. For compartmentalization elements, impermeability and insulation requirements must be met for a sufficient time to enable:

- Escape for the occupants of the building in safe conditions.
- Safety of fire-fighting operations.
- Minimization of adjacent and public infrastructure damage.

The definition of a building's TRRF is based on the fact that it is a value defined according to the probability of the fire occurring and its consequences. It is not, therefore, the duration of the fire, the response time of the fire brigade.

In view of the difficulty of calculation, this "time" is usually established by consensus in normative committees. In the Brazilian case, the TRRF is set up by standard ABNT NBR 14432:2001, as shown in Table 3.1, from some examples.

Table 3.1: Fire resistance rating (TRRF), in minutes

FIRE RESISTANCE RATING (TRRF), IN MINUTES, ACCOURDING TO ABNT NBR 14432:2001					
Occupancy	**Building Width**				
	H ≤ 6m	6m ≤ h ≤ 12m	12m ≤ h ≤ 23m	23m ≤ h ≤ 30m	H > 30m
Residence	30	30	60	90	120
Hotel	30	60	60	90	120
Commercial	60	60	60	90	120
Office	30	60	60	90	120

3.3 Tabular Method

In this method, minimum concrete cover is established for columns, beams or slabs and the TRRF. All values are tabulated.

The minimum dimensions stipulated must also be within the limits of ABNT NBR 6118:2023. According to ABNT NBR 15200:2024, to meet the requirements in a fire situation, the tabular design method is the simplest one. This method is developed according to the TRRF and is based on the principle that the temperature in a point of the concrete cross section becomes lower as the point moves away from the surface (Costa & Silva, 2003), that is, the further away the reinforcement from the outer face, the lower its temperature.

Tests suggest that the verification of structures in fire situations should consider only longitudinal reinforcement, since concrete elements, in this type of situation, usually fail by bending or axial load plus bending, and not by shear (ABNT NBR 15200:2024).

Tables 3.2 and 3.3 shows the minimum dimensions (b_{min} and b_{wmin}) of the beams and the distance from the center of the steel bar to the concrete surface (c_1) of the tensile reinforcements, as a function of the TRRF. The dimensions of interest for the different types of beam cross sections are defined in Figures 3.2 and 3.3.

Table 3.2: Minimum dimensions for simply supported beams (ABNT NBR 15200:2024)

TRRF [min]	Combination of bmin/c1 [mm/mm]				bw,min [mm]
	1	2	3	4	
30	80/25	120/20	160/15	190/15	80
60	120/40	160/35	190/30	300/25	100
90	140/60	190/45	300/40	400/35	100
120	190/68	240/60	300/55	500/50	120
180	240/80	300/70	400/65	600/60	140

Table 3.3: Minimum dimensions for continuous beams (ABNT NBR 15200:2024)

TRRF [min]	Combination of bmin/c1 [mm/mm]				bw,mín [mm]
	1	2	3	4	
30	80/15	160/12	-	-	80
60	120/25	190/12	-	-	100
90	140/37	250/25	-	-	100
120	190/45	300/35	450/35	500/30	120
180	240/60	400/50	550/50	600/40	140

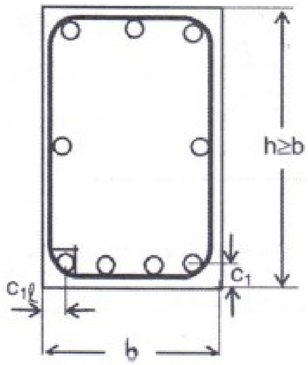

Figure 3.2: Concrete cover c_1 e c_{1l} (ABNT NBR 15200:2024)

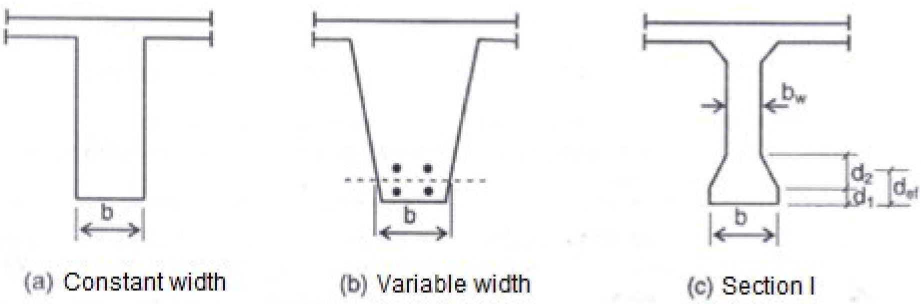

Figure 3.3: Definition of dimensions for different types of beam cross sections (ABNT NBR 15200:2024)

This method is the most usual for checking structures in a fire situation, also known as a prescriptive method. Despite being an easy method to apply, it has the great disadvantage of not evaluating the specifics of the case, resulting in overinvestment in some cases and/or situations of unsafe designs (Spinardi et al., 2017).

3.4 General Analytical Method

This method is based on the following hypotheses:

1. According to ABNT NBR 15200:2024, $S_{d,fi}$ can be adopted as 70% of design load effects in normal situation (S_d), thus ignoring any effects generated by the deformations imposed in a fire situation.

2. Based on the temperature distribution in the cross section, the resisting moment in a fire situation is calculated from computer programs or technical literature.

3. Resisting stresses can be calculated by the criteria established in ABNT NBR 6118:2023 for normal situations, adopting medium resistances for concrete and steel in a fire situation. This average value of resistance is obtained by uniformly distributing it in the concrete section, or in the total reinforcement, the total loss of resistance by heating the concrete or reinforcement, respectively (ABNT NBR 15200:2024).

3.5 Advanced Calculation Method

This method considers the following aspects:

1. Load combinations referring to a structure in a fire situation are calculated strictly according to ABNT NBR 8681:2004.

2. The effects of thermal deformations that are restricted are added, and the calculation of these stresses and the material stresses must be performed by non-linear models capable of considering the redistribution of the stresses that occur in a structure during fire.

3. The resistant forces are calculated with temperature distribution according to TRRF.

3.6 Experimental Method

This method is justified only in special cases in which the fire resistance is higher than that calculated by the methods of ABNT NBR 15200:2024, dealing with the experimental evaluation of the element under analysis and will not be treated in detail in this research.

3.7 European Standard Considerations - *Eurocode 2 - Part 1-2*

Eurocode 2 - Part 1–2 is a European standard and applies to buildings and other concrete civil structures. This standard deals with the requirements for resistance, use, durability and fire resistance in RC structures, applying to structures that perform compartmentalization and load support functions when exposed to fire (EUROCODE 1992–1–2, 2002). It presents some general principles and rules for the application of tabulated and calculated values in the structure, aiming to fulfill specific requirements in relation to the resistant function and its performance.

This brief presentation of Eurocode 2 highlights its role as the foundation for the Brazilian standard ABNT NBR 15200:2024, a key focus of this research. Eurocode 2 is more comprehensive and includes concepts not found in ABNT NBR 15200:2024, which is more concise and direct.

3.7.1 Tabulated Values - Beams

Tables 3.4 and 3.5 are applied to beams that may be exposed to a fire situation on three sides, that is, the upper side or any other side, maintaining an insulating function. For the beams exposed on the four sides, the height of the beam cannot be less than the minimum width required by Tables 3.4 and 3.5. The total cross-sectional area of the beam (A_c) should be less than twice the square of the minimum beam width ($2 \,.\, {b_{min}}^2$) (EUROCODE 1992–1–2, 2002).

Table 3.4: Minimum dimensions and distances to the axis of beams simply supported by reinforced or prestressed concrete (EUROCODE 1992–1–2, 2002)

R = TRRF [min]	Combination of bw/a				b,mín [mm]
	1	2	3	4	
30	80/25	120/20	160/15	190/15	80
60	120/40	160/35	190/30	300/25	100
90	140/60	190/45	300/40	400/35	100
120	190/68	240/60	300/55	500/50	120
180	240/80	300/70	400/65	600/60	140

Table 3.5: Minimum dimensions and distances to the axis of continuous reinforced or prestressed concrete beams (EUROCODE 1992–1–2, 2002)

R = TRRF [min]	Combination of bw/a				b,mín [mm]
	1	2	3	4	
30	80/15	160/12	-	-	80
60	120/25	190/12	-	-	100
90	140/37	250/25	-	-	100
120	190/45	300/35	450/35	500/30	120
180	240/60	400/50	550/50	600/40	140

The values presented in Tables 3.4 and 3.5 can only be applied if the beam sections are in accordance with Figure 3.4. When there are cases where the width is variable (Figure 3.4 (b)) the value of b_{min} refers to the distance from the center of gravity of the positive reinforcement. The effective height (d_{eff}) of the lower flange of "I" beams should not be less than Equation 3.4, Figure 3.4 (c) (EUROCODE 1992–1–2, 2002).

$$d_{eff} = d_1 + 0{,}5 \,.\, d_2 \geq b_{min} \tag{3.4}$$

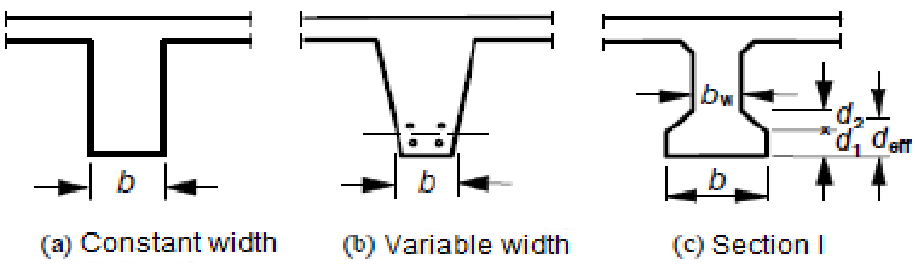

Figure 3.4: Definition of dimensions for different types of beam section (NE 1992–1–2, 2002)

This rule does not apply if it is possible to inscribe an imaginary cross section in the real section that meets the minimum fire resistance requirements (Figure 3.5). In the case of $b_{min} > 1{,}4\, b_w$ the cover for the concrete reinforcement must be increased according to Equation 3.5 (EUROCODE 1992–1–2, 2010):

$$a_{eff} = \left(1{,}85 - \frac{d_{eff}}{b_{min}} . \sqrt{\frac{b_w}{b}}\right) \geq a \tag{3.5}$$

where a is concrete cover and a_{eff} is effective concrete cover.

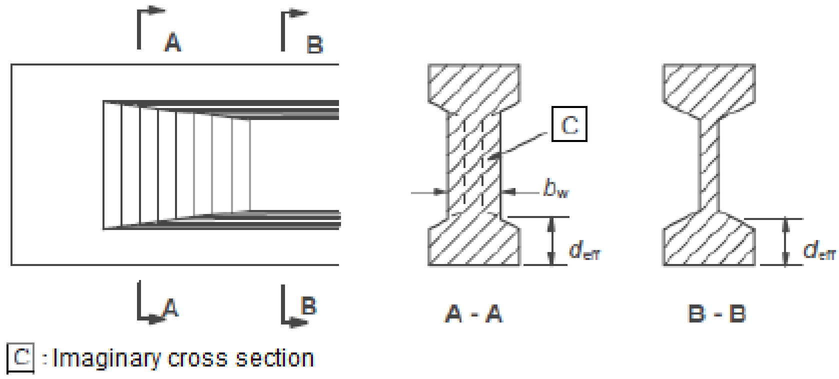

Figure 3.5: "I" beam with variable bw web width meeting the requirements of an imaginary cross section (EUROCODE 1992–1–2, 2002)

In the lower corners of the beams, there is a concentration of temperature and for this reason the cover between the faces of the beam and the axis of the lower corner reinforcements must be increased by 10 mm (EUROCODE 1992–1–2, 2002).

In the case of beams simply supported, the minimum values stipulated are in Table 3.4, as shown. For the case of continuous beams, Table 3.5 indicates minimum values of the distance from the axis of the reinforcement to the bottom face and sides of the beam, however these values are only valid if they obey the following indications: (i) respect the constructive rules applied and (ii) be such that the redistribution of calculation momentum does not exceed 15%. Otherwise, all continuous beams under analysis must be considered as simply supported beams (EUROCODE 1992–1–2, 2002).

It is important to note that Table 3.5 will only be applied to continuous beams if the rotation capacity of the supports is sufficient for the required fire situation. In the event that they still do not obey such indications for the realization of a simplified calculation method, they may be based on other methods that may be more rigorous and precise for any other case to be analyzed (EUROCODE 1992–1–2, 2002).

For standard fire resistances greater than R90 (equivalent to TRRF 90 in the Brazilian standard), the area of the upper reinforcement section in each support must obey an average distance of 0,3 l_{eff}, l_{eff} being the effective span length, measured at from the support center. Therefore, the minimum area of the upper reinforcement, in the section at a certain distance from the support axis considered, follows Equation 3.6 (EUROCODE 1992–1–2, 2002):

$$A_{S,req}(X) = A_{S,req}(0) \; . \; \left(1 - 2{,}5 \; . \frac{x}{l_{eff}}\right) \tag{3.6}$$

where $A_{S,req}(X)$ is the minimum area of the compression reinforcement in section x, not less than $A_S(X)$; $A_{S,req}(0)$ is the area of the compression reinforcement section needed in the support; x the distance of the section under consideration, with $x \leq 0{,}3.\, l_{eff}$; and l_{eff} the effective span length.

3.7.2 Calculation Methods

Eurocode 2 standardizes some calculation methods, but there are some considerations for these methods (EUROCODE 1992–1–2, 2002):

- Avoid concrete spalling or, if not avoided, its influence should be considered in the structure's performance.
- In general, an ambient temperature of 20 ºC is allowed for the thermal insulation function.

In Eurocode (2002), fire resistance can be demonstrated in three ways:

- In terms of time ($t_{fi,d} > t_{fi,req}$)
- In terms of load capacity ($R_{fi,d,t} > E_{fi,d,t}$)
- In terms of temperature ($\theta_d < \theta_{cr,d}$)

Table 3.6: Three Alternative Methods of Comparing Fire Severity with Fire Resistance (NISTIR, 2009)

Domain	Units	FIRE RESISTANCE	≥	FIRE SEVERITY
Time	minutes or hours	Time to failure (FRR)	≥	Fire duration as calculated or specified by code
Temperature	°C	Steel temperature to cause failure	≥	Maximum steel temperature reached during the fire
Strength	kN or kN.m	Load capacity (strength/stability) at elevated temperature	≥	Applied load during the fire

The most used nowadays to this type of analysis is the load capacity or the Strength based analysis, which is why it will be explored in the following sections.

3.7.2.1 Simplified Calculation Methods

In the cross sections of the beams, simplified calculation methods may be used to determine the ultimate resistant capacity of an element of RC in a fire situation. These methods are applicable to structures subject to standard fires (EUROCODE 1992–1–2, 2002).

Simplified calculation methods are performed based in:

- Temperature profiles (based on Eurocode appendix and/or previous research).
- Reduced cross-section (Isotherm 500º and Zone Method).

Normally, simplified calculations are performed by reducing the cross-section. This reduction can occur, in general, in two ways:

- **500 ºC Isotherm Method:** Concrete with temperature below 500 ºC retains full strength and the rest is disregarded.

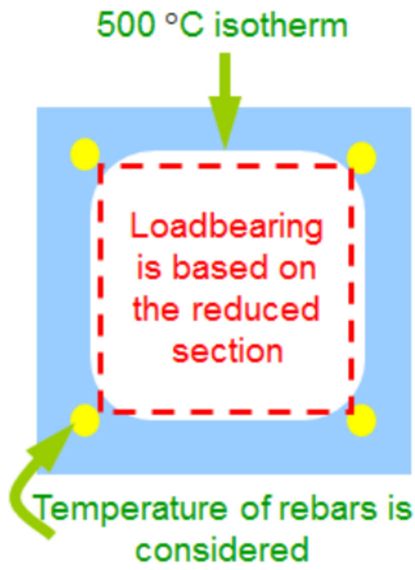

Figure 3.6: 500 ºC Isotherm Method (Robert el al., 2012)

- **Zone Method:** Cross section is divided into zones. Mean temperature and corresponding Strength of each zone is used. This method is more accurate for small cross sections than 500º C isotherm method (Robert el al., 2012).

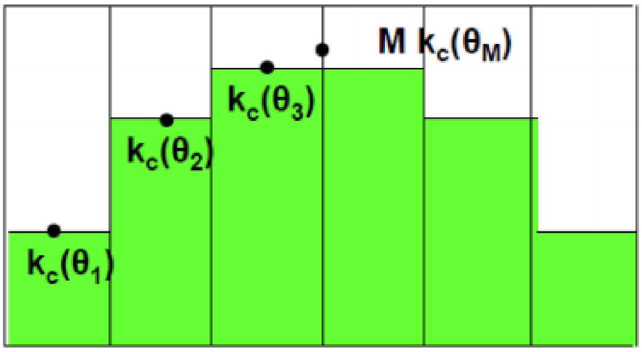

Figure 3.7: Zone Method (Robert el al., 2012)

Another method, used a little less, is the temperature profiles. Figures 3.8 and 3.9 shows temperature profiles of beams exposed to fire when the maximum gas temperature is reached, these abacuses are restricted to elements with siliceous aggregates. Figure 3.10 shows the standardization from which figures relating to temperature profiles are presented.

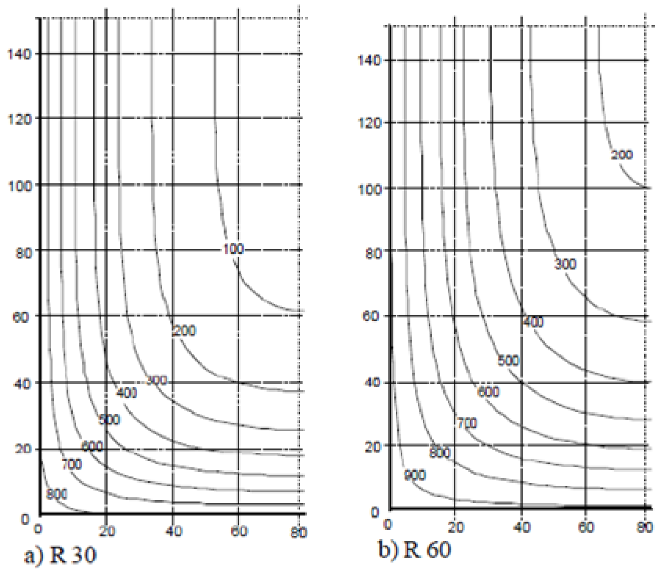

Figure 3.8: Temperature profiles (ºC) for a beam, h x b = 600 x 300 (EUROCODE 1992–1–2, 2002)

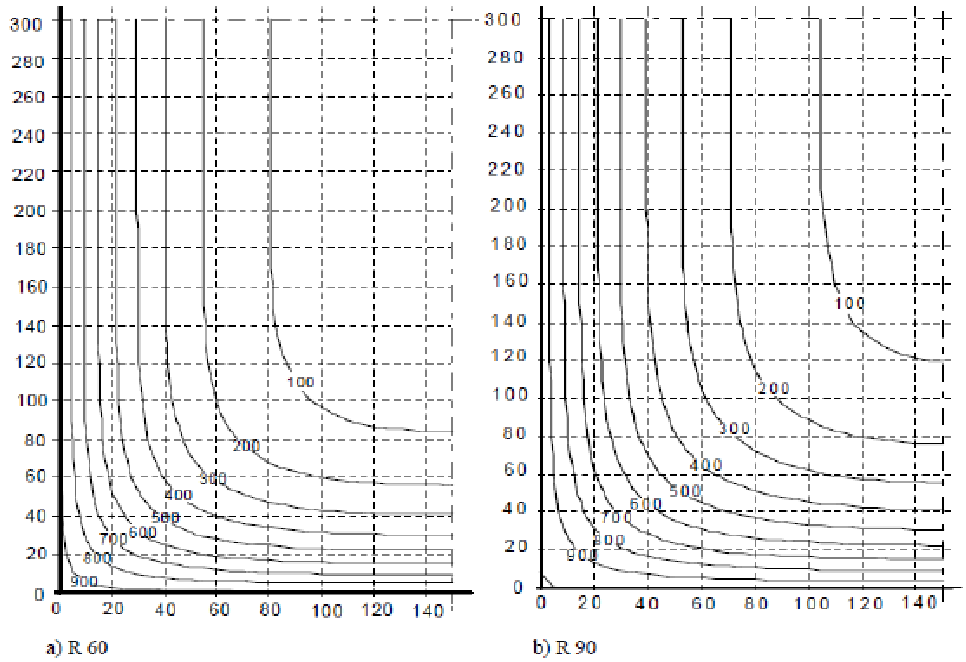

Figure 3.9: Temperature profiles (ºC) for a beam, h × b = 600 × 300 (EUROCODE 1992–1–2, 2002)

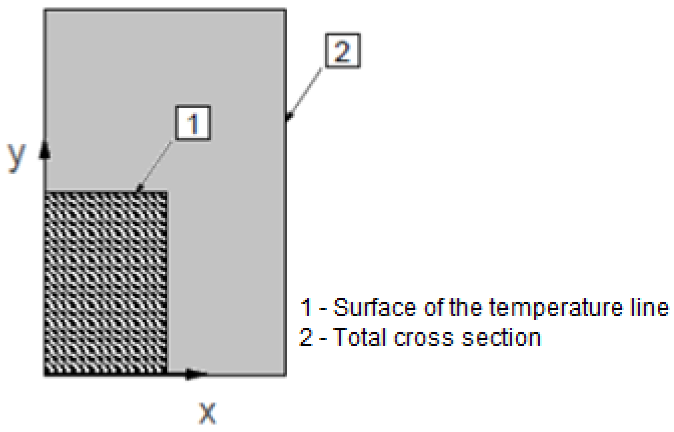

Figure 3.10: Cross-sectional surface for which the abacus with temperature lines is displayed (EUROCODE 1992–1–2, 2002)

3.7.2.2 Advanced Calculation Methods

These methods seek a realistic analysis of the structure in a fire situation, approaching a viable model of the behavior of the structure and based on the physical behavior of the materials. Advanced methods must include the temperature distribution inside the structural elements and their mechanical behavior. Therefore, two responses will be obtained for this type of calculation: (i) those of thermal actions and (ii) those of mechanical responses (EUROCODE 1992–1–2, 2010). Usually, the use of such methods is linked to the finite element methods (FEM) software (e.g. ANSYS, DIANA, SAFIR).

3.8 Ultimate Limit State in a Fire Situation

In usual cases, the design requirement in relation to the ultimate limit state of a structural element can be described by:

$$S_d \leq R_d \tag{3.7}$$

where S_d represents the design loads (or load effects) and R_d the design resistance.

Similarly, in a fire situation, the ultimate limit state can be assessed by the following equation:

$$S_{d,fi} \leq R_{d,fi} \tag{3.8}$$

where $S_{d,fi}$ represents the loads (or load effects) in a fire situation and $R_{d,fi}$ the design resistance in a fire situation.

From Equation 3.8, the flexural ultimate limit state for a RC beam, under fire situation, can be described as:

$$R_{d,fi} - S_{d,fi} \geq 0 \tag{3.9}$$

where:

$$S_{d,fi} = \gamma_g . M_g + \gamma_q . \sum_{2}^{n} (\varphi_{2j} . M_q) \qquad and \qquad R_{d,fi} = M_R \tag{3.10}$$

Substituting the information given in Equation 3.10 in 3.9, it is obtained:

$$M_R - (\gamma_g . M_g + \gamma_q . \textstyle\sum_2^n (\varphi_{2j} . M_q)) \geq 0 \tag{3.11}$$

where M_g is moment due to dead loads, M_q is the moment due to live loads and M_R is the resisting moment.

A summary of flexural ultimate limit states, for RC beams under fire, for different design codes is presented in Table 3.7.

Table 3.7: Summary of flexural ultimate limit state in a fire situation according to different codes

Code	Flexural ultimate limit state
ACI	$M_R - (M_g + M_q)$
EUROCODE 2	$M_R - (M_g + 0{,}3\, M_q)$
ABNT NBR 8681:2004	$M_R - (1{,}2\, M_g + 0{,}28\, M_q)$

3.9 Summary

This chapter provides a comprehensive overview of methodologies for designing RC beams in fire scenarios. It begins by introducing the Brazilian standards relevant to the design and assessment of RC structures (ABNT NBR 8681:2004, ABNT NBR 6120:2019, ABNT NBR 6118:2023, ABNT NBR 14432:2001, and ABNT NBR 15200:2024), detailing their respective scopes and applications within fire safety design.

The chapter then discusses various approaches for evaluating fire resistance in RC beams, covering the tabular, general analytical, advanced calculation, and experimental methods. Each method's applicability and limitations in assessing fire scenarios are addressed. In addition, the European standard Eurocode 2 - Part 1-2 is considered, with particular attention to its guidelines on temperature profiles in RC beams as a function of fire exposure time. The Eurocode's simplified calculation approaches, such as the 500 ºC Isotherm and Zones Method, are explored alongside advanced methods, offering a comparative view of European and Brazilian practices.

Finally, the concept of the Ultimate Limit State in fire situations is introduced, rounding out the chapter with a focus on the criteria for determining structural adequacy under extreme thermal conditions.

4

UNCERTAINTIES AND STRUCTURAL RELIABILITY

4.1 Introduction

The main objective of the structural fire design is to guarantee good structural performance under these adverse conditions. In general, the verification of the structure in a fire situation aims to (ABNT NBR 15200:2024):

- Limit the risk to human life.
- Limit the risk of property loss.
- Limit the risk to adjacent buildings and the society itself.

It is considered that these objectives can be achieved if it is demonstrated that the structure maintains the following functions (ABNT NBR 15200: 2012):

- **Firebreak function** - the structure does not allow the fire to pass over it or the heat to pass through it in sufficient quantity to generate combustion on the side opposite the initial fire. The structural function comprises thermal insulation and sealing against the passage of flames.
- **Load-bearing function** - the structure maintains its bearing capacity to support the structure as a whole or of each of its parts, avoiding global collapse or progressive local collapse.

The main objective of structural fire design is to ensure, with an acceptable level of probability, that the structure remains stable during a fully developed fire for enough time to allow occupants to escape and/or enable Fire Department personnel to intervene. Additionally, it must maintain property integrity and ensure the continuity of operations.

However, most of the planning and design of buildings to be structurally safe under fire conditions ends up being conducted without the benefit of complete information; consequently, the performance guarantee cannot be fully satisfied. Many decisions that are made during the planning and design process are invariably made under conditions of imprecision and uncertainty.

All quantities (except physical and mathematical constants) that go into structural engineering calculations are associated with some uncertainty. This fact is implicitly recognized in current technical standards. Therefore, under fire situation, there is invariably a probability of failure of the building structure, along with the associated consequences. The development of design standards requires the quantification of these uncertainties by appropriate means, and a study of their interaction in the structure under analysis should be conducted (Hart, 1982).

4.2 Uncertainties in Engineering Design

In general, structural reliability analysis is related to the rational treatment of the uncertainties in the structural design and to the problems associated with rational decision making. Uncertainties need to be identified and classified so that their relevance to the problem in question can be determined.

4.2.1 Basic Variables

For the purposes of quantifying uncertainties in the field of structural engineering, and for further reliability analysis, it is necessary to define a set of basic variables. They are defined as the set of variables that govern the static or dynamic response of the structure. The basic variables are the mechanical characteristics of the materials (e.g., elastic modulus), the geometric characteristics (e.g., dimensions of the cross section), the external loads (e.g., wind), etc. (Melchers, 1999).

4.2.2 Types of Uncertainties

In structural engineering, a wide range of uncertainties must be considered, including environmental conditions, human error, and the prediction of future events. Several quantitative techniques are available for systematically identifying these uncertainties. These techniques involve a thorough analysis of the problem, accounting for all potential consequences and possibilities, while focusing on those with a finite probability of occurrence. Moreover, all techniques rely on the availability of up-to-date information to support these assessments (Melchers, 1999).

To illustrate “where” and “how” different types of uncertainties can arise in man's attempt to understand and use a natural phenomenon to serve his project, the schematic diagram is presented in Figure 4.1 (Melchers, 1999).

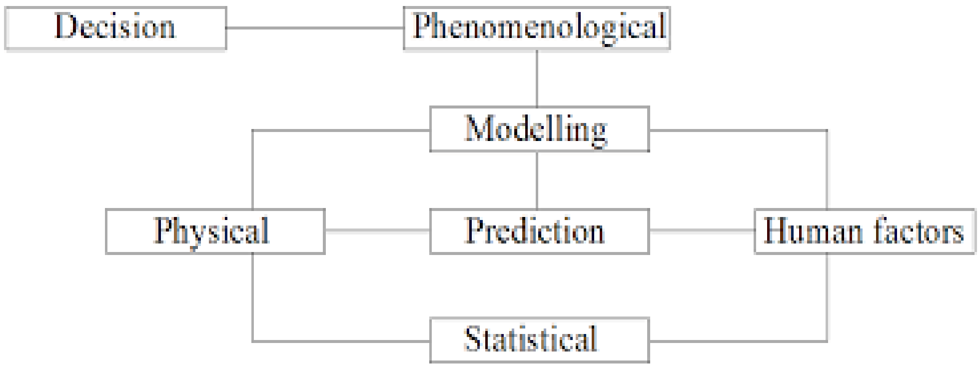

Figure 4.1: Interrelationship of uncertainties in the assessment of reliability (Melchers, 1999)

Figure 4.1 can represent the flow for conducting a fire project, for example. To do this, it is necessary that the designer tries to know and understand as much as possible about the fire phenomenon. In a scientific approach to the problem, it would be necessary to adjust a model that could approximate the effects of the phenomenon.

For the model to be more accurate, the designer must rely on his own observation of the physical aspects of the project in question and make his own prediction on any aspect that is not apparent in the observation. The accuracy of its modeling would be better in proportion to the extent that observations similar to those made by other human beings could be used - that is, if it had access to the available statistical data. The accuracy or reliability of such data depends, of course, on human factors. The various aspects are dynamically interrelated, and uncertainties definitely arise in each area. These uncertainties are explained later in the case of structural fire.

4.2.2.1 Phenomenological Uncertainties

Fire is certainly a phenomenon that has had a major impact on human life since its earliest existence on earth. The development of fire science has accelerated in the last 150 years, being a complex area that involves many disciplines, but it is primitive compared to other technological fields (Quintiere, 1998). An example of this uncertainty is in the field of fire engineering, and specifically in structural fire design, where the effect of fire on the behavior of the structural element is not yet fully understood or quantified. The effect on the entire structure is even less understood. Most of the knowledge about the structural response to fire is empirical and based on many assumptions and hypotheses.

4.2.2.2 Physical Uncertainties

Physical uncertainty is identified with the inherent random nature of a basic variable (Melchers, 1999). The structural responses of an entire structure or elements under fire conditions depend, in part, on the properties of the material at elevated temperatures. These properties are not known exactly, and this gives rise to physical uncertainty.

Specific examples include:

- The physical dimension of a structural element at elevated temperature (cross section).
- The temperature of fire.
- The variation of Young's modulus with temperature.
- The variability in the actual permanent load during fire situation.

Physical uncertainty can be reduced, but not eliminated, with greater availability of statistical data, or greater effort in quality control (Ang & Tang, 1975). It is a "fundamental" property of the variable in question. Physical uncertainty must be estimated from observations of the variable or be subjectively assessed.

4.2.2.3 Statistical Uncertainties

In most cases of engineering projects, values related to the properties of the materials used in the calculation are inferred from statistical analysis of sample observations. The data can be collected in order to build a probabilistic model of the physical variability of a property. This will imply, first, in the selection of an appropriate probability distribution type and then in the determination of numerical values for the distribution parameters (Ang & Tang, 1975).

In practice, however, very large sample sizes are needed to establish reliable estimates of the numerical values of the parameters (for example, mean and standard deviation). Therefore, for a given data set, the distribution parameters can be considered as random variables, whose uncertainty depends on the sample size or any previous knowledge (Ang & Tang, 1975). This uncertainty is called statistical uncertainty, and, unlike physical uncertainty, it arises only as a result of the lack of information.

4.2.2.4 Uncertainties in Modeling

The design and analysis of structural fires uses, at some point, mathematical models that relate the desired output variables (for example, the resisting moment) with the values of a set of input variables, or basic variables (for example, compressive strength of concrete and yield Strength of steel). These models are deterministic in shape.

In addition, such models can be based on an understanding of the mechanical problem (for example, heat transfer models) or they can be highly empirical (for example, parametric time-temperature relationship). However, with rare exceptions, it is rarely possible to make highly accurate predictions about the structural response of both, the elements and the entire structure, under fire conditions (Thoft-Christensen & Baker, 1982). In other words, the response of the structural elements to fire and load, under fire conditions, contains an uncertainty component in addition to the uncertainties of the variables relevant to the problem.

This additional source of uncertainty is called modeling uncertainty and occurs as a result of simplifications, assumptions, unknown boundary conditions and also as a result of the unknown effects of other variables and their interactions, which are not included in the model. In many elements and structures, the model's uncertainties have a great effect on structural reliability and should not be neglected (Thoft-Christensen & Baker, 1982).

4.2.2.5 Uncertainties in Forecasting

The fire project involves predicting the future state of the structure under analysis, for example, the prediction of fire occurrence and the resulting structural response. The strength of a forecast depends on the state of available knowledge. As new knowledge related to the structural response under fire conditions becomes available, the forecast and the project become more refined, with a concomitant reduction of uncertainties. In other words, the accuracy of any prediction made depends not only on the properties of the structure, but also on the designer's knowledge of it, as well as the forces and influences that are likely to act on it in a fire condition.

4.2.2.6 Uncertainties in the Decision

In the structural fire design, or, for that matter, any project or enterprise, a series of decisions have to be made and, precisely for this reason, there are uncertainties in decision making. Examples of these uncertainties are related to decisions, for example, whether the limit state has been exceeded and / or whether the recovery or demolition of a compromised structure is worthwhile. After a fire has occurred, the engineer has to decide, based on the certainty of his own engineering judgment or experience, whether the structure damaged by the fire is repairable, whether it still serves or has violated the ultimate limit state. Another example is the choice of the failure criteria for structural elements exposed to fire - if the failure analysis should be done in the domains of temperature, load or time.

4.2.2.7 Uncertainties in Human Factors

It can be said that the biggest source of uncertainty in the design, construction, operation or use and maintenance of any engineering system comes from the "human factor". The uncertainty resulting from human involvement in the engineering system usually manifests itself when the system fails, and human error is determined to be the main cause. For example, human error causes 20 to 90% of all major system failures or accidents, as illustrated in Table 4.1 (Stewart & Melchers 1997).

Table 4.1: Proportion of systems failure due to human factors (Stewart & Melchers, 1997)

System	% error / accidents
Aircraft	60-70%
Air Traffic Control	90%
Buildings and Bridges	75%
Dams	75%
Missiles	20-53%
Offshore platforms	80%
Nuclear	80%

4.3 Structural Reliability

According to ISO 2394 (International Organization for Standardization, 2015) reliability is the ability of a structure or structural member to fulfil the specified requirements, during the working life, for which it has been designed. In that document it is noted that reliability is often expressed in terms of probability, and this concept covers safety, serviceability, and durability of a structure.

Structural reliability problems can be framed as a supply-versus-demand issue. In structural safety contexts, supply and demand are represented by the structure's resistance, R, and the load effects, S, respectively. This framework emphasizes ensuring that the structure's capacity (resistance) is adequate to withstand the effects of applied loads throughout its service life. The probability that resistance exceeds load effects, $P\ (R > S)$, indicates the structure's survival probability. Conversely, the complementary probability, $P\ (R < S)$, represents the probability of failure.

Given the probability distributions of R (resistance) and S (load effects), considered as statistically independent, continuous random variables, and assuming a single failure mode, the probability of failure P_f is given by (Ang and Tang, 1990):

$$P_f = P\,(R - S < 0) = P\,(M < 0) \tag{4.1}$$

If the probability density functions of R and S are available, that is $f_R\ (r)$ and $f_S\ (s)$ are known, and if R and S are continuous and statistically independent random variables, the probability of failure P_f can then be expressed by Equation 4.2.

$$P_f = \mathrm{P}\ (R - S < 0) = \int_0^{\infty} \int_0^{s} \mathrm{f}_R(\mathrm{r})\, \mathrm{f}_S(\mathrm{s})\ dr\ ds \tag{4.2}$$

This equation is illustrated in Figure 4.2, which shows the probability density function (PDF) of R and S.

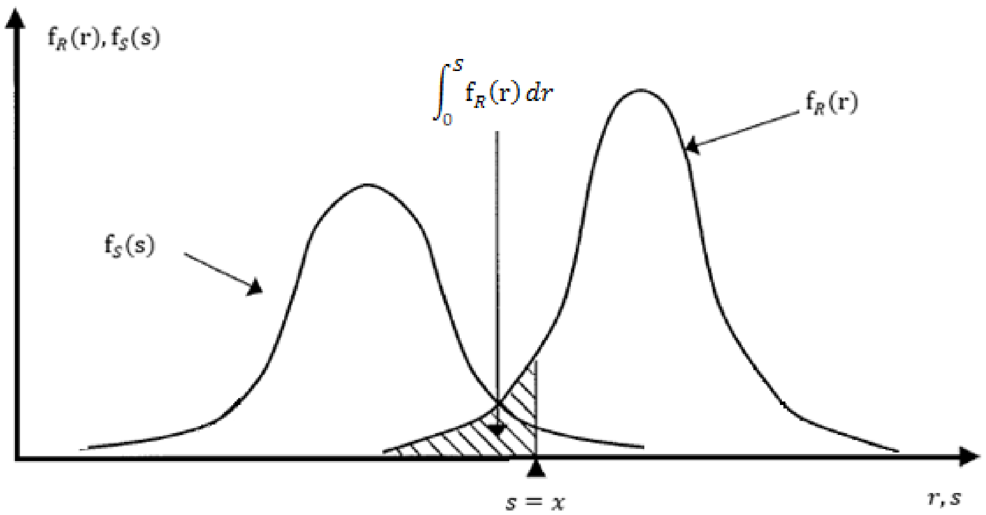

Figure 4.2: Basic reliability problem represented by R *and* S *PDFs.*

In statistical theory, for a random variable X, the cumulative distribution function (CDF) $F_x\ (x)$ is given by Equation 4.3, provided that $x \geq y$ (Ang & Tang, 1975).

$$F_X(x) = P(X \leq x) = \int_0^x f_X(y)\, dy \tag{4.3}$$

Equation 4.2 can then be written in the form:

$$P_f = P(R - S < 0) = \int_0^\infty F_R(s)\, f_S(s)\, ds \tag{4.4}$$

The integral of Equation 4.4 is known as the convolution with respect to the load effects, *S*.

To determine the reliability of this "capacity x demand" problem, it is necessary to evaluate the "convolution integral" shown in Equation 4.4 to obtain the probability of failure. The probability of no failure, or of safe performance, is a direct measure of reliability. However, in reality, the problem is generally not as simple as described earlier.

First of all, the closed integration of Equation 4.2, or 4.4, is only possible for some special cases, for example, when both (*R* and *S*) are random variables with normal distributions. In general, it is necessary to resort to numerical integration. Second, the simplified formulation of Equation 4.4 is not enough for many real-life problems. Several random variables will influence "capacity" or "supply" (Ang & Tang, 1990).

It follows that, in general, the strength or capacity of a structural component is a function of several random variables. If the vector $\boldsymbol{X}$ represents the basic variables of the problem, then the limit state equation $G(R, S) = R - S = 0$ can be generalized as $G(X) = 0$. Consequently, Equation 4.2 can be generalized as (Ang & Tang, 1990):

$$P_f = P(G(\mathbf{X}) \leq 0) = \int \ldots \int_{G(\mathbf{X}) \leq 0} f_x(\mathbf{x})\, dx \tag{4.5}$$

In this Equation 4.5, $f_x(\boldsymbol{x})$ is the joint probability density function for the vector of *n* basic variables.

Equation 4.5 adds considerably to the complexity of calculating the probability of failure. However, techniques have been developed to deal with these problems. Two broad classes of the most used techniques are the "First Order Reliability Method" (FORM), "Second Order Reliability Method" (SORM), and Monte Carlo Simulation (MCS).

4.3.1 Safety Margin

For a linear limit state function, such as the safety margin *M*, defined by $M = R - S$, the probability of failure can be determined using Equation 4.5. Since both *R* and *S* are random variables, the safety margin M will also be a random variable, with a probability density function represented by $f_M(m)$. If $f_M(m)$ is known, the probability of failure P_f can be obtained as:

$$P_F = \int_{-\infty}^{0} f_M(m)dm = F_M(0) \tag{4.6}$$

When resistance R and load effects S are statistically independent normal variables, the safety margin M will also follow a normal distribution. In this case, the mean of the safety margin, μ_M, is calculated using Equation 4.7, and the standard deviation of the safety margin, σ_M, is determined by Equation 4.8. The probability of failure, P_f, is then given by Equation 4.9 (Ang and Tang, 1990):

$$\mu_M = \mu_R - \mu_s \tag{4.7}$$

$$\sigma_M = \sqrt{\sigma_R^2 + \sigma_S^2} \tag{4.8}$$

$$P_F = F_M(0) = \Phi\left(\frac{-\mu_M}{\sigma_M}\right) = 1 - \Phi\left(\frac{\mu_M}{\sigma_M}\right) \tag{4.9}$$

where μ_R and μ_S are the mean of the resistance and load effects, respectively; σ_R and σ_S are the standard deviations of resistance and load effects, respectively; and Φ is the cumulative distribution function of the standard normal variable.

As seen in Equation 4.9, the probability of failure is a function of the ratio between the mean and standard deviation of the safety margin. The reliability index, β, is defined as the ratio μ_M / σ_M (see Equation 4.10). As can be seen from Figure 4.3, the reliability index is the distance between the mean of the safety margin and the limit condition ($M = 0$) in terms of the number of standard deviations. Graphically, the probability of failure is represented by the area under the PDF, $f_M(m)$, for values of M less than zero.

$$\beta = \frac{\mu_R - \mu_S}{\sqrt{\sigma_R^2 + \sigma_S^2}} = \frac{\mu_M}{\sigma_M} \tag{4.10}$$

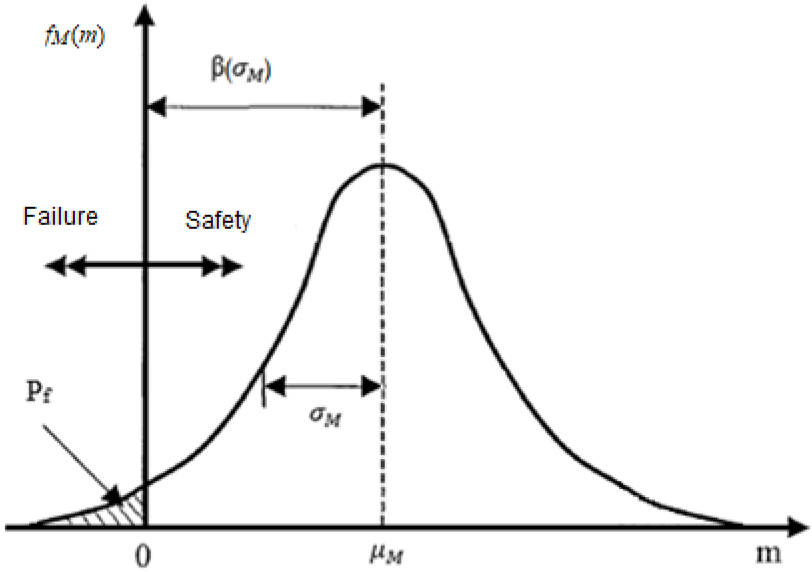

Figure 4.3: PDF of the safety margin M

4.3.2 First Order Second Moment (FOSM)

The calculation of P_f requires knowledge of $f_R(r)$ and $f_S(s)$, or the joint distribution $f_{R,S}(r, s)$ (for statistically dependent variables). In practice, R and S are functions of multiple random variables, and the required information is not readily available. Furthermore, if the available information on the uncertainties associated with the basic variables is limited to their mean and standard deviation (and covariance, in the case of statistical dependence), the "First Order Second Moment" (FOSM) method can be used to calculate the reliability index (Ang and Tang, 1990).

In the FOSM method, the terminology "second moment" refers to the description of all random variables only in terms of their mean (the "first moment"), their variance (the "second moment") and covariance.

In this context, the problem can be formulated in terms of the basic design variables Xi. For each set of values for these variables, it is necessary to define whether the structure has failed or not. To define the "state" of the structure, a performance function $g(X)$ is used, where $X = (X_1, X_2, ..., X_n)$ is the vector of basic variables. The limit performance can be defined as $g(X) = 0$, which represents the "limit state" of the structure. Therefore, $g(X) > 0$ is the safe state, and $g(X) < 0$ is the failure state. Geometrically, the limit state function, $g(X) = 0$, is an n-dimensional surface (or hypersurface) called the failure surface.

Given the statistics of the basic variables and the corresponding performance function, the reliability index, β, can be calculated. The FOSM uses the statistics of the random variables only up to the second moment, i.e., the mean and variance. This method is based on the linearization of the performance function at the "design point" (or the "most probable failure point").

Considering a problem defined by n statistically independent variables, Xi, the reduced variables $X'i$ are represented by Equation 4.8, and the limit state function $g(X') = 0$ is given by Equation 4.12.

$$X'_i = \frac{X_i - \mu_{x_i}}{\sigma_{x_i}} \text{ ; where } i = 1,2,3, \ldots, n \tag{4.11}$$

$$g\left(\sigma_{X_1} X'_1 + \mu_{X_1}, \ldots, \sigma_{X_n} X'_n + \mu_{X_n}\right) = 0 \tag{4.12}$$

Figure 4.4 shows the safety region and the failure region in the reduced variable space for n = 2. As the failure surface moves away from the origin in the reduced variable space, the region where $g(X) > 0$, which represents the safety region, increases. Conversely, when the failure surface moves closer to the origin, the safety region decreases.

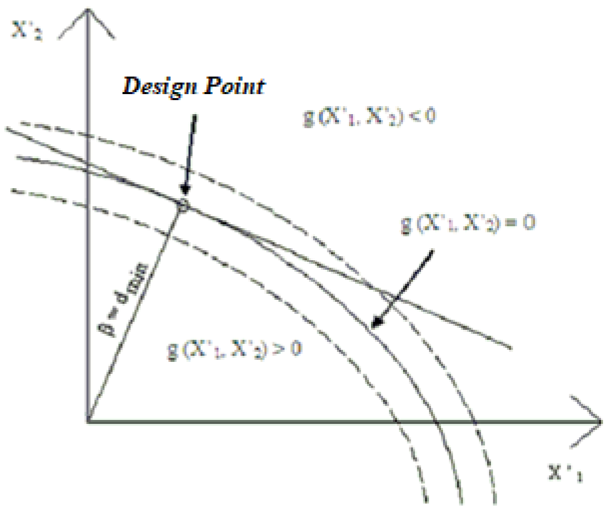

Figure 4.4: Safety and failure states in the reduced variable space

The point on the failure surface with the smallest distance to the origin in the reduced variable space is the design point, $\boldsymbol{x}^{*\prime} = x_1^{*\prime}, x_2^{*\prime} \ldots x_n^{*\prime}$. This smallest distance, d_{min}, is taken as the reliability index, β, and can be determined through an optimization procedure that minimizes the distance D subject to the constraint $g(X) = 0$ (i.e., the design point lies on the failure surface).

Using the method of Lagrange multipliers, it can be shown that, for uncorrelated variables, the reliability index is given by Equations 4.13 and 4.14, in matrix and scalar notation, respectively (Ang and Tang, 1990):

$$\beta = \frac{-\boldsymbol{G}^{*T}\boldsymbol{X}'^{*}}{(\boldsymbol{G}^{*T}\boldsymbol{G}^{*})^{1/2}} \tag{4.13}$$

$$\beta = \frac{-\sum x_i'^{*}\left(\frac{\partial g}{\partial X'_i}\right)_*}{\sqrt{\sum\left(\frac{\partial g}{\partial X'_i}\right)_*^2}} \tag{4.14}$$

where $G*$ is the gradient vector at the design point, given by Equation 4.15:

$$\boldsymbol{G} = \left(\frac{\partial g}{X_1'^{*}}, \frac{\partial g}{X_2'^{*}}, \ldots.., \frac{\partial g}{X_n'^{*}}\right) \tag{4.15}$$

Since the design point is not known a priori, an iterative procedure can be used to calculate the reliability index. It can be shown that the calculation of the reliability index through Equations 4.13 and 4.14 is equivalent to the linearization of the performance function (i.e., first-order expansion in a Taylor series) at the design point (Ang and Tang, 1990).

In the more general case, the determination of the design point and the calculation of the corresponding reliability index require the use of iterative procedures (Ang and Tang, 1990; Melchers, 1999). The metric obtained through FOSM is the reliability index, β.

4.3.3 First Order Reliability Methods (FORM)

In reliability analysis, the FOSM is used to calculate the reliability index based on limited information on the basic variables, specifically their means and standard deviations. If the probability distributions of all basic variables are known, the failure probability can be determined. FOSM is consistent with uncorrelated normal variables. However, if the variables are correlated or non-normal, a more complex process is needed to obtain the reliability index β and the corresponding probability of failure (Ang and Tang, 1990; Melchers, 1999). Once β is determined, the failure probability can be found as $P_f \approx \Phi(-\beta)$. In literature, this latter approach is known as "First Order Reliability Method" (FORM).

FORM involves linearization of the performance function by approximating the failure surface with a tangent hyperplane at the design point. This process changes the boundary between the "safe state" and the "failure state." The reliability estimate obtained through this approximation can be either conservative or non-conservative, depending on whether the actual failure surface is concave or convex relative to the origin of the reduced variables (Ang and Tang, 1990). To refine the reliability estimate, second-order terms from the Taylor series expansion of the performance function can be included, leading to the Second Order Reliability Method (SORM).

4.3.4 Monte Carlo Simulation

In Structural Reliability, MCS is a tool used to predict the performance of a structure by utilizing a specific set of values for the random variables generated according to their respective probability distributions. The process involves running repeated simulations, where each simulation provides a performance measure based on the defined performance function.

For the implementation of MCS, two key components are required: the deterministic relationship to describe the structure's response, typically represented by the performance function, and the probability distributions for all the variables involved in the structure's response (Diniz 2008). Haldar and Mahadevan (2000) detail MCS through the following steps: (a) define the problem considering all relevant random variables; (b) quantify the probabilistic characteristics of these variables, including their probability density functions for continuous variables or probability mass functions for discrete variables, along with their statistical parameters; (c) generate numerical values for these variables through simulations; (d) deterministically evaluate the problem for each set of realizations of the random variables; (e) extract probabilistic information from the conducted simulations; and (f) determine the precision and efficiency of the simulation.

One of the main tasks in MCS is generating random numbers from prescribed probability distributions; for a given set of generated random numbers, the simulation process is deterministic. In theory, simulation methods can be applied to large and complex systems, where the rigid idealizations and/or simplifications required for analytical models can often be relaxed, resulting in more realistic simulation models. In practice, however, MCS may be limited by economic constraints and computational capacity (Ang and Tang 1990).

The use of MCS in structural performance assessment can be conducted in two ways (Diniz 2008):

- Calculate the statistics (mean, standard deviation, and distribution type) of the system's response. In this case, a sample of the structure's response is first obtained, then a probability distribution is fitted to the sample data, and the distribution parameters are estimated;

- Calculate the probability of unsatisfactory performance of the structure. In this case, a performance function is established, and a sample of possible results is simulated. The number of unsatisfactory performances is counted, and the failure probability is obtained by the rate of unsatisfactory performances.

Considering N as the total number of simulations (sample size) and N_f as the number of cases where $g(X) < 0$, the failure probability can be estimated using Equation 4.16:

$$P_f = \frac{N_f}{N} \tag{4.16}$$

A sample from MCS is similar to a sample of experimental observations. Therefore, the results from MCS can be treated statistically; such results can also be presented in the form of histograms, with applicable estimation and statistical inference methods. For these reasons, MCS is also a sampling technique and, as such, shares the same issues as sampling theory; that is, the results are also subject to sampling errors. Generally, finite sample solutions are not "exact" (unless the sample size is infinite) (Ang and Tang, 1990).

MCS is frequently used in calculating failure probabilities associated with different failure modes of structures. Therefore, estimating the error associated with the failure probability obtained from a finite sample of n elements is of interest. Equally important, and particularly due to the computational cost involved in MCS, it is crucial to determine the number of simulations required (sample size) to achieve an acceptable level of precision.

Shooman (1968) proposed Equation 4.17 to estimate the percentage error, where P_f is the estimated failure probability and n is the sample size.

$$\%\text{erro} = 200\sqrt{\frac{1-P_f}{nP_f}} \tag{4.17}$$

This equation can be applied as follows: for example, if in 10.000 simulations a failure probability equal to 0,01 was obtained using Equation 4.14, then, the estimated percentage error according to Equation 4.17 is 20%, that is, the probability of failure is in the range 0,01 ± 0,002. If a narrower range is desired, for example, $0{,}01 \pm 0{,}001$, the reverse operation must be performed, resulting in n equal to 39.600 simulations.

4.3.5 Life-Cycle Cost Analysis

The pursuit of a sustainable built environment has shifted the focus from solely considering initial construction costs to evaluating expenses throughout the entire lifespan of a structure. Life-cycle cost analysis (LCCA) involves estimating a range of costs, including those related to construction, inspection, maintenance, and potential failures, among others. This approach also addresses challenges related to system reliability, time-dependent reliability (such as modeling deterioration and stochastic loads), structural health monitoring (inspection, maintenance, and repair), assessment of the condition of existing or retrofitted structures, and optimization. In this context, the main objective may be "Minimization of Life-Cycle Costs" or "Maximization of Net Benefits." Since costs and benefits occur at different times, they must be discounted to their present values (Diniz, 2008).

In these methods, the problem is approached rigorously and comprehensively. However, several issues need to be addressed: (i) deciding on the appropriate discount rate for the analysis; (ii) determining the type and frequency of inspections—whether at constant or variable intervals; (iii) defining the type of repairs required; (iv) addressing costs related to the potential loss of human life; and (v) estimating the probabilities of failure for all possible failure modes. Although these methods introduce greater complexity, they have been successfully applied in real-world cases, such as developing maintenance strategies for bridges. Furthermore, optimized designs are expected to significantly reduce the operational costs associated with infrastructure (Thoft-Christensen & Baker, 1982; Frangopol & Estes, 1997).

The life-cycle cost analysis has turned out to be a very important and essential tool for Performance-Based Design (PBD). It is related to the analysis of costs over the life-cycle of the structure, seeking to facilitate and improve the decision-making process of the designer and enabling the calibration of codes.

According to Rackwitz (2000) and Vrouwenvelder (2002), life-cycle costs allows to evaluate optimum reliability levels, which can then function as a generalized target for reliability-based design applications.

In terms of a fire situation analysis, life-cycle costs (Y) can consider the (i) total building construction and maintenance cost (C), (ii) obsolescence cost (A), (iii) fire-induced material damages (D_M), (iv) fire-induced loss to human life and limb (D_L), and (v) reconstruction cost after fire-induced failure (D_R). The life-cycle cost function can then be described as follows (Van Coile and Hopkin, 2018):

$$Y(\theta) = C(\theta) + A(\theta) + D_M(\theta) + D_L(\theta) + D_R(\theta) \tag{4.18}$$

where θ is the design vector.

It must be pointed out that the variables D_M, D_L and D_R are dependent on the probability of failure of the structural element. The evaluation of all these parameters, together, could help in optimizing a design, assuming the structure will be rebuilt in case of failure, for example, or assisting in decision making on the need of protecting some structural elements against fire or not, etc.

4.3.6 Levels of Reliability Methods

Building on the methods discussed in previous sections - such as FORM, FOSM, MCS, and Life-Cycle Cost Analysis - this section introduces the levels of reliability methods, which categorize these approaches based on their complexity and the information required. These levels, as established by Madsen et al. (1986), Diniz (2006), and Lind et al. (1992), allow for a structured choice of the reliability format depending on the precision needed and data available, from simpler, less data-intensive approaches to advanced, probabilistic methods that incorporate comprehensive data.

- **Level 0 - Allowable Stress Method:** in this method, a comparison is made between the stress resulting from the maximum expected load, calculated in the linear elastic regime, with an allowable stress. All loads are treated similarly; the allowable stress is determined by dividing the limit stress by a safety factor.

- **Level 1 - Limit State Methods:** the uncertainties associated with the design variables are considered through partial safety factors. A characteristic value is used for each uncertain value. These methods are known as semi-probabilistic design, or load and resistance factors design (LRFD), since partial safety factors are calibrated using higher level methods and used in the design process. Current design recommendations for RC structures (e.g. ABNT NBR 6118, EUROCODE 2, ACI 318) follow limit state methods.
- **Level 2 - Reliability Index Methods:** methods that employ two values for each "uncertain" parameter (usually mean and variance) and a measure of the correlation between parameters (usually covariance) in the computation of the reliability index. The reliability index β is used as a measure of reliability in this level. FOSM, as described in section 4.4.1, is used in the calculation of the reliability index.
- **Level 3 - Probability of Failure Methods:** in these methods, the probability distributions of the basic variables involved are specified and the probability of failure is used as a measure of reliability. FORM, SORM and MCS are used in the calculation of the probability of failure.
- **Level 4 – Minimization of Costs Involved over the Life-cycle:** These methods combine reliability with structural optimization. All costs incurred over the service life of the structure (initial, inspection, maintenance, repairs, failure and demolition) must be calculated and referred to the present time. The objective then is to minimize the total cost, having as a constraint condition the level of reliability defined as acceptable.
- **Level 5 - Life-Quality Index (LQI):** This method introduces a more comprehensive approach by incorporating factors that influence the overall well-being of users and the environment over the service life of the structure. This approach not only accounts for failure probabilities but also integrates considerations such as user safety, economic and environmental impacts, and sustainability.

In summary, the levels of reliability methods outlined—from Level 0 (Allowable Stress Method) to Level 5 (Life-Quality Index)—provide a progressive framework for structural reliability analysis, balancing simplicity with analytical rigor. Each level serves distinct purposes: Levels 0 and 1 apply conservative, deterministic approaches suitable for preliminary assessments, while Levels 2 and 3 introduce probabilistic measures, refining safety evaluations through reliability indices and probabilities of failure. Level 4 takes a life-cycle perspective, incorporating cost considerations over the structure's lifespan, which is essential for sustainable, economically efficient design. Finally, Level 5 extends the scope of reliability beyond structural performance and costs, integrating societal and life-quality factors. Together, these levels support an adaptable methodology, allowing engineers to select the most appropriate level of analysis based on project-specific goals, data availability, and the desired balance between precision and practicality.

4.3.7 Calibration of Technical Standards

The role of technical standards in the design of structures and infrastructures is to establish the requirements that engineers must follow to ensure the level of safety demanded by society at any given time. These standards are developed by technical committees, which are responsible for calibrating and specifying how the variables used in engineering designs should be treated, ensuring that they meet the necessary safety standards.

Calibration of a standard, as explained by Ditlevsen and Madsen (1996), is a process conducted by a competent authority, typically the technical committee. This process involves determining equations, minimum and maximum values, safety coefficients for various variables such as nominal values, partial safety factors, among others. These values are chosen based on a design formulation that is specified and calibrated by a higher-level method, including structural reliability studies.

In the context of partial safety factors, also known as LRFD (Load and Resistance Factor Design), the variables involved include characteristic values of the quantities of interest. These values represent the expected levels of these quantities based on statistical data.

Furthermore, weighting coefficients plays an essential role in LRFD. They are used to increase the loads and decrease the resistances. In this way, the weighting coefficients adjust the characteristic values to include a safety margin, ensuring that the structure can support the applied loads throughout its life span. These weighting coefficients are determined through a detailed analysis that considers material variability, uncertainties related to loading, among other factors, attempting to reflect a balance between safety and cost-effectiveness.

Calibration of these standards can be conducted at different levels of superior reliability methods, each with an increasing degree of detail. A level 1 method, for instance, uses simplifications that allow for more direct and practical application with the use of partial safety factors. These methods are generally simpler and more accessible for daily use by engineers. However, the validity and accuracy of a level 1 method must be justified based on higher-level methods. This calibration process is essential to ensure that the requirements of technical standards are founded on reliability principles.

A level 2 method, on the other hand, involves a more detailed and complex analysis, considering variability and uncertainties more explicitly. The primary task of the level 2 method is to justify that the level 1 method achieves a reliability index, known as the target reliability index, β_{target}. This reliability index is a statistical measure that indicates the relative safety of a structure or structural component in relation to the probability of failure.

The biggest challenge that calibration of technical standards in structural engineering faces, particularly regarding existing structures, is numerically defining the target reliability index, β_{target}. This metric serves as a reference to ensure that designed structures meet an acceptable safety level. The idea is to calibrate design methods based on the reliability indices observed in previous practices, as well as considering new industry studies.

The association of the reliability index with each failure mode is the only practical alternative (Nowak and Collins, 2013). The failure mode refers to the way a system or structural element loses its initial design characteristics or, ultimately, its ability to carry loads, analyzed under ultimate limit states and serviceability limit states. In this way, the incorporation of probabilistic concepts in design, via the limit state method, is applied to the reliability of components (a single failure mode) of structural components, such as beams, slabs, and columns, and not to the reliability of systems (Diniz, 2006).

This means that when designing structures, the reliability of each structural component is considered in isolation, rather than the interaction between all the components of the structure. Each structural component has its own function, importance for the structural integrity, and different failure modes having varying consequences. For example, the failure of a column, which supports vertical loads, may have more severe consequences than the failure of a beam. Therefore, different failure modes (brittle or ductile) and the importance of the component to the structural integrity determine the choice of different target reliability index (β_a) values. A brittle failure mode, which occurs suddenly and without warning, may be more critical than a ductile failure mode, which shows signs of deformation before failure. Therefore, components with brittle failure or those essential to the stability of the structure should have a higher β_a.

As seen, the calibration of standards is a complex process aimed at ensuring that designed structures meet safety, performance, and usability requirements. According to Lind and Davenport (1972), this process goes through five stages: (i) defining the scope, (ii) defining the objectives of the standard, (iii) establishing demand frequency (loading conditions), (iv) selecting the metric space of the standard, and (v) selecting the format of the standard.

The first step in the calibration process is defining the scope of the standard. This stage involves determining which types of structures or components will be covered by the standard, as well as the context in which they will be applied. For example, a standard for concrete structures may include different types of concrete, construction methods, and environmental conditions. In the second stage, the specific objectives of the standard are defined. These objectives usually include ensuring safety, durability, and functionality of the structures, which must be quantifiable and measurable.

The third step involves establishing the loading conditions that the structure must withstand. This includes identifying the types and magnitudes of the loads the structure will face during its lifetime, such as permanent loads (self-weight), variable loads (use loads), and occasional loads (winds, earthquakes, etc.). Statistical and historical load studies are often used in this phase to determine appropriate load distributions. The fourth step is selecting the metric space of the standard, which should be consistent with international practices and facilitate comparison and application of the standards in different contexts. This includes deciding how material properties, applied forces, and geometric dimensions will be measured and represented.

Finally, the fifth step is selecting the format of the standard. This refers to the structure and organization of the standard, including how design rules, safety coefficients, and other requirements will be presented. There are different possible formats, such as the partial safety factors format (or the limit state method). The choice of format should consider ease of use by engineers, clarity of instructions, and the ability to ensure the safety and functionality of the structures.

4.3.8 Target Reliability Index

The reliability index (β) is a central concept in structural reliability. This index plays a crucial role in the calibration of partial safety factors to ensure a desired level of safety for a given structure, as presented before. Melchers (1987) explains that the index incorporates uncertainties from various factors such as load effects, material properties, and environmental conditions, thus offering a probabilistic framework for evaluating safety beyond traditional deterministic methods. This approach allows engineers to establish an acceptable safety margin based on quantified risks, supporting more effective design and maintenance decisions that balance safety and cost efficiency.

In calibrating these safety factors, an initial statistical characterization of the random variables involved is essential, as outlined by Sagrilo (2003), along with setting a target safety level that reflects the structural class and materials used. Once these parameters are established, reliability analysis methods like FORM or MCS can assess whether the proposed safety factors meet the required level to meet the required reliability target.

The calibration of the partial safety factors can be defined based on an optimization problem. The main objective is to minimize the error between the points on the response surface in terms of reliability and the target reliability index (β_a). A minimization problem is then established (Faber and Sorensen, 2002).

This target reliability index can be determined for a specific class of structures, components, or limit states, and its value typically evolves over time. As the structure ages, the reliability index tends to decrease, reflecting the increasing uncertainty associated with the material properties and environmental factors. Therefore, the target reliability index should not necessarily remain constant throughout the structure's lifetime; rather, it can be adjusted based on the anticipated changes in the structure's performance over time (fib MC 2010, 2011). The optimal value of the target safety level, in turn, is influenced by a balance between the expected costs of failure and the expenses associated with improving safety through updates, especially in the context of existing structures. This process can be framed within a life-cycle cost analysis.

According to fib MC 2010 (CEB-FIP, 2011), the choice of the target reliability level must consider the possible consequences of failure in terms of risk to life or injury, potential economic losses and the degree of inconvenience in society. The choice of the target reliability level also considers the costs and efforts required to reduce the risk of failure. Due to the great differences in the result of such considerations, attention must be given to differentiating the level of reliability of the structures yet to be built (new structures that are still in the design phase) and those that already exist.

Normally, in the genuine process of calibrating technical design standards, the correct choice of the reliability index should consider the reference period, the consequences of failure and the cost of the safety measure for each specific case. The differentiation of the level of reliability based on the different consequences of failure and the cost of the safety measure should be based on well-founded analysis (CEB-FIP, 2011).

To achieve this, information on the reliability of structural elements is essential. However, target safety levels for RC beams in fire situations are not well-established in the literature, highlighting the need for further research in this area.

4.4 Summary

This chapter provides a comprehensive overview of the various uncertainties encountered in fire engineering design, including phenomenological, physical, statistical, modeling, forecasting, decision-making, and human factor uncertainties. Each type was described in terms of its origin and potential impact on a given structure or structural element. Key concepts in structural reliability were then introduced, covering failure, failure probability, and acceptable failure probability, as well as the importance of the safety margin and the target reliability index. Following this foundation, the chapter briefly presented methods for reliability analysis, beginning with a description of First Order Second Moment (FOSM) and First Order Reliability Methods (FORM). The MCS, identified as the most suitable method for the reliability analysis of RC structures under fire conditions, was detailed. Finally, the chapter introduced the concept of life-cycle cost analysis in reliability-based design, providing a basis for integrating long-term cost considerations. This discussion culminated in an examination of the hierarchical Levels of Reliability Methods, which guide the selection of analysis approaches based on the desired balance between simplicity and precision. Finally, the calibration of technical standards and target reliability indices are discussed.

5

State-of-the-art on Reliability of RC Beams Exposed to Fire

5.1 Introduction

A state-of-the-art review of the reliability evaluation of RC beams exposed to fire is presented in this section. Papers were identified through a search on the Web of Science, google scholar, and detailed searches within the journals Journal of Structural Fire Engineering, Fire Technology, and Fire Safety Journal, supplemented with references known by the authors. References listed in identified papers were investigated, as well as references to the identified papers. Only a very limited number of papers related to the topic were identified. Some papers, specific to beams, which at first sight appear relevant to the proposal were not included in this review, as their content was found to be beyond the scope of this research. These papers deal with, for example, the use of carbon fiber reinforced polymer (CFRP) sheets in beams, and the estimation of residual load-carrying capacity and reliability after fire (Li and Tang, 2005; Tang, 2006; Bai et al., 2007; Bai et al., 2009; Cai and Feng, 2019). The same goes for prestressed concrete beams (Eamon and Jensen, 2012).

A timeline of studies about the topic is shown in Figure 5.1, highlighting the main advances over time. In this literature review, three distinct lines of research were verified, which do not refer to each other. This suggests that these research lines have so far been developed independently and that there is an opportunity to synthesize them.

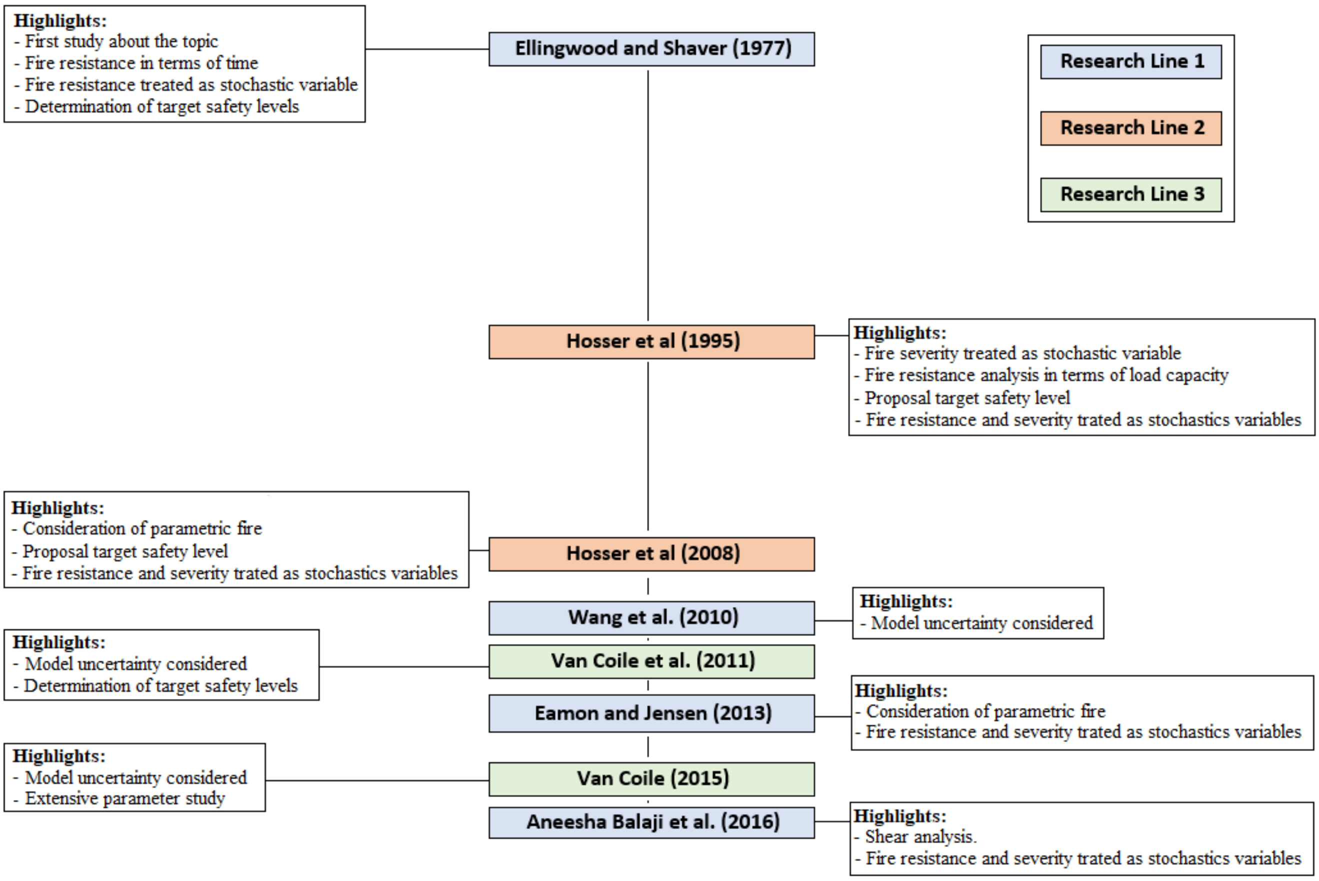

Figure 5.1- Timeline of the papers.

5.2 Ellingwood and Shaver (1977)

The first identified study on the reliability of RC beams exposed to fire was developed by Ellingwood and Shaver in 1977. In this study, methods for analytically predicting the behavior of RC beams subjected to fire are presented. The parameters that are important for predicting beam behavior are identified through a sensitivity study, considering the reliability of a T-beam. The loads were assumed deterministic, and the resistance was given by a Weibull distribution. The application of reliability analysis techniques for developing fire-resistant design procedures is also examined in that paper.

5.3 Hosser et al. (1995)

This study presents an application in order to evaluate the reliability of RC beams under standard fire exposure, using FORM as the probabilistic approach, considering the Eurocode equations. Target reliabilities are proposed, based on normal design reliability targets (considering the natural fire safety concept, whereby the target reliability for normal design is divided by the fire frequency, i.e., without considering the specific costs and benefits of fire protection). The study concludes that the uncertainty in the reinforcement temperature is dominant for the reliability evaluation.

5.4 Hosser et al. (2008)

Based on the study developed in 1995, this research also presents an application in order to evaluate the reliability of RC beams under both standard and natural fires. In this more recent paper, the authors use MCS in combination with an in-house non-linear code for structural fire analysis. Again, target reliability is proposed, based on the same premises as the previous study (e.g. a simple frequency scaling of the normal design target reliability). The study highlights that uncertainty in the fire characteristics dominates the overall reliability.

5.5 Wang et al. (2010)

In this study, a simple time-variant analytical model of the resistance of RC beams under fire has been studied. The reliability index of different specifications of concrete beams at different times has been analyzed, considering standard fire exposure.

The influence of key parameters on the evolution of the reliability index with time has been presented, and the results have shown that increasing the reinforcement ratio and concrete cover thickness is an effective measure to improve the fire resistance of RC beams. Wang et al. (2010) considered random dead and live loads but treated the beam resistance as deterministic.

5.6 Van Coile et al. (2011)

Van Coile et al. (2011) present a simple computational tool, which provides insight into the time and temperature dependent reliability of concrete beams during fire. The uncertainty of basic variables is considered through MCS, resulting in a quantification of the uncertainty regarding the bending moment capacity during fire and the corresponding evolution of the safety level.

The results of these probabilistic simulations are compared with the design values specified in the Eurocodes, providing insight into the reliability level achieved by the current design documents. A specific finding was that the fire resistance of a beam can be increased by altering the beam configuration (e.g. increasing the nominal concrete cover), or by decreasing the uncertainty on the concrete cover, for example through improved quality control (Van Coile et al., 2011).

5.7 Eamon and Jensen (2013)

In Eamon and Jensen (2013), a procedure for conducting a reliability analysis of RC beams subjected to a fire is presented. This involved identifying relevant load combinations, specifying critical load and resistance random variables, and establishing a high-temperature performance model for beam capacity. Based on the procedure, an initial reliability analysis is conducted using currently available data based on a previous study by Jensen (2010). Significant load random variables are taken as dead load, sustained live load, and fire temperature. Resistance was taken in terms of moment capacity, with random variables taken as steel yield strength, concrete compressive strength, positioning of reinforcement, beam width, and thermal diffusivity (Eamon and Jensen, 2013).

A semi-empirical model is used to estimate the beam moment capacity as a function of fire exposure time, considering standard and parametric fire exposures. This model is calibrated to experimental data available in the literature. The effect of various beam parameters was considered, including concrete cover, beam width, aggregate type, concrete compressive strength, dead-to-live load ratio, reinforcement ratio, support conditions, mean fire temperature, and other parameters. Using the suggested procedure, the reliability was evaluated from zero to four hours of fire exposure using MCS. It was found that reliability decreased nonlinearly as a function of time, while the most significant parameters were concrete cover, span/depth ratio when axial restraints are present, mean fire temperature and support conditions (Eamon and Jensen, 2013).

5.8 Van Coile (2015)

This doctoral dissertation contains an extensive parameter study on the reliability of concrete beams, considering standard ISO 834 heating. Improved probabilistic models are used relative to Van Coile et al. (2011), and the underlying cross-sectional capacity evaluation is done through an improved nonlinear fiber model which uses the constitutive laws of EN 1992-1-2:2004 as a basis. Again, the mean value and standard deviation of the concrete cover are found to have a very large impact on the reliability, while the effect of the cross-section variation is rather small. Also, the effect of considering uncertainty on the strength reduction factors is found to be small, but the applied model was based on a limited amount of tests. Recent investigations by Qureshi et al. (2020) have shown that the actual variability at elevated temperatures is much higher than adopted in (Van Coile, 2015).

5.9 Aneesha Balaji et al. (2016)

Aneesha Balaji et al. study a methodology for computing the probability of structural failure of RC beams subjected to fire. The significant load variables considered are dead load, sustained live load and fire temperature. Resistance is expressed in terms of moment capacity and shear capacity with random variables taken as yield strength of steel, concrete class (or grade of concrete), beam width and depth. The flexural capacity is determined based on the design equations recommended in Indian standards and the simplified method named "500ºC isotherm method", detailed in Eurocode for simplified fire design for standard fire exposure. The shear capacity is evaluated in a simplified way through analytic equations of the Indian code IS 456:2000. A transient thermal analysis is conducted using finite element software ANSYS.

Reliability is evaluated from the initial state to 4 hours of fire exposure based on the first order reliability method (FORM). A procedure is coded in MATLAB for finding the reliability index and the procedure is validated with available literature. The effect of various parameters such as effective cover, yield strength of steel, grade of concrete, distribution of reinforcement bars and aggregate type on reliability indices are studied. Effective cover of concrete and yield strength of steel are found to have a significant effect on reliability of beams (Aneesha Balaji et al., 2016).

5.10 References Analysis

Analyzing the mentioned references, significant differences are found with respect to: (i) the failure mode considered, (ii) fire specification, and (iii) reliability calculation (i.e. the consideration of stochastic variables). This is explored in the following and summarized in Table 5.1.

A probabilistic evaluation of RC beams in fire situation demands basically (i) a deterministic model of the phenomenon and (ii) statistics of stochastic variables and their distributions. A brief overview on both aspects is presented in the following for the identified references, presenting the variables that were considered as deterministic or probabilistic in each study.

For the establishment of the deterministic analysis model, three points are fundamental: (i) how the fire resistance will be considered (in terms of time, temperature or strength), (ii) if the limit states of bending and/or shear were analyzed and (iii) how the heat transfer inside the concrete was developed (e.g. Finite Element (FE) software). This aspect is explored in Table 5.2A and Table 5.2B

For the establishment of the probabilistic model, two points are crucial: (i) which and how many variables were treated as probabilistic or deterministic and (ii) if the used statistics (mean, variance) are up to date with the current state-of-the-art.

Table 5.1: Summary of how failure mode, fire and reliability are managed in references.

	FAILURE MODE		**FIRE**		**RELIABILITY**		
	Bending Analysis	Shear Analysis	Standard Fire	Parametric Fire	Fire Resistance*	Fire Severity*	Target Safety Levels
Ellingwood and Shaver (1977)	X		X		P	D	X
Hosser et al. (1995)	X		X		P	P	X
Hosser et al. (2008)	X		X	X	P	P	X
Wang et al. (2010)	X		X		D	P	
Van Coile et al. (2011)	X		X		P	D	X
Eamon and Jensen (2013)	X		X	X	P	P	
Van Coile (2015)	X		X		P	D	
Aneesha Balaji et al. (2016)	X	X	X		P	P	
* P – Probabilistic / D – Deterministic							

Table 5.2A: Type of fire resistance analysis, heat transfer mechanism, and mechanical response of the RC beam.

	Ellingwood and Shaver (1977)	**Hosser et al. (1995)**	**Hosser et al. (2008)**	**Wang et al. (2010)**
Fire resistance analysis	In terms of time ($t_{fi,d}$>$t_{fi,req}$)	In terms of load capacity ($R_{fi,t}$>$E_{fi,t}$)	In terms of load capacity ($R_{fi,t}$>$E_{fi,t}$)	In terms of load capacity ($R_{fi,t}$>$E_{fi,t}$)
Heat transfer	Experimental tests	Average concrete temperatures (background could not be verified as part of the current review)	Temperature distribution in the cross-section was calculated by the program FIRES-T. Natural fire in accordance with a model proposed in Zehfuss & Hosser (2007).	Temperature distribution in the cross-section was defined according to temperature profiles studied by the authors in another research.
Mechanical response	Experimental tests	Calculations based in Eurocode equations	Calculated by an in-house non-linear code.	The cross-section of the beam has been divided into an elastic zone and a plastic zone based on the section temperature studied by the authors in another research.

Table 5.2B: Type of fire resistance analysis, heat transfer mechanism, and mechanical response of the RC beam.

	Van Coile et al. (2011)	**Eamon and Jensen (2013)**	**Van Coile (2015)**	**Aneesha Balaji et al. (2016)**
Fire resistance analysis	In terms of load capacity ($R_{fi,t}>E_{fi,t}$)	In terms of load capacity ($R_{fi,t}>E_{fi,t}$)	In terms of load capacity ($R_{fi,t}>E_{fi,t}$)	In terms of load capacity ($R_{fi,t}>E_{fi,t}$)
Heat transfer	Temperature distribution in the cross-section was calculated by the finite element software DIANA.	For standard fire exposure, Wickstrom (1985) equations determine the reduced cross-section. For parametric exposures, the temperature distribution in the cross-section was calculated by the finite element program SAFIR.	Temperature distribution evaluated through an in-house finite difference code.	Temperature distribution in the cross-section was calculated by the finite element program ANSYS.
Mechanical response	Calculated by an in-house fiber model.	500 °C isotherm method to determine the reduced cross-section.	Calculated by an in-house fiber model.	500 °C isotherm method to determine the reduced cross-section.

5.10.1 Failure Mode

When considering system reliability, it is important to recognize that failure of a single component may or may not mean failure of the larger structure. Systems can be classified as series or parallel systems. Series systems are characterized by the fact that the failure of one element leads to the immediate failure of the entire system, while, in the parallel system, the system has redundancy, and all parallel elements must fail before the system fails. However, most structures do not fit the idealized classification as series or parallel, as they are a combination of series and parallel subsystems. Therefore, it is necessary to identify the elements that are critical for system stability. This issue has not been explored in the listed references and the failure probabilities thus refer to single mode failure probabilities.

For the case of a RC beams, failure modes related to ultimate limit states are classified into two major types: (i) flexural failure and (ii) shear failure. Among the works identified herein, the shear limit state is evaluated in only one of them, with the others being limited to the analysis of the bending limit state.

5.10.2 Fire Severity

Fire severity is usually defined in terms of a standard fire exposure time period. In this aspect, internationally known curves have emerged that aim to enable this standardization. An example is the ISO 834 fire (ISO 834:2019), as mentioned in Chapter 2, which does not depend on the dimensions, purpose of the compartment or the thermal characteristics of the materials (Costa & Rita, 2004). It is worth mentioning that any extrapolation of conclusions about a standard fire to a real fire must be carefully analyzed, as the behavior of the standard curve is not faithful to the curve of a real fire (Costa & Silva, 2003).

To solve this issue, parametrized fires have been proposed. The great advantage of these curves, as mentioned before, is that they allow considering the compartment geometry, fire load density and ventilation characteristics, while at the same time maintaining the simplicity of a straightforward analytical formula (Van Coile, 2015).

That way, in terms of fire severity, the analysis may be performed using the (i) standard fire (ISO-834) and (ii) parametric fires curves. It is clear that the standard fire curve does not adequately represent the fire in a room, as it does not consider extremely consequential factors, such as ventilation and the fire load present in it (Harmathy, 1970; Law, 1973). However, despite these limitations, the use of standard fire curves is the form of analysis most found in the analyzed references. Parametric fire exposure is considered in only two of the studies (Hosser et al., 2008 and Eamon and Jensen, 2013). Both studies demonstrate the great impact of this consideration on the reliability of RC beams exposed to fire.

5.10.3 Fire Resistance

The properties of the materials vary according to the temperature of the gases to which they are submitted by the action of fire and, therefore, it is essential to know the temperatures in these structural elements. The thermal action on concrete and steel is translated by the reduction of mechanical properties, which, under high temperatures, experience a decrease in strength and Young’s modulus.

In the literature, especially the Eurocode (2002), adequate fire resistance can be demonstrated in three ways: (i) In terms of time ($t_{fi,d}>t_{fi,req}$), (ii) in terms of load capacity ($R_{fi,d,t}>E_{fi,d,t}$) and (iii) in terms of temperature ($\theta_d< \theta_{cr,d}$). Only the first work on the theme, developed by Ellingwood and Shaver (1977), performs its analysis in terms of time, the other studies focus on the evaluation of the load capacity.

5.10.4 Structural Assessment

Regarding the structural assessment, the following methods to account for the strength loss due to fire were identified in the papers: (i) 500º C Isotherm Method: Concrete with temperature below 500 ºC retains full strength and the rest is disregarded, and (ii) Finite Element Methods (FEM).

In the cross sections of the beams, simplified calculation methods may be used to determine the ultimate resistant capacity of an RC element in a fire situation. These methods are applicable to structures subject to standard fires (Eurocode 1992–1–2, 2002). Simplified calculation methods are performed reducing the cross-section, based on: (i) temperature profiles (based on Eurocode appendix and/or previous research) and (ii) reduced cross-section (Isotherm 500º and Zone Method). Some authors state that the zone method is more accurate for small cross sections than 500º C isotherm method (Robert el al., 2012) and that it could be promising for natural fires (Hertz, 1985), but this method was not used in any of the selected papers referenced in this study.

However, despite the possibility of applying simplified methods, in the identified papers, mainly FEM was used for the structural assessment. More specifically the software DIANA, SAFIR and ANSYS have been used for this purpose, as well as in-house codes. Eamon and Jensen (2013) mention that the 500º isotherm method shows results with little deviation from the FEM when the standard fire is applied.

5.10.5 Model Uncertainty

The formulation of the structural design based on reliability implies the recognition that the physical variables considered in engineering problems are subject to variability.

The importance of studying model uncertainty in structural engineering can be summarized as follows (Szerszen and Nowak, 2003):

1. **Reliability Assessment:** In structural engineering, it is essential to ensure that a structure can withstand its intended loads and maintain its stability over its design life. To achieve this, engineers use mathematical models to simulate structural behavior. However, these models are based on assumptions that may not fully represent the true behavior of the structure. Therefore, analyzing model uncertainty is crucial for assessing the accuracy and reliability of structural predictions, ensuring that engineering designs account for potential deviations from real-world behavior.
2. **Risk Assessment:** Model uncertainty can contribute significantly to the risk associated with a structure. For instance, if the model underestimates the loads that a structure will be subjected to, it may lead to the design of a structure that is under-designed and more susceptible to failure. Conversely, if the model overestimates the loads, it may lead to a structure that is over-designed, resulting in higher construction costs. Therefore, studying model uncertainty can help in assessing and mitigating the risks associated with structural engineering projects.
3. **Optimization of Designs:** Structural engineers are often tasked with optimizing the design of a structure to achieve specific performance criteria. However, the accuracy of the optimization depends on the accuracy of the model used. Therefore, studying model uncertainty can help in optimizing the design of a structure by identifying the key parameters and assumptions that have the most significant impact on the performance of the structure.
4. **Code Development:** The codes and standards used in structural engineering are based on mathematical models that are intended to provide a safe and reliable design. However, these models are subject to uncertainties that can significantly affect the performance of the structure. Therefore, studying model uncertainty can help in the development of more accurate and reliable codes and standards.

In conclusion, studying model uncertainty is crucial in structural engineering as it helps in evaluating the reliability of the analysis, assessing and mitigating risks, optimizing the design of structures, and developing more accurate and reliable codes and standards. Structural engineers must therefore pay close attention to the modeling assumptions and simplifications made in their analysis and consider the uncertainties associated with them.

According to Guedes Soares (1997), because the same structural problem can be evaluated according to different engineering theories, an additional source of uncertainty must be incorporated into the reliability formulation. Therefore, the model error concerns the uncertainty in the representation of the physical behavior of a structure (Melchers & Beck, 2018).

In the case of the references under analysis, only Wang et al. (2010), Van Coile et al. (2011) and Van Coile (2015) mention the inclusion in their calculations of a parameter related to the uncertainty in the model. In Wang et al. (2010), a factor to compute the uncertainties is applied in the used resistance model, however, the value is not mentioned. In Van Coile et al. (2011) a lognormal factor with mean of 1,2 and standard deviation of 0,15 is used to compute the uncertainties in the model, based on the Joint Committee on Structural Safety (JCSS) probabilistic model code, used for room temperature conditions. Considering that the performance in fire is expected to be less conservative than for normal design situations (i.e. because of the loss of reserve strength beyond the reinforcement yield plateau), a less optimistic model uncertainty was adopted in Van Coile (2015). For the resistance effect a lognormal distribution with a mean of 1,1 and coefficient of variation of 0,1 was used. The model uncertainty for the load effect was taken in accordance with the JCSS (see Jovanović et al., 2020 for an overview of the total load model).

5.11 Discussion

5.11.1 Failure Mode

Aneesha Balaji et al. (2016) point out the importance of reinforcement yield strength for the shear limit state and highlight the importance of considering the possibility of shear failure.

In this research it is observed that the reliability with respect to shear is less than that of flexure in the initial stages of fire (from time 0 to 2,5 hours of fire exposure) and after that the condition reverses. This implies that at the initial stages of fire, for the beam considered in that study, the limit state of shear is more critical and after about 2,5-hour limit state of flexure becomes more relevant.

Nevertheless, the shear capacity model used by Aneesha Balaji et al. is a simplified one, being an adaptation of an Indian standard model for usual design conditions. Some authors state that little information is available about this failure mode in fire (e.g. Eamon and Jensen, 2013). Shear capacity evaluation of concrete beams during fire is a topic of ongoing research (Gernay et al., 2021).

5.11.2 Fire Severity and Resistance

To interpret the reliability analysis, it is important to evaluate how fire resistance and severity are treated, whether they are treated in a deterministic or in a probabilistic way. On one hand, it is clear that over the years studies tend to consider both parameters (fire resistance and severity) in a probabilistic way, bringing a more realistic assessment. About this, only the research developed by Hosser et al. (1995 and 2008), Eamon and Jensen (2013) and Aneesha Balaji et al. (2016) treated both of them in a probabilistic way. It is important to mention that the study conducted by Aneesha Balaji et al. is closely related to the one conducted by Eamon and Jensen, with regard to the methodologies and statistical values of the variables involved.

5.11.3 Stochastic Variables and Uncertainties in the Models

With respect to the probabilistic description of the stochastic variables, a great variability in the types of (i) distribution, (ii) mean values and (iii) correlation coefficients are noticeable. A summary of the random variables considered in the references is summarized in Table 5.4 and 5.5. An example is the values related to the COV of concrete strength used by Aneesha Balaji et al. (2016) and Van Coile et al. (2011), with 41% of difference. This highlights that the probabilistic models for RC concrete beams exposed to fire are not fully consolidated in the literature and require further investigation.

Likewise, uncertainties in the model are not treated in all studies, as mentioned before. As clearly seen from the previous sections, ultimate conditions for RC beams, i.e. ultimate stress and ultimate strain, cannot be predicted with certainty. The uncertainties associated with such predictions, or model errors, may be much more significant than those associated with inherent variabilities (Ang & Tang, 1990). In this sense, it is noticed the inexistence in the literature of a database of experiments in RC beams on fire that could subsidize the calculation of the uncertainties in the models used by different authors. This fact justifies the absence of the use of this factor in the papers, or the use of the same ones used at room temperature.

Also, the uncertainty in the thermal properties is not fully considered. Material strengths at elevated temperatures exhibit a large variability and there are no consolidated probabilistic models in the literature to quantify it. Recently, studies related to probabilistic models for temperature-dependent strength of steel and concrete are available (Qureshi et al., 2020) and can serve as a reference for future studies.

For the case of loads (dead and live) in fire situation, some recent studies point out a consolidated probabilistic load model, where the recommended distribution, mean and COV are listed in Table 5.3 (Jovanović et al., 2020). Based on historical data, the study of Jovanović et al. indicates that relative differences of the probability of failure in the order of 10% can be observed in function of the load models used (Jovanović et al., 2020), proposing the parameters presented in Table 5.3 for dead and live loads in case of fire.

Table 5.3: Probabilistic characteristics of live and dead load (Jovanović et al., 2020)

Load	Distribution	Mean	COV
Dead Loads	Normal	Equal to the nominal permanent load	0,10 (for a first assessment, if not evaluated on a project basis).
Live Loads	Gamma	0,2 times the nominal live load	0,60 for large load areas (> 200 m^2) and 0,95 for smaller load areas (<100 m^2).

Regarding the determination of target safety levels, only three of the authors address this issue for RC beams (Hosser et al (1995 and 2008); Ellingwood and Shaver (1977); Van Coile et al. (2011)) and a life-cycle costs analysis dedicated to RC beams was not found within the available literature on this topic.

Table 5.4: Summary of the parameters of the random variables considered

		Ellingwood and Shaver (1977)			Hosser et al. (1995)			Hosser et al. (2008)			Wang et al. (2010)			Van Coile et al. (2011)		
Variable		**Used Distrib.**	**Mean (μ)**	**COV.**	**Used Distrib.**	**Mean (μ)**	**COV.**	**Used Distrib.**	**Mean (μ)**	**COV.**	**Used Distrib.**	**Mean (μ)**	**COV.**	**Used Distrib.**	**Mean (μ)**	**COV.**
Concrete Parameters	h (mm)	Deterministic			Deterministic			Deterministic			Deterministic			Normal	h	5
	b (mm)				Deterministic			Deterministic						Normal	b	5
	f_c (MPa)				Log Normal	$1{,}29.f_c$	0,15	Log Normal	$1{,}26.f_c$	0,13				Log Normal	$1{,}135.f_c$ *	0,06
	E_c (GPa)	Variable not considered in the analysis			Variable not considered in the analysis			Variable not considered in the analysis			Variable not considered in the analysis			Log Normal	E_c	0,15
	d (mm)	Normal	d	0,08	Log Normal	d	0,15	Deterministic			Deterministic			Beta $[0;3d_{nominal}]$	d	0,07
	Thermal diffusivity (α) m^2/s	Variable not considered in the analysis			Variable not considered in the analysis			Variable not considered in the analysis			Variable not considered in the analysis			Variable not considered in the analysis		
	Reduction Factor of concrete strength	N/a			N/a			N/a			N/a			Beta $[3d_{nominal}; 3d_{nominal}]$	**	0 at 20°C 0,045 at 700°C
Steel Parameters	f_y (MPa)	Log Normal	f_y	0,09	Log Normal	$1{,}09.f_y$	0,05	Normal	$1{,}12.f_y$	0,055	Deterministic			Normal	$1{,}145.f_y$	0,05
	A_s (mm²)	Deterministic			Deterministic			Deterministic						Normal	$1{,}02.A_s$	0,02
	Reduction Factor of Steel strength	N/a			N/a			N/a			N/a			Beta $[3d_{nominal}; 3d_{nominal}]$	**	0 at 20°C 0,065 at 600°C

* $\mu = \frac{f_{ck}}{(1-2.COV)}$

** Mean taken from the EUROCODE nominal curve

		Eamon and Jensen (2013)			Van Coile et al. (2015)			Aneesha Balaji et al. (2016)		
Variable		Used Distrib.	Mean (μ)	COV.	Used Distrib.	Mean (μ)	COV.	Used Distrib.	Mean (μ)	COV.
Concrete Parameters	h (mm)	Deterministic			Deterministic			Deterministic		
	b (mm)	Normal	1,01. b	0,04	Deterministic			Normal	1,01. b	0,04
	f_c (MPa)	Normal	1,10 – 1,23.f_c	0,145	Log Normal	1,43.f_c	0,15	Normal	1,10 – 1,23.f_c	0,145
	E_c (GPa)	Variable not considered in the analysis			Variable not considered in the analysis			Variable not considered in the analysis		
	d (mm)	Normal	0,99.d	0,04	Beta [0;3$d_{nominal}$]	d	0,02	Normal	0,99.d	0,04
	Thermal diffusivity (α) m^2/s	Normal	α	0,06	Variable not considered in the analysis			Normal	α	0,06
	Reduction Factor of concrete strength	N/a			Beta [3$d_{nominal}$;3$d_{nominal}$]	**	0 at 20°C 0,045 at 700°C	N/a		
Steel Parameters	f_y (MPa)	Normal	1,145.f_y	0,05	Log Normal	1,162.f_y *	0,07	Normal	1,145.f_y	0,05
	A_s (mm)	Deterministic			Normal	A_s	0,02	Deterministic		
	Reduction Factor of Steel strength	N/a			Beta [3$d_{nominal}$;3$d_{nominal}$]	**	0 at 20°C 0,065 at 600°C	N/a		

* $\mu = \frac{f_{ck}}{(1-2.COV)}$
** Mean taken from the EUROCODE nominal curve

Table 5.5: Summary of the parameters of the random variables considered

		Ellingwood and Shaver (1977)			Hosser et al. (1995)			Hosser et al. (2008)			Wang et al. (2010)			Van Coile et al. (2011)		
Variable		**Used Distrib.**	**Mean (μ)**	**COV.**	**Used Distrib.**	**Mean (μ)**	**COV.**	**Used Distrib.**	**Mean (μ)**	**COV.**	**Used Distrib.**	**Mean (μ)**	**COV.**	**Used Distrib.**	**Mean (μ)**	**COV.**
Loads/Fire Severity Parameters	Fire Temp. (T) (°C)	Variable not considered in the analysis			Log Normal	0,80.T	0,20	Variable not considered in the analysis			Variable not considered in the analysis			Variable not considered in the analysis		
	Dead Load (DL) (kN/m)	Deterministic			Normal	DL	0,05	Normal	DL	0,10	Normal	DL	0,07	Deterministic		
	Live Load (LL) (kN/m)				Gumbel	0,66.LL	0,40	Gumbel	0,52.LL	0,50	Extr. value type I distrib.	LL	0,30			
Model Uncertainty (θ)		Not considered			Not considered			Not considered			Not considered			Log Normal	1,2.θ	0,15

Transversal Section

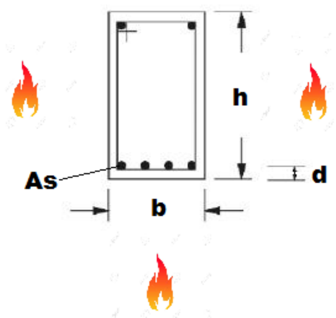

		Eamon and Jensen (2013)			Van Coile et al. (2015)			Aneesha Balaji et al. (2016)		
Variable		Used Distrib.	Mean (μ)	COV.	Used Distrib.	Mean (μ)	COV.	Used Distrib.	Mean (μ)	COV.
Loads/Fire Severity Parameters	Fire Temp. (T) (°C)	Normal	T	0,45	Variable not considered in the analysis			Normal	T	0,45
	Dead Load (DL) (kN/m)	Normal	1,05.DL	0,05	Normal	DL	0,1	Normal	1,05. DL	0,05
	Live Load (LL) (kN/m)	Gamma	0,24.LL	0,65	Gumbel	$\frac{0{,}2\,\chi}{1-\chi}DL$	1,1	Extr. value type I distrib.	LL	0,30
Model Uncertainty (θ)		Normal	1,02.θ	0,06	Log Normal	1,06.θ	0,16	Not considered		

χ – Load ratio defined in the research

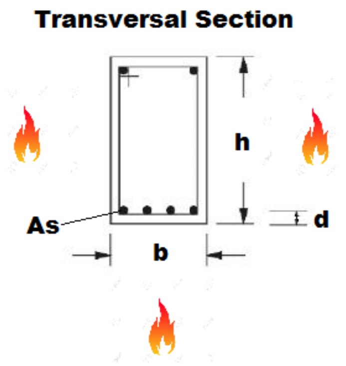

5.12 Gaps Identified

Three main gaps have been identified: (i) Probabilistic evaluation of bending and shear capacity for standard fires and parametric fires; (ii) Failure probability evaluation (especially for the case of parameterized fire); (iii) Evaluation of target safety levels for reliability-based design (e.g. through life-cycle costs).

It is worth highlighting that all the presented studies can be considered as case study applications. This means that there was no analysis of a large spectrum of cases and that most papers are limited to assessing the influence of the parameters of (i) concrete, (ii) steel, (iii) beam, (iv) fire and (v) loads on the reliability of RC beam (see Table 5.6).

However, a target failure probability (or in other words, a target reliability index) is necessary. Obtaining such target reliability indices can be considered part of the code calibration process. In accordance with Rackwitz (2000) and Vrouwenvelder (2002), life-cycle costs allow us to evaluate optimum reliability levels, which can then function as a generalized target for reliability-based design applications. Studies dedicated to steel structures (Hopkin et al., 2020) and RC slabs (Van Coile et al., 2014) are available. No published studies, which focused on RC beams, in particular, are available, making this an important topic for research.

About the mentioned life-cycle costs analysis, it has turned out to be an important and essential tool for PBD. It is related to the analysis of costs over the life-cycle of the structure, seeking to facilitate and improve the decision making of the designer and enabling the calibration of codes. The possession of the target reliability index enables the development of partial safety factors. These two important points of study (parametric fire and life-cycle costs) were not addressed or have not been extensively explored in previous research on concrete beams exposed to fire and ended up becoming important points of research.

This question reinforces the fact that the theme of probabilistic models for RC beams exposed to fire is not fully consolidated in the literature and is worth investigating.

Table 5.6: Beam reliability impact of the parameters analyzed by the authors

<table>
<tr><td colspan="2"></td><th>Ellingwood and Shaver (1977)</th><th>Wang et al. (2010)</th><th>Van Coile et al. (2011)</th><th>Eamon and Jensen (2013)</th><th colspan="2">Aneesha Balaji et al. (2016)</th></tr>
<tr><th colspan="2" rowspan="2">PARAMETERS
IN FIRE SITUATION</th><th colspan="6">BEAM RELIABILITY IMPACT</th></tr>
<tr><th>Bending</th><th>Bending</th><th>Bending</th><th>Bending</th><th>Bending</th><th>Shear</th></tr>
<tr><th rowspan="3">Concrete</th><td>Concrete Strength ↑</td><td>Not rated</td><td>↑</td><td>↑</td><td>↑</td><td>↔</td><td>↔</td></tr>
<tr><td>Concrete Cover ↑</td><td>↑↑↑</td><td>↑↑↑</td><td>↑↑↑</td><td>↑↑↑</td><td>↑↑↑</td><td>↑↑</td></tr>
<tr><td>Aggregate (Silic. x Carb.)</td><td rowspan="2">Not rated</td><td>Not rated</td><td>Not rated</td><td>↑*</td><td>↑*</td><td>↑*</td></tr>
<tr><th rowspan="3">Steel</th><td>Reinforcement Ratio ↑</td><td>↑↑</td><td rowspan="2">Not rated</td><td>↑</td><td colspan="2">Not rated</td></tr>
<tr><td>Reinforcement Yield Strength ↑</td><td>↑↑↑</td><td>Not rated</td><td>Not rated</td><td>↔</td><td>↑↑↑</td></tr>
<tr><td>Bar diameter ↑</td><td>Not rated</td><td>Not rated</td><td>Not rated</td><td>Not rated</td><td>↓</td><td>↓</td></tr>
<tr><th rowspan="3">Beam</th><td>Span/ Depth ratio ↑</td><td rowspan="3">Not rated</td><td rowspan="3">Not rated</td><td rowspan="3">Not rated</td><td>↓↓↓</td><td colspan="2" rowspan="3">Not rated</td></tr>
<tr><td>Restraint level ↑</td><td>**Axial: ↓
Rotational: ↓↓</td></tr>
<tr><td>Width ↑</td><td>↑↑↑</td></tr>
<tr><th>Fire</th><td>Standard x Parametric</td><td>Not rated</td><td>Not rated</td><td>Not rated</td><td>↑↑↑</td><td colspan="2">Not rated</td></tr>
<tr><th>Loads</th><td>Load ratio ↑</td><td>Not rated</td><td>Not rated</td><td>Not rated</td><td>↓↓</td><td colspan="2">Not rated</td></tr>
<tr><td colspan="2">↑↑↑ - High Positive Impact
↑↑ - Medium Positive Impact
↑ - Low Positive Impact</td><td colspan="4">↓↓↓ - High Negative Impact
↓↓ - Medium Negative Impact
↓ - Low Negative Impact</td><td colspan="2">↔ - Indifferent</td></tr>
<tr><td colspan="8">* Carbonate performs better than siliceous.
** The axial restraint decreases the moment capacity as temperature increases; the reverse occurs when Span/Depth ratio is small.</td></tr>
</table>

5.13 Summary

In this chapter, the gaps in literature with respect to the reliability evaluation of RC beams exposed to fire have been determined through a literature review.

It was noticed in this study the lack of a consolidated model for the strength of the beam in fire, given the scarce investigations in the scope of the reliability of RC structures in a fire situation. There is little literature on this topic, making it difficult to run advanced calculation models, being the reason for several of the authors end up using in-house or simplified calculation models. The advantage of using this last approach was the ease in conducting the modeling of the resistance behavior of the beam in fire, as well as its accuracy, despite the simplicity.

Based on the studies in the area and in the great variability found, it is concluded that deterministic or "single value" analysis in this kind of design can give very misleading results if the variability of material properties and the full range of scenarios are not taken into account.

This is especially true for the fire case, for the very reason that fire behavior, and its effect on material properties, generates huge scatter in the data. In these circumstances, the application of the reliability assessment would highlight any deficiencies or gaps in the design and would provide a good basis for its re-examination, in order to satisfy the expected performance requirement.

All existing studies considered the standard fire exposure, thereby neglecting uncertainty in the fire exposure. In this point, studies into the reliability of RC beams considering parametric fire exposure will add to the topic a more realistic view of the reliability of the built environment.

Besides that, the reliability study of RC beams under fire subjected to pure bending was investigated by all the presented research, but with respect to shear capacity, only one study could be obtained as part of this review, still being a simplified study. Research focusing on the shear performance is thus necessary to obtain a complete picture of the reliability in case of fire. Along the same lines, studies are based on single span beams. The case of continuous beams is little known and explored in literature.

Once this probabilistic assessment is made, target safety levels can be established, in order to be a reference for code calibration and design application, i.e. to allow a reliability-based design. The absence of such life-cycle cost analysis is considered an obstacle for the application of reliability-based considerations in structural fire design.

6

RELIABILITY OF RC BEAMS EXPOSED TO FIRE DESIGNED ACCORDING TO ABNT NBR 15200

6.1 Introduction

In this chapter, a comprehensive framework is presented to evaluate the performance and reliability of RC beams under fire conditions. The study begins with the selection of an appropriate model to characterize the resisting moment of RC beams, focusing on their behavior at elevated temperatures. This is followed by model validation and calibration.

Further, a characterization of the RC beam case studies under consideration is provided, highlighting key geometric and material properties. The statistical description of the relevant random variables is then explored, covering both the resistance and load effects statistics, which are essential for accurately capturing the variability in the system's response to fire. Finally, the performance function with respect to the flexural ultimate limit state for RC beams exposed to fire is developed. This performance function is then used in conjunction with MCS in order to assess the reliability of each selected RC beam. This approach allows for an in-depth discussion of the reliability levels obtained and their implications, considering critical parameters such as concrete cover, load ratios, steel area, and temperature. The chapter concludes with a discussion of these results, offering insights into the factors that most significantly influence the fire performance of RC beams.

6.2 Model Selection

In line with the methods for designing RC structures in fire situations presented in this chapter, compiled in Brazilian and European standards, according to Robert et al. (2012), a PBD assessment can be done at three levels: (i) assessing an element individually, (ii) assessing part of the structure or (iii) assessing the structure as a whole, as presented in the previous sections and outlined in Figure 6.1.

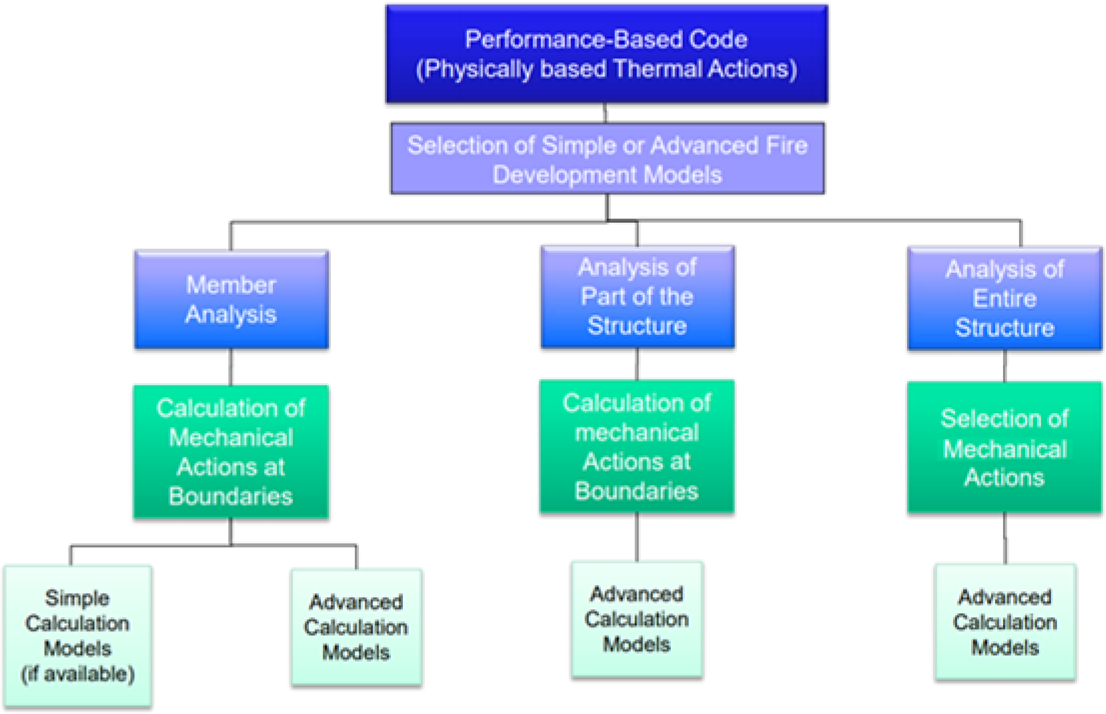

Figure 6.1: Choice of the calculation model (ROBERT el al., 2012)

Analytical formulations and the Finite Element Method (FEM) are two commonly used deterministic models for structural assessment. The main differences between these methods are as follows (Robert et al., 2012):

1. **Modeling Capabilities:** Analytical formulations are typically used for simple structural systems with linear behavior. On the other hand, FEM can be used to model complex geometry, material nonlinearities, and boundary conditions.
2. **Accuracy:** Analytical formulations are faster and more accurate than FEM for simple structures with linear behavior. However, for complex structures or systems with nonlinear behavior, FEM is typically more accurate.
3. **Computational Requirements:** Analytical formulations are typically less computationally intensive than FEM, which can be more expensive than analytical formulations in terms of software, hardware, and human resources.
4. **Verification:** Analytical formulations are often easier to verify as they are derived from fundamental principles and equations. FEM, on the other hand, requires validation through experimentation or comparison to analytical solutions.
5. **Design Optimization:** FEM is often used for design optimization, as it allows for rapid evaluation of many design alternatives. Analytical formulations, on the other hand, may require significant modifications to equations or assumptions for each new design.

In summary, analytical formulations are suitable for simple structures with linear behavior, while FEM is better suited for complex structures with nonlinear behavior. Analytical formulations are typically faster and more accurate than FEM for simple structures, but FEM is more accurate for complex structures. FEM is often used for design optimization, but it can be more expensive than analytical formulations.

In this research, the analysis of a simple single element (beam) was adopted. The idea is to calibrate a simplified model (to be presented in this section), able to adequately represent the behavior of the structure in fire, validated with advanced methods (FEM). This solution proved to be the most reasonable for the development of this research, considering the complexity of the subject, the time available for the research and the reasonable accuracy of the results obtained.

In these terms, the FEM model could be considered a surrogate model, that is, a model used when an outcome of interest cannot be easily measured or computed, so a model of the outcome is used instead (Forrester et al., 2008), once the volume of experimental data about the subject is insufficient to establish a real comparison.

In this sense, reinforcing the possibility of using simplified methods, Rigberth (2000) has demonstrated that:

- Both simplified methods (zone method and 500 ºC isotherm method) provide very good results for fire-exposed tensile zones, considering the standard fire.
- The simplified method generates slightly conservative estimates of fire resistance than the exact numerical model (advanced method).
- This isotherm of 500 ºC method gives good results for cross-sections with the compressive zones exposed to the standard fires, presenting conservative results for natural fires and parametrical models.

6.2.1 Resisting Moment Model

In this section, a methodology for the analysis of RC beams resisting moment is presented. The proposed model was used by Eamon and Jensen (2013) in their research about the reliability of beams in fire situations. All the equations used are based on equations already developed and consolidated in the literature about the theme of the analysis of RC structures in fire situations (NISTIR, 2009; Wickstrom, 1986; BSI, 1987; Purkiss, 2007).

Research was conducted about the topic (Coelho, 2018). On that occasion, a simplified model was used in which the reduction in the strength of concrete and steel was obtained by means of reduction factors established in ABNT NBR 15200:2024 (Figures 2.7 and 2.8). However, it was considered that concrete and steel had the same temperature increase due to the fire effect, considering only the different reduction factors for steel and concrete. Such consideration ends up making the model very conservative.

The comparison of the results of resisting moment as a function of the temperature increase can be seen in Figure 6.2, for a specific beam configuration analyzed (the results were remarkably similar for the other configurations). It is noticed that, until 500 ºC, Coelho (2018) model behaves, in a way, less conservative than the model of Eamon and Jensen (2013). However, after 500 ºC the reduction is very drastic since the slow heat transfer in the concrete is disregarded.

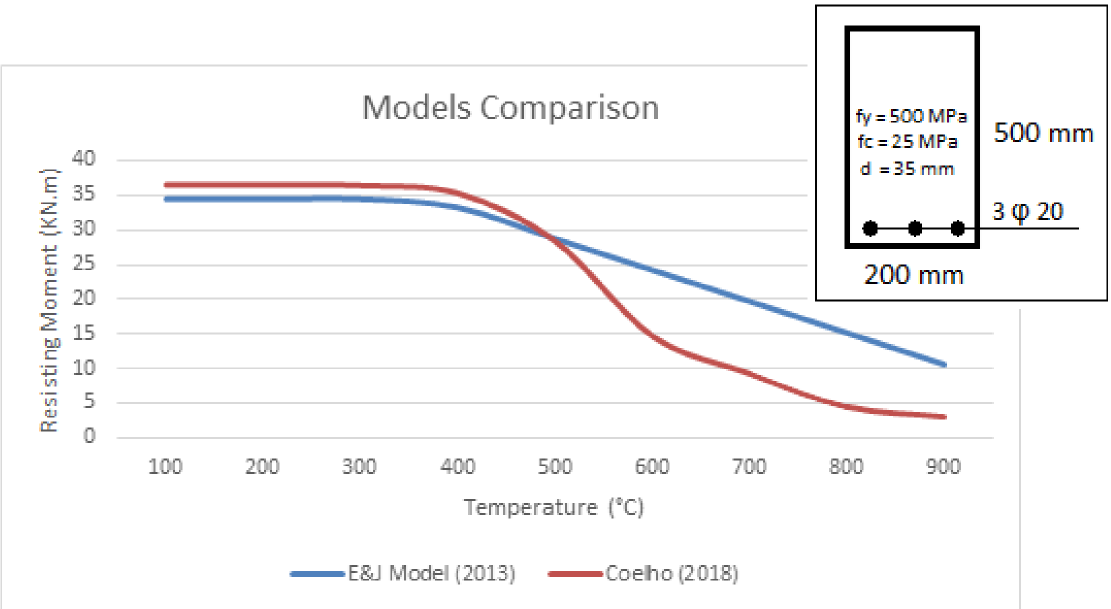

Figure 6.2: Resisting moment according to Coelho (2018) and Eamon & Jensen (2013)

Considering that analysis in fire situations, as well as current standards, in general, are linked to the resistance of 20, 30, 60, 90 and 120 minutes of exposure to a standard fire and that for 20 minutes of exposure to standard fire (ISO 834), for example, there is a gas temperature of approximately 780 ºC, it was decided to use the model proposed by Eamon and Jensen (2013) in this research.

In this model, for rectangular beams in which all steel reinforcement yields are at ultimate capacity, nominal resisting moment as a function of temperature, $M_R(T)$, can be computed as (NISTIR, 2009):

$$M_R(\mathrm{T}) = \left(A'_s.f_y(T_r)\right).(d-d') + (A_s - A'_s).f_y(T_r).\left(d - \frac{a(T_c)}{2}\right) + M_r\,(T) \quad (6.1)$$

where A_s and A'_s are the areas of tensile and compressive steel, while d and d' are the depths of the tensile and compressive steel centroids, respectively, which remain temperature independent. Steel yield stress, $f_y(T_r)$, is a function of the temperature in the reinforcing bar (T_r); concrete compressive strength, $f_c'(T_c)$, is a function of the temperature in the concrete (T_c); $a(T_c)$ is the depth of the concrete compressive stress block, given by $a(T_c) = \frac{(A_s-A'_s).f_y(T_r)}{0,85.f_c'(T_c).b(T_c)}$; and $M_r(T)$ is additional resistance due to axial and/or rotational thermally-induced restraints on the section (if considered/known).

To determine how internal temperature changes in the section as a function of time for a standard fire exposure (t; hours) and external temperature (T), a specially calibrated version of Wickstrom's model (Wickstrom, 1986) can be used.

In this model the temperature of the steel reinforcement T_r is given by (Wickstrom, 1986):

$$T_r = \left(n_w.\left(n_x + n_y - 2.n_x.n_y\right) + \left(n_x.n_y\right)\right)T \quad (6.2)$$

where n_w represents the ratio of the beam surface temperature rise and that of the fire temperature; n_x and n_y are used to determine the ratio between the temperature rise on the surface to that of an interior point in the section, as a function of fire temperature, position and time. These values are defined as (Wickstrom, 1986):

$$n_w = 1 - 0,0616t^{-0,88} \qquad n_{s(s=x,y)} = 0,18\ln\left(\frac{\alpha_r t}{s^2}\right) - 0,81 \quad (6.3)$$

where *s* is the distance of the center of the reinforcement bar considered to the outer edge of the concrete section, measured in the x or y coordinate direction, *t* is time of fire exposure in hours and α_r is the thermal diffusivity ratio.

Thermal diffusivity ratio is given as:

$$\alpha_r = \frac{\alpha}{\alpha_c} = \frac{\frac{k}{\rho . c_p}}{\alpha_c} \tag{6.4}$$

where α is thermal diffusivity, k is thermal conductivity, ρ is density, c_p is the specific heat capacity and α_c is a thermal diffusivity reference value of 0,417 × 10^{-6} m^2/s.

The thermal diffusivity ratio was used in the study conducted by Eamon and Jensen (2013) as a model calibration factor, considering the results obtained via FEM.

However, these values are not presented in their research. To obtain them, in order to use in this research, a series of tests and comparisons of results were performed with the software SAFIR and a code in Python. This factor varies, depending on the settings of the section.

Once the value of T_r is defined, it is necessary to evaluate the strength reduction of concrete and steel. The steel yield strength reduction factor *r* can be taken as (BSI, 1987):

$$r = \frac{720 - (T_r + 20)}{470} \ ; 0 \leq r \leq 1 \tag{6.5}$$

The value of f_y (T_r) can then be obtained as follows:

$$f_y(T_r) = f_y . r \tag{6.6}$$

According to some researchers, concrete properties have minimal impact on the resisting moment, which is governed by the tensile steel, and the choice of concrete model used have little influence on the final results (Eamon and Jensen, 2013). Due to this, f_c'(T_c) is held constant in the analysis, but the size of the effective compression block is reduced.

Thus, to take into account the reductions of concrete compressive strength, the position of the 500 ºC isotherm in the section is needed. For compressive blocks exposed to fire from the sides of the section, using the Wickstrom model, it is given by the following, measured from the outer edge of the beam (Purkiss, 2007):

$$x_{500} = \sqrt{\frac{\alpha_r t}{\exp\left(4{,}5+\frac{480}{0{,}18 n_w T}\right)}} \tag{6.7}$$

Once this is located, the effective width of the compression block as a function of concrete temperature (T_c) becomes: b (T_c) = b – 2.x_{500}, where the multiplier 2 in the right side of this equation is due to the assumption that the fire is encroaching on both sides of the beam and *t* is time of fire exposure in hours.

6.2.2 Selected Beams

The RC beams analyzed in the present study, for the bending ULS, have a rectangular cross section of 20 cm wide (b) by 50 cm high (h), are simply supported, subject to uniformly distributed loads, corresponding to their own weight and to imposed load, and are supposed to belong to a commercial building, up to 23 m high. This configuration is common in buildings with a 5 m (L) span between columns. Only the f_{ck} value of 25 MPa will be adopted, since this parameter showed low influence in this type of study, as seen, in summary, in Table 5.6, about previous research results. The yield strength of longitudinal reinforcement steel (f_{yk}) of 500 MPa is considered.

Table 6.2 contains information on the characteristics of the longitudinal reinforcement and coverings for the beams being analyzed, such as steel area (As), longitudinal reinforcement ratio (ρ), distance from the steel bar axis to the concrete face (d'), lateral and longitudinal cover (c_1). Two different concrete cover distances, 4,5 cm and 3,5 cm, will be considered, intentionally reducing the cover thickness. In some cases, these values fall below the minimum requirement established by ABNT NBR 6118 for beams in urban areas. Specifically, for structures classified under aggressive environmental class 2, the standard prescribes a minimum concrete cover of 3,0 cm.

Considering a specific weight of 25 kN/m³ for RC, the self-weight of the beam was calculated and served as a basis for defining configurations that would not meet the boundary criteria. It is important to mention that although this condition is basic, it is often neglected in these types of studies (Jovanovic et al., 2020).

Table 6.1: Geometric details of the beams under analysis

Reinforcement		A_s (cm²)	ρ (%)	d' (cm)	c_1 (cm)
Case 1	**4 ϕ 10 mm**	3,2	0,32	4,5	4,0
Case 2	**4 ϕ 10 mm**	3,2	0,32	3,5	3,0
Case 3	**4 ϕ 12,5 mm**	5,0	0,50	4,5	3,9
Case 4	**4 ϕ 12,5 mm**	5,0	0,50	3,5	2,9
Case 5	**4 ϕ 16 mm**	8,0	0,80	4,5	3,7
Case 6	**4 ϕ 16 mm**	8,0	0,80	3,5	2,7
Case 7	**3 ϕ 20 mm**	9,45	0,95	4,5	3,5
Case 8	**3 ϕ 20 mm**	9,45	0,95	3,5	2,5

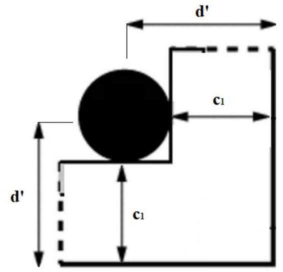

Each configuration will be evaluated for three distinct load ratios (r) defined as the "live load (LL)" / "permanent load (PL)" + "live load (LL)" ratio, r = LL / (PL+LL), model proposed by (Jovanovic et al., 2020). The default values for this ratio will be r = 0,25; 0,5 and 0,75. Therefore, in summary, 4 different beam configurations will be analyzed in 3 loading situations for 2 different concrete covers and 2 fire conditions (ISO and Parametric) in 5 time steps, totalizing 240 situations, which will be the basis for analyzes and generalizations.

In terms of parametric fire, it will be considered a compartment with twelve windows, two doors and the dimensions and characteristics as shown in Figure 2.7 and detailed in section 3.8.2.

6.2.3 Model Validation and Calibration

Although this semi-empirical model proposed has been validated by Eamon and Jensen (2013), a new validation and confirmation of this model was considered relevant. In-house codes (based on FEM) results from Van Coile's studies (2015), and validated within the research group, were available for the current research, which performed a comparison between the three models for some beam configurations. Additionally, a comparison with experimental test results was conducted to assess the accuracy of the models under analysis.

In fire-exposed beam design, it is essential to ensure that flexural failure remains ductile, meaning that yielding of the tensile reinforcement occurs before concrete failure. In this study, this aspect was addressed through the use of SAFIR, which inherently considers the nonlinear behavior of materials at high temperatures and allows for the evaluation of stress redistribution in the cross-section. The program enables the identification of whether the failure mode is ductile (with reinforcement yielding) or brittle (due to concrete crushing before yielding). If a brittle failure mode was observed, this was taken into account in the reliability assessment to ensure an adequate safety level.

The results obtained can be seen in Figure 6.3 for one of the beam configurations (the convergence results were remarkably similar for the other configurations evaluated), requiring only an update in the thermal diffusivity ratio (calibration factor).

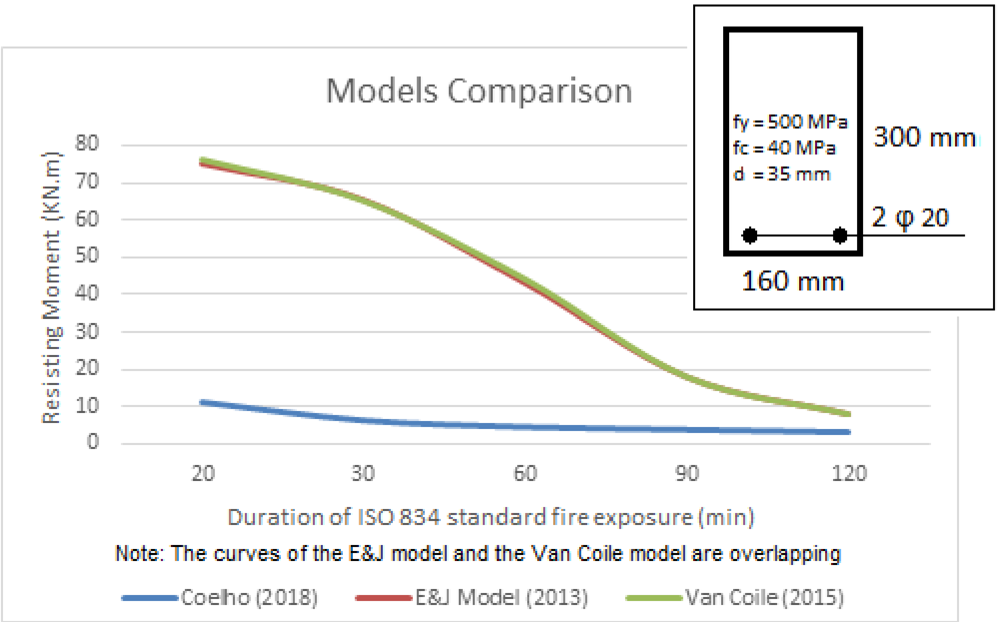

Figure 6.3: Comparative graph of the values obtained for the moment of resistance in Coelho (2018), Eamon & Jensen (2013) and Van Coile (2015)

From the results obtained, the convergence of this model with FEM and the need to abandon the model used in (Coelho, 2018) is clearly perceived, since for high temperatures (especially between 20 and 90 minutes) it is extremely conservative. In addition, the reasonableness of adopting such a method for continuity of research was verified.

It remains then necessary to validate and calibrate the data for the beams that will be studied in this research.

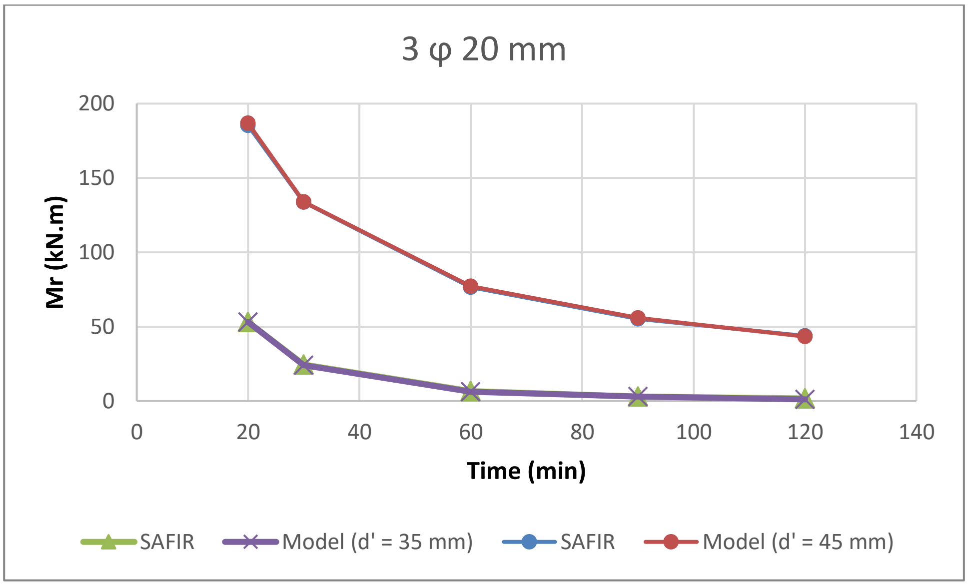

Figure 6.4: Resisting moment for the configuration of 3 ϕ 20 mm exposed to standard fire

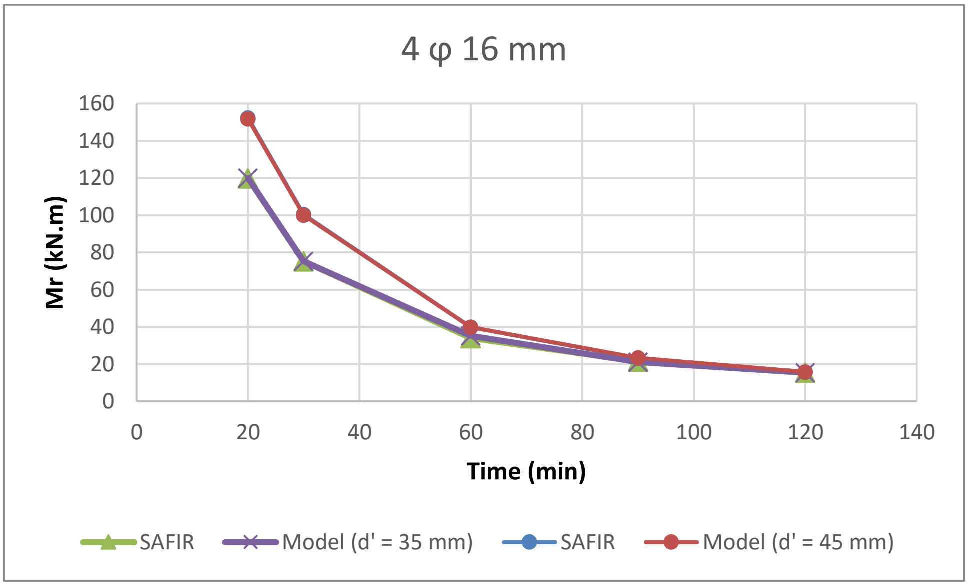

Figure 6.5: Resisting moment for the configuration of 4 ϕ 16 mm exposed to standard fire

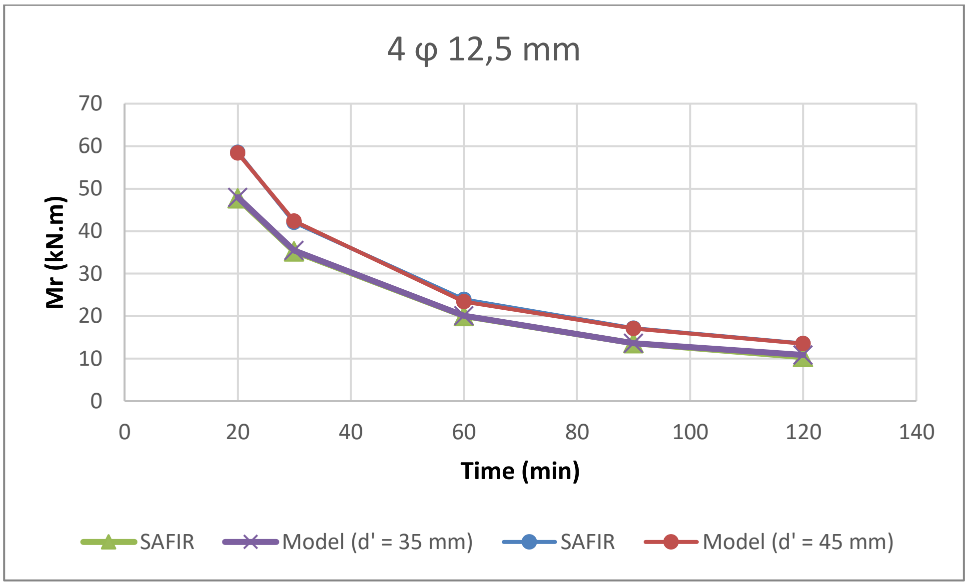

Figure 6.6: Resisting moment for the configuration of 4 ϕ 12,5 mm exposed to standard fire

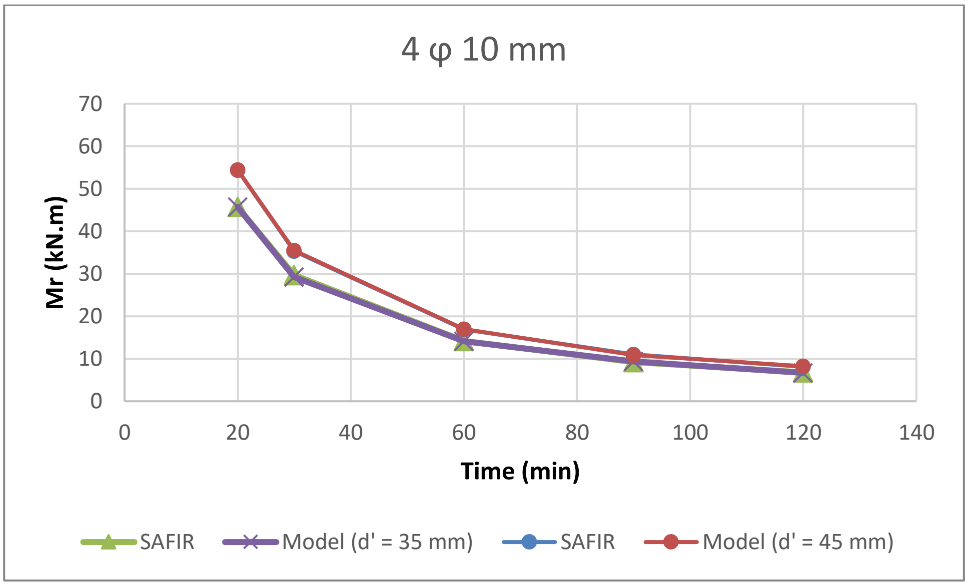

Figure 6.7: Resisting moment for the configuration of 4 ϕ 10 mm exposed to standard fire

The results obtained from the model show strong agreement with those generated via FEM (SAFIR), serving as a calibration reference for both approaches. The accuracy exceeds 95% for these specific cases. Additionally, some curves appear to overlap.

It is interesting to verify the discrepancy in the case of 3 ϕ 20 mm, a configuration that, due to the diameter of the bar, exposes the steel more to temperature variation (due to less concrete cover), resulting in a greater loss of resistance. This variation can also be seen, to a lesser extent, in the other settings, especially at 20 and 30 min of exposure, a difference that reduces, depending on the diameter of the bars used. Such evidence reinforces the importance of the concrete cover in maintaining the strength of reinforcement.

Another notable point is that variations due to concrete cover thickness occur primarily within the first 60 minutes of exposure. This is because, under standard fire conditions, the temperature stabilizes around 1.000°C by this time, explaining the observed behavior.

Regarding parametric fire analysis, the compartment under consideration will be treated as a hotel space with specific dimensions, characteristics, and features, including twelve windows and two doors, as illustrated in Figure 2.7. In addition, a fire load of 377 MJ/m² (hotel) and the existence of automatic fire suppression and detection will be considered. The results are shown in Figures 6.8 to 6.11

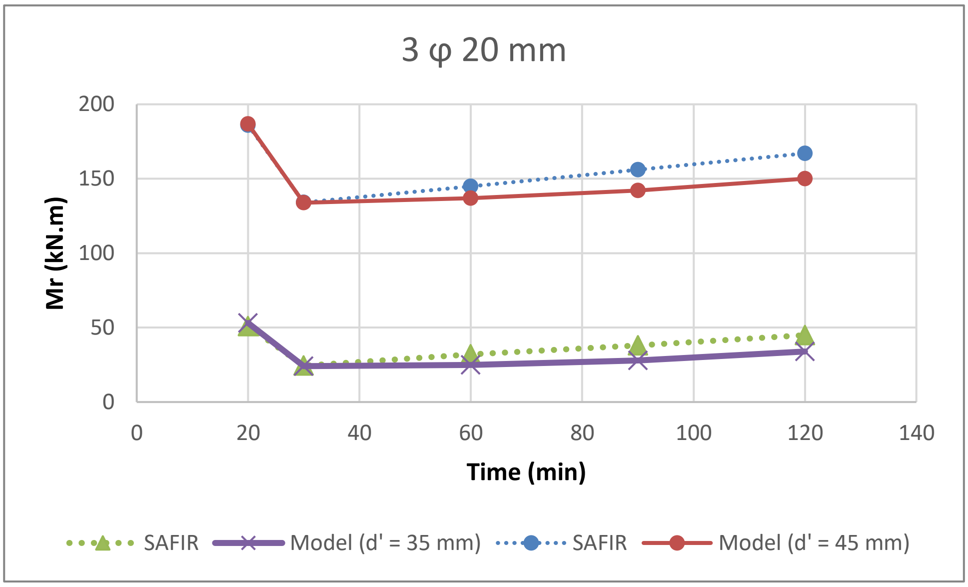

Figure 6.8: Resisting moment for configuration of 3 ϕ 20 mm exposed to parametric fire

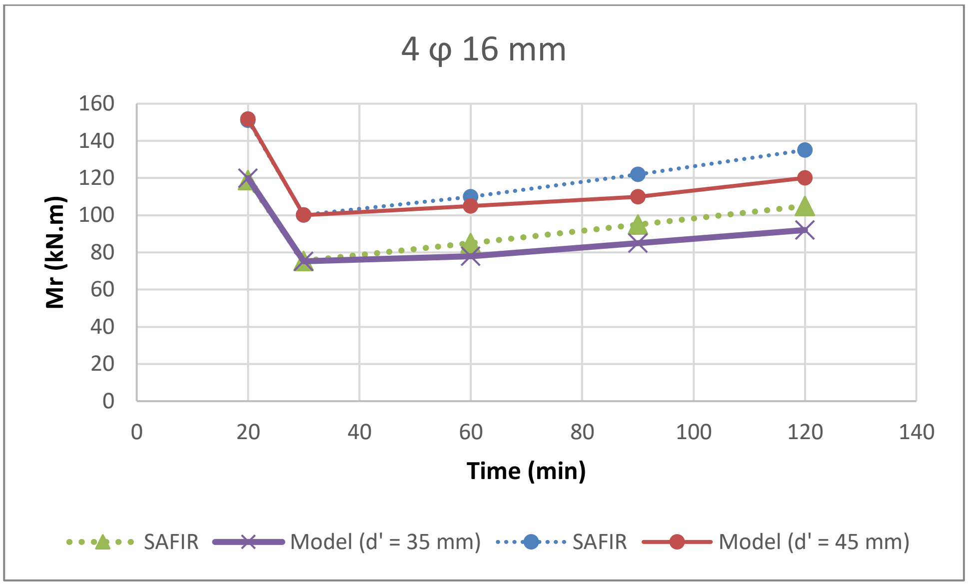

Figure 6.9: Resisting moment for configuration of 4 ϕ 16 mm exposed to parametric fire

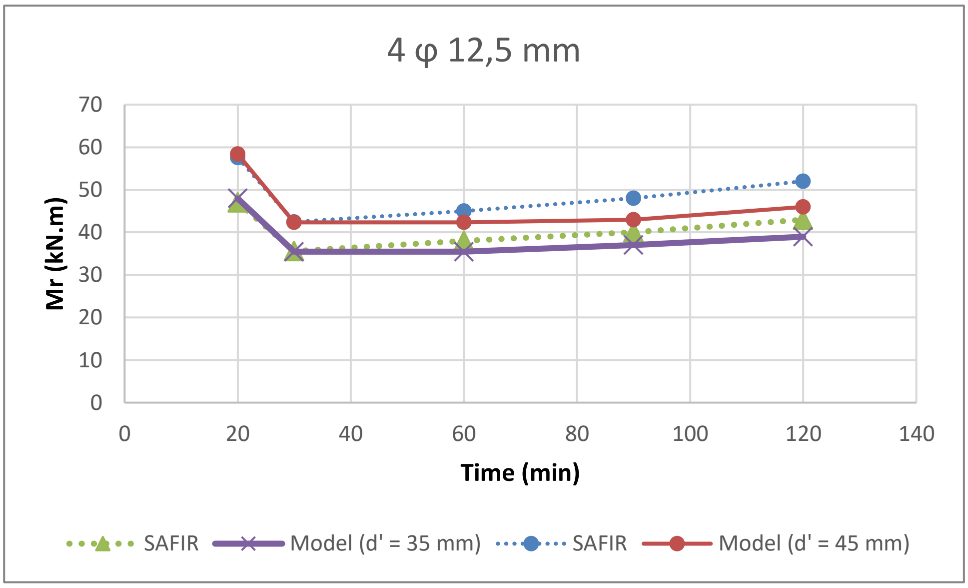

Figure 6.10: Resisting moment for configuration of 4 ϕ 12,5 mm exposed to parametric fire

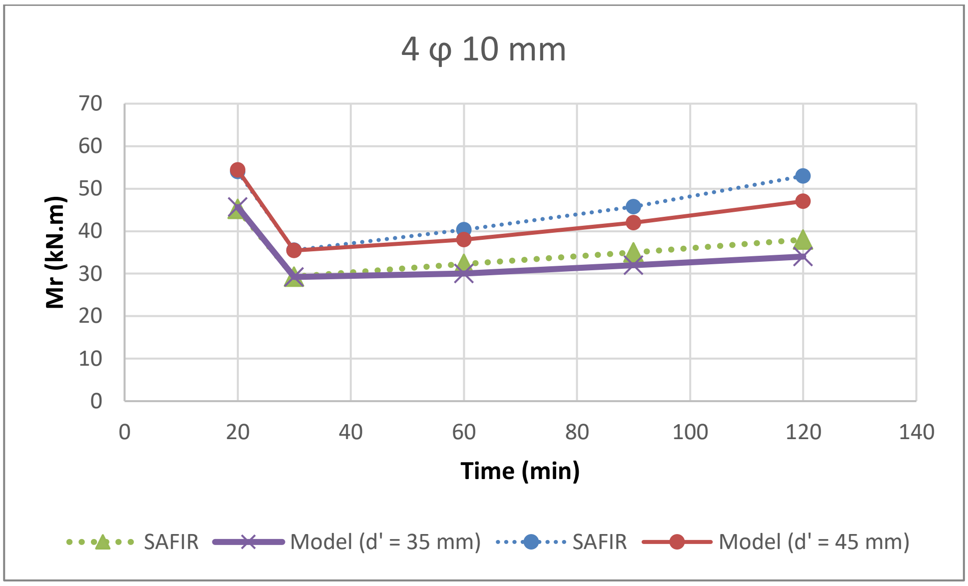

Figure 6.11: Resisting moment for configuration of 4 ϕ 10 mm exposed to parametric fire

In cases of parameterized fire exposure, the finite element analysis (FEM) indicates that the resisting moment at 60 minutes of exposure would be higher than at 20 minutes. This occurs because, given the characteristics of the compartment, the gas temperature at 60 minutes reaches 522.21 °C, which is lower than the peak temperature observed at 20 minutes of exposure (see Figure 2.8, which illustrates the temperature evolution within the compartment under study).

However, it is crucial to emphasize that this temperature refers to the gas phase inside the compartment and does not imply that the entire cross-section of the beam immediately reaches this temperature. Heat transfer within the structural element occurs gradually, meaning that the internal temperature distribution in the section depends on thermal inertia, conductivity, and exposure duration. Consequently, even if the external fire temperature decreases after a peak, parts of the section may still be heating up due to the delayed thermal response of the material. This explains why, in certain scenarios, the structural response may indicate an increase in the resistant moment at later stages of fire exposure.

As discussed in detail in sections 2.3.1 and 2.3.2 and presented by various authors (Krishna et al., 2018; Malik et al., 2021; Coelho et al., 2024) the characteristics of this type of materials (concrete and steel) can undergo changes as temperature increases. These changes may include corrosion, alterations in dimensions, reduction in strength, and permanent modifications in the microstructure of both of them.

The thermal behavior of concrete differs significantly during the cooling process. Unlike steel, whose thermal properties are reversible, concrete retains the maximum temperature it reached at various integration points. Additionally, its mechanical properties continue to degrade, with an average strength reduction of about 10% during cooling. For instance, concrete with a compressive strength of $f_c = 50$ MPa at room temperature may drop to $f_c = 20$ MPa at maximum temperature and further decrease to $f_c = 18$ MPa upon cooling back to ambient conditions. In the case of steel, a residual loss of strength of about 10% is also considered (Maraes et al., 2017). Furthermore, it is important to note that thermal elongation in both materials is not reversible.

It can be seen that for the parameterized fire case, the proposed model deviates from the "real" values, with the greatest deviation at 120 min, reaching 85% of the values obtained via FEM, in the worst case, i.e. more conservative results are obtained. For this study, this deviation will be considered acceptable; however, attention is recommended when using these equations, because depending on the case, the deviations may be greater and unreasonable, requiring validation, calibration and evaluation of boundary conditions with each model change.

6.3 Statistical Description of the Basic Variables

6.3.1 Obtaining Resistance Statistics

Resistance statistics of an RC beam corresponding to different temperatures can be obtained via MCS. This requires: (i) a deterministic relationship that defines the strength of the beam as a function of temperature; and (ii) the statistics of the random variables associated with the calculation of the resistant bending moment.

The random variable that represents moment resistant ($\mathrm{M}_R(\mathrm{T})$) is given by the following functional relation:

$$\mathrm{M}_R(\mathrm{T}) = \boldsymbol{\theta_R}\left[\left(\boldsymbol{A'_s}.F_y(T_r)\right).(D - D') + (\boldsymbol{A_s} - \boldsymbol{A'_s}).F_y(T_r).\left(D - \frac{\frac{(\boldsymbol{A_s} - \boldsymbol{A'_s}).F_y(T_r)}{0{,}85.\,\mathrm{F}_c'(T_c).B(T_c)}}{2}\right)\right] \quad (6.8)$$

In Equation 6.8 the only deterministic variable in this model is the temperature T_r, all other variables are assumed as random.

A_s and **A'_s** are the areas of tension and compression steel, respectively; D and D' are the depths of the tension and compression steel centroids, respectively; $F_c'(T_c)$ is the concrete strength as a function of temperatures of the concrete (T_c); $F_y(T_r)$ is the steel yield strength as a function of the temperature in each bar (T_r); $B(T_c)$ is the width of the beam as a function of the temperature in the concrete (T_c); $\boldsymbol{\theta_R}$ is the variable representing the uncertainty in the resistance model.

The statistics of the basic random variables associated with the resisting moment are summarized in Table 6.3. The data in this table has been compiled from the available literature. Considering the results obtained in section 6.2.2, regarding the model of the resisting moment, in this study the same statistics of the model error assumed in Van Coile (2015) are used here.

Table 6.2: Statistics of random variables associated with RC beam resistance

Variables		**Distribution**	**Mean**	**COV**	**Ref.**
Steel	Reinforcement area, **A_s** (mm²)	Normal	**A_s**	0,02	[1]
	Steel yield stress, F_y (MPa)	Log-Normal	1,16 f_{yk}	0,07	[1]
Concrete	Height, H (cm)	Normal	h	0,04	[1]
	Concrete strength, F_c (MPa)	Log-Normal	1,23 f_{ck}	0,15	[1]
	Width, B (cm)	Normal	b	0,04	[1]
	Cover, D' (cm)	Log-Normal	d'	0,1	[1]
Model Error	Model error (resistance), $\boldsymbol{\theta_R}$	Log-Normal	1,10 $\boldsymbol{\theta_R}$	0,1	[2]
Reference: [1] JCSS - Probabilistic Model Code, 2002. [2] VAN COILE, R. "Reliability-based decision making for concrete elements exposed to fire". Doctoral dissertation. Ghent University, 2015.					

With the information listed above, the statistics of the strength of each beam (minimum, maximum, mean and COV) can be obtained for each time of fire exposure considered from the MCS 100.000 (one hundred thousand). These statistics are presented in Tables 6.4 to 6.11, where $M_{R\text{-}MCS}$ represents the random moment resistant variable obtained by MCS and $M_R(T)$ is the resisting moment.

Table 6.3: Resisting moment statistics for the beam with d' = 45 mm, 3 ϕ 20 mm, as a function of fire exposure.

Configuration	**3 ϕ 20 mm / d' = 45**				
Standard Fire					
Resisting Moment – M_{R-MCS} (MCS) (kN.m)				**$M_R(T)$ (kN.m)**	**μM_{R-MCS} / $M_R(T)$**
Time of fire exposure (min)	**Min.**	**Mean**	**Max.**		
20	153,87	218,01	305,54	186,78	1,17
30	108,68	156,14	220,04	133,90	1,17
60	62,21	89,85	130,48	77,16	1,16
90	43,12	64,99	95,99	55,83	1,16
120	34,89	50,38	76,75	43,39	1,16
Parametric Fire					
Time of fire exposure (min)	**Min.**	**Mean**	**Max.**	**$M_R(T)$ (kN.m)**	**μM_{R-MCS} / $M_R(T)$**
20	152,98	218,72	308,57	186,78	1,17
30	108,27	155,78	226,27	133,90	1,16
60	105,31	158,03	234,94	137,22	1,15
90	134,69	166,81	243,71	142,57	1,17
120	123,07	175,79	322,90	150,25	1,17

Table 6.4: Resisting moment statistics for the beam with d' = 35 mm, 3 ϕ 20 mm, as a function of fire exposure.

Configuration	**3 ϕ 20 mm / d' = 35**				
Standard Fire					
Resisting Moment – $M_{R\text{-}MCS}$ (MCS) (kN.m)				**M_R(T) (kN.m)**	**$\mu M_{R\text{-}MCS}$ / M_R(T)**
Time of fire exposure (min)	**Min.**	**Mean**	**Max.**		
20	42,67	61,83	87,00	53,11	1,16
30	19,36	28,05	40,61	24,11	1,16
60	4,77	7,15	10,50	6,15	1,16
90	2,36	3,43	5,19	2,95	1,16
120	0,92	1,35	1,93	1,15	1,17
Parametric Fire					
Time of fire exposure (min)	**Min.**	**Mean**	**Max.**	**M_R(T) (kN.m)**	**$\mu M_{R\text{-}MCS}$ / M_R(T)**
20	43,54	62,95	91,17	53,12	1,19
30	17,29	25,92	38,13	24,12	1,07
60	20,90	29,52	41,73	25,23	1,17
90	24,73	33,36	45,57	28,51	1,17
120	31,49	40,11	52,32	34,28	1,17

Table 6.5: Resisting moment statistics for the beam with d' = 45 mm, 4 ϕ 16 mm, as a function of fire exposure.

Configuration	4 ϕ 16 mm / d' = 45				
Standard Fire					
Resisting Moment – $M_{R\text{-}MCS}$ (MCS) (kN.m)				**$M_R(T)$ (kN.m)**	**$\mu M_{R\text{-}MCS}$ / $M_R(T)$**
Time of fire exposure (min)	**Min.**	**Mean**	**Max.**		
20	120,84	175,79	260,07	151,79	1,16
30	81,64	115,77	163,98	100,05	1,16
60	32,26	46,06	64,65	39,88	1,15
90	18,46	26,88	38,09	23,29	1,15
120	12,50	18,14	26,34	15,73	1,15
Parametric Fire					
Time of fire exposure (min)	**Min.**	**Mean**	**Max.**	**$M_R(T)$ (kN.m)**	**$\mu M_{R\text{-}MCS}$ / $M_R(T)$**
20	123,36	176,13	250,84	151,79	1,16
30	81,51	115,88	161,63	100,05	1,16
60	81,84	118,16	166,59	105,26	1,12
90	92,87	129,19	177,61	110,42	1,17
120	104,38	140,70	189,13	120,26	1,17

Table 6.6: Resisting moment statistics for the beam with d' = 35 mm, 4 ϕ 16 mm, as a function of fire exposure.

Configuration	**4 ϕ 16 mm / d' = 35**				
Standard Fire					
Resisting Moment – $M_{R\text{-}MCS}$ (MCS) (kN.m)				**M_R(T) (kN.m)**	**$\mu M_{R\text{-}MCS}$ / M_R(T)**
Time of fire exposure (min)	**Min.**	**Mean**	**Max.**		
20	98,34	138,79	196,42	119,93	1,16
30	61,37	86,94	121,49	75,24	1,16
60	27,93	40,57	57,34	35,13	1,15
90	16,82	24,38	35,31	21,13	1,15
120	11,83	17,77	26,11	15,40	1,15
Parametric Fire					
Time of fire exposure (min)	**Min.**	**Mean**	**Max.**	**M_R(T) (kN.m)**	**$\mu M_{R\text{-}MCS}$ / M_R(T)**
20	97,59	138,14	192,20	119,93	1,15
30	60,74	87,84	123,29	75,24	1,17
60	61,33	88,58	128,35	78,26	1,13
90	72,85	99,94	135,39	85,42	1,17
120	81,20	108,30	143,75	92,56	1,17

Table 6.7: Resisting moment statistics for the beam with d' = 45 mm, 4 ϕ 12,5 mm, as a function of fire exposure.

Configuration	**4 ϕ 12,5 mm / d' = 45**				
Standard Fire					
Resisting Moment – $M_{R\text{-}MCS}$ (MCS) (kN.m)				**$M_R(T)$ (kN.m)**	**$\mu M_{R\text{-}MCS}$ / $M_R(T)$**
Time of fire exposure (min)	**Min.**	**Mean**	**Max.**		
20	46,41	69,00	96,28	58,40	1,18
30	34,65	50,02	71,51	42,35	1,18
60	19,16	27,60	40,99	23,37	1,18
90	14,07	20,18	28,68	17,08	1,18
120	11,11	15,96	22,50	13,53	1,18
Parametric Fire					
Time of fire exposure (min)	**Min.**	**Mean**	**Max.**	**$M_R(T)$ (kN.m)**	**$\mu M_{R\text{-}MCS}$ / $M_R(T)$**
20	47,65	68,83	98,26	58,40	1,18
30	35,58	49,55	76,19	42,35	1,17
60	36,86	50,60	74,03	43,25	1,17
90	38,74	52,49	75,91	44,86	1,17
120	40,52	54,49	81,13	46,57	1,17

Table 6.8: Resisting moment statistics for the beam with d' = 35 mm, 4 ϕ 12,5 mm, as a function of fire exposure.

Configuration	**4 ϕ 12,5 mm / d' = 35**				
Standard Fire					
Resisting Moment – $M_{R\text{-}MCS}$ (MCS) (kN.m)				**$M_R(T)$ (kN.m)**	**$\mu M_{R\text{-}MCS}$ / $M_R(T)$**
Time of fire exposure (min)	**Min.**	**Mean**	**Max.**		
20	39,41	56,66	80,74	47,97	1,18
30	29,04	41,88	62,06	35,47	1,18
60	16,63	23,75	33,64	20,11	1,18
90	11,20	16,04	22,59	13,59	1,18
120	8,81	12,83	18,25	10,87	1,18
Parametric Fire					
Time of fire exposure (min)	**Min.**	**Mean**	**Max.**	**$M_R(T)$ (kN.m)**	**$\mu M_{R\text{-}MCS}$ / $M_R(T)$**
20	39,11	56,46	83,63	47,97	1,18
30	29,53	42,05	59,15	35,46	1,19
60	30,00	42,80	60,09	36,52	1,17
90	31,41	43,93	61,03	37,55	1,17
120	33,60	46,12	63,22	39,42	1,17

Table 6.9: Resisting moment statistics for the beam with d' = 45 mm, 4 ϕ 10 mm, as a function of fire exposure.

Configuration	**4 ϕ 10 mm / d' = 45**				
Standard Fire					
Resisting Moment – $M_{R\text{-}MCS}$ (MCS) (kN.m)				**$M_R(T)$ (kN.m)**	**$\mu M_{R\text{-}MCS}$ / $M_R(T)$**
Time of fire exposure (min)	**Min.**	**Mean**	**Max.**		
20	45,14	64,35	89,70	54,18	1,19
30	29,01	41,91	60,46	35,45	1,18
60	13,40	20,01	28,12	16,93	1,18
90	8,94	12,88	18,49	10,91	1,18
120	6,74	9,73	14,46	8,24	1,18
Parametric Fire					
Time of fire exposure (min)	**Min.**	**Mean**	**Max.**	**$M_R(T)$ (kN.m)**	**$\mu M_{R\text{-}MCS}$ / $M_R(T)$**
20	44,20	63,88	92,11	54,42	1,17
30	27,78	41,43	58,05	35,45	1,17
60	29,29	42,26	60,51	38,26	1,10
90	36,72	49,69	67,94	42,47	1,17
120	41,64	55,28	73,53	47,25	1,17

Table 6.10: Resisting moment statistics for the beam with d' = 35 mm, 4 ϕ 10 mm, as a function of fire exposure.

Configuration	**4 ϕ 10 mm / d' = 35**				
Standard Fire					
Resisting Moment – M_{R-MCS} (MCS) (kN.m)				**$M_R(T)$ (kN.m)**	**μM_{R-MCS} / $M_R(T)$**
Time of fire exposure (min)	**Min.**	**Mean**	**Max.**		
20	37,52	54,01	77,72	45,68	1,18
30	23,21	34,53	48,35	29,22	1,18
60	11,60	16,66	23,90	14,10	1,18
90	7,67	11,06	16,40	9,36	1,18
120	5,51	7,90	11,27	6,68	1,18
Parametric Fire					
Time of fire exposure (min)	**Min.**	**Mean**	**Max.**	**$M_R(T)$ (kN.m)**	**μM_{R-MCS} / $M_R(T)$**
20	35,23	52,34	73,15	45,68	1,15
30	24,57	34,19	50,49	29,22	1,17
60	24,23	34,92	51,77	30,32	1,15
90	28,34	37,97	58,78	32,45	1,17
120	30,71	40,33	61,14	34,47	1,17

6.3.2 Obtaining Load Statistics

In the problem analyzed here it is considered that only permanent loads and live loads act on the beam, as mentioned in section 2.2. Thus, the random variable "bending moment in fire situation", $M_{S,fi}$, is given as:

$$M_{S,fi} = \boldsymbol{\theta}_S.(M_{PL} + M_{LL}) \tag{6.9}$$

where M_{PL} is the random variable "moment caused by permanent load (PL)", M_{LL} is the random variable "moment caused by the live load corresponding to the fire situation (LL)" and $\boldsymbol{\theta}_S$ is the random variable that represents the model error associated with the calculus (Table 6.12).

Table 6.11: Statistics of random variables associated with loads

Variables		**Distribution**	**Mean**	**COV**	**Ref.**
Loads	Permanent Load, M_{PL}	Normal	M_{PL}	0,1	[1]
	Live Load, M_{LL}	Gamma	$0,2.M_{LL}$	0,95	[1]
Uncertainties in the model	Uncertainties in load model, $\boldsymbol{\theta}_S$	Log-Normal	$\boldsymbol{\theta}_S$	0,1	[1]
Reference: [1] JOVANOVIĆ, B., VAN COILE, R., HOPKIN, D., ELHAMI KHORASANI, N., LANGE, D., & GERNAY, T. "Review of current practice in probabilistic structural fire engineering: permanent and live load modelling". Fire Technology, 2020.					

Thus, the generation of statistics corresponding to the bending moment in fire situation ($M_{s,fi}$) involves obtaining the statistics of the random variables PL (permanent load) and LL (live load corresponding to the fire situation) which can be obtained for each beam considered, as a function of the "r" ratio, from the procedure described below.

For each beam it is assumed that the bending moment (M_{Sd}) is equals the design resistant moment (M_{Rd}), i.e. $M_{Sd} = M_{Rd}$. For the acting loads considered, the design load effects (M_{Sd}) is given by:

$$M_{Sd} = \gamma_g . M_{Dn} + \gamma_q . M_{Ln} \tag{6.10}$$

where M_{Dn} is bending moment due to the nominal permanent load PL_k, γ_g is the partial safety factor of the permanent load, M_{Ln} is the bending moment due to the nominal live load LL_k and γ_q is the live load partial safety factor.

For a simply-supported beam subject to uniformly distributed loads, the moments M_{Dn} e M_{Ln} are given by:

$$M_{Dn} = \frac{(PL_k).L^2}{8} \tag{6.11}$$

$$M_{Ln} = \frac{(LL_k).L^2}{8} \tag{6.12}$$

Substituting equations 6.12 and 6.11 into 6.10 gives:

$$M_{Sd} = \gamma_g . \frac{(PL_k).L^2}{8} + \gamma_q . \frac{(LL_k).L^2}{8} \tag{6.13}$$

Using the information in Table 6.12, for the ratio “mean / characteristic value”, it is obtained:

$$PL_k = \mu_{\mathrm{PL}} \tag{6.14}$$

$$LL_k = \frac{\mu_{\mathrm{LL}}}{0{,}2} \tag{6.15}$$

where μ_{PL} e μ_{LL} are the means of permanent load and live load, respectively.

Substituting Equations 6.14 and 6.15 in 6.13, gives:

$$M_{Sd} = \frac{L^2}{8} . \left(\gamma_g . \mu_{\mathrm{PL}} + \gamma_q . \frac{\mu_{\mathrm{LL}}}{0{,}2}\right) \tag{6.16}$$

For the load ratio $\left(r = \frac{5.\mu_{\mathrm{LL}}}{\mu_{\mathrm{PL}} + 5.\mu_{\mathrm{LL}}}\right)$, equation 6.16 can be rewritten as:

$$M_{Sd} = \frac{L^2}{8} . \mu_{LL} . \left(\frac{5.(1-r)}{\mathrm{r}} . \gamma_g + \frac{\gamma_q}{0{,}2}\right) \tag{6.17}$$

Live load averages, μ_{LL}, and permanent load, μ_{PL}, can then be obtained:

$$\mu_{\mathrm{LL}} = \frac{8}{L^2} . \frac{M_{Sd}}{\left(\frac{5.(1-r)}{\mathrm{r}} . \gamma_g + \frac{\gamma_q}{0{,}2}\right)} \tag{6.18}$$

$$\mu_{\mathrm{PL}} = \mu_{\mathrm{LL}} . \frac{5.(1-r)}{\mathrm{r}} \tag{6.19}$$

where γ_g e γ_q are equal to 1,4 (load partial safety factors adopted for ULS) and $M_{Sd} = M_{Rd}$.

For each beam configuration under analysis and for each ratio r considered (r = 0,25; 0,5 e 0,75) the averages μ_{LL} e μ_{PL} can then be calculated from equations (6.18), (6.19) and the design resistant moment by the Equation 6.8. This information is presented in Table 6.13.

Table 6.12: Means μ_{PL} and μ_{LL} for different configurations and load ratios, fck = 25 MPa.

Reinforcement Steel	**r = 0,25**		**r = 0,5**		**r = 0,75**	
	μ_{PL} (kN)	μ_{LL} (kN)	μ_{PL} (kN)	μ_{LL} (kN)	μ_{PL} (kN)	μ_{LL} (kN)
4 ϕ 10 mm (d' = 4,5)	11,89	0,79	7,93	1,59	3,96	2,38
4 ϕ 10 mm (d' = 3,5)	12,16	0,81	8,11	1,62	4,05	2,43
4 ϕ 12,5 mm (d' = 4,5)	18,19	1,21	12,13	2,43	6,06	3,64
4 ϕ 12,5 mm (d' = 3,5)	18,61	1,24	12,41	2,48	6,20	3,72
4 ϕ 16 mm (d' = 4,5)	28,66	1,91	19,10	3,82	9,55	5,73
4 ϕ 16 mm (d' = 3,5)	29,35	1,96	19,56	3,91	9,78	5,87
3 ϕ 20 mm (d' = 4,5)	33,09	2,21	22,06	4,41	11,03	6,62
3 ϕ 20 mm (d' = 3,5)	33,89	2,26	22,60	4,52	11,30	6,78

6.4 Performance Function of Beams Subjected to Fire

The reliability analysis of the structural element in question (beam exposed to fire under bending, at ULS) involves assessing the probability of failure (or reliability index) conditioned on the occurrence of fire

The corresponding performance function is given by:

$$g(\boldsymbol{X}) = R - S \tag{6.20}$$

where $\boldsymbol{X}$ is the vector of random variables; R is the resisting moment and S the load effects.

R and S are functions of a number of random variables; thus Equation 6.20 may be rewritten explicitly as:

$$g(\boldsymbol{X}) = \boldsymbol{\theta_R}\left[\left(\boldsymbol{A_s'}.F_y(T_r)\right).(D - D') + (\boldsymbol{A_s} - \boldsymbol{A_s'}).F_y(T_r).\left(D - \frac{\frac{(\boldsymbol{A_s} - \boldsymbol{A_s'}).F_y(T_r)}{0{,}85.\,\mathrm{F}_c{}'(T_c).B(T_c)}}{2}\right)\right] - \boldsymbol{\theta_S}.[M_{PL} + M_{LL}] \tag{6.21}$$

6.4.1 Code for Reliability Analysis of RC Beams under Fire

The MATLAB code developed for the research presented herein uses MCS to assess the reliability of RC beams in fire scenarios (see Annex B). The code's primary purpose is to quantify the probability of failure of concrete beams under fire conditions by simulating the randomness in the key parameters that influence structural behavior under elevated temperatures. One of the fundamental aspects of the simulation is the definition and use of a performance function, which determines the failure condition of the beam (Equation 6.21). This performance function accounts for load effects and the temperature-dependent reduction in material strength, and it operates based on randomly generated input variables representing the uncertainty in the beam's properties and fire exposure.

To accurately simulate fire conditions, the code includes both standard and parametrized fire models. The standard fire model follows typical fire temperature curves, which are widely used in structural fire safety studies and design codes. On the other hand, the parametrized fire model considers specific compartment characteristics and adjusts the temperature curve accordingly. By including both fire models, the code allows a comparison between conservative, generalized fire scenarios and those tailored to realistic building compartment conditions. This dual approach helps in evaluating the reliability of RC beams under both standardized and more realistic fire exposures, enhancing the code's applicability to diverse real-world situations.

A critical aspect of the code is its reliance on random variables to capture the variability in key parameters, such as material properties and load ratios. These variables are generated using stochastic techniques within each MCS cycle, ensuring that the resulting reliability indices and failure probabilities reflect a broad range of possible conditions. Specifically, the code generates random distributions for concrete and steel properties under fire, load ratios, and duration of exposure, which directly influence the temperature-dependent properties of the beam. These variables are essential for accurately calculating the beam's resistant moment and assessing its ability to withstand the applied loads in fire situations.

The simulation proceeds through multiple loops, each corresponding to different cases, load ratios, fire durations, and fire types (standard and parametrized). For each combination, the code initiates a MCS cycle, setting distinct seeds to enhance randomness across trials. This approach ensures that each fire type and exposure duration is independently evaluated, providing a more comprehensive understanding of how these variables impact the reliability of the beam. Each simulation cycle calculates temperature-dependent material properties, evaluates the resistant moment, and compares it to load effects, storing the results for subsequent statistical analysis.

Reliability indices and failure probabilities are calculated at the end of each simulation cycle. The code aggregates the results across different cases, providing an array of reliability indices and failure probabilities for each scenario. These metrics are crucial for assessing the overall safety level of RC beams under fire exposure and for comparing the relative risks associated with standard versus parametrized fire models. The output provides a statistical basis for understanding how different fire scenarios and structural properties impact the probability of failure, helping guide design decisions aimed at enhancing structural resilience.

Finally, the code includes a visualization step, where it plots reliability indices, failure probabilities, and resistant moment statistics across all simulated cases. These figures offer a visual summary of the results, enabling easier interpretation of the reliability analysis. The use and results are presented in the next section.

6.4.2 Probabilistic Calculation - Monte Carlo Simulation

To assess the reliability of the beam under fire conditions, it is essential to consider the variation in all relevant parameters. This is achieved through the Monte Carlo Simulation (MCS) method, where parameters are treated as random variables with values defined by their respective probability distribution functions. The characterization of these parameters is summarized in Tables 6.3 and 6.12, serving as the foundation for the simulations.

The execution of this method involves an intermediate step in which the resistant moment and load effect moment are simulated for different conditions under analysis. This step is crucial, as it provides statistical insights into the system's behavior and forms the basis for Tables 6.4

to 6.11, which summarize the mean, maximum, and minimum resistant moments at different temperatures, as well as Table 6.13, which relates to load effects. This intermediate analysis is necessary to ensure a structured and interpretable approach, avoiding direct Monte Carlo evaluation of the probability of failure without first understanding the fundamental variations in the system's response.

Beyond this intermediate objective, the MCS in this study serves as a tool for obtaining the probability of failure for all established conditions. To achieve reliable results, 1.000.000 (one million) simulations with random values were performed for each beam, respecting the mean, coefficient of variation (COV), and probability distribution of each variable. The results are presented in the following figures. Additionally, an example of one of the case studies and the code used to perform the MCS can be found in Annex A and B, respectively.

Figures 6.12 to 6.19 display the reliability index and probability of failure for each selected beam. It is important to note that some curves overlap, and the points are connected by straight lines solely for visualization purposes. The analysis was conducted specifically at key time intervals—20, 30, 60, 90, and 120 minutes—ensuring that the reliability assessment is based on targeted evaluations rather than an indiscriminate direct Monte Carlo approach, which could lead to a less structured interpretation of results.

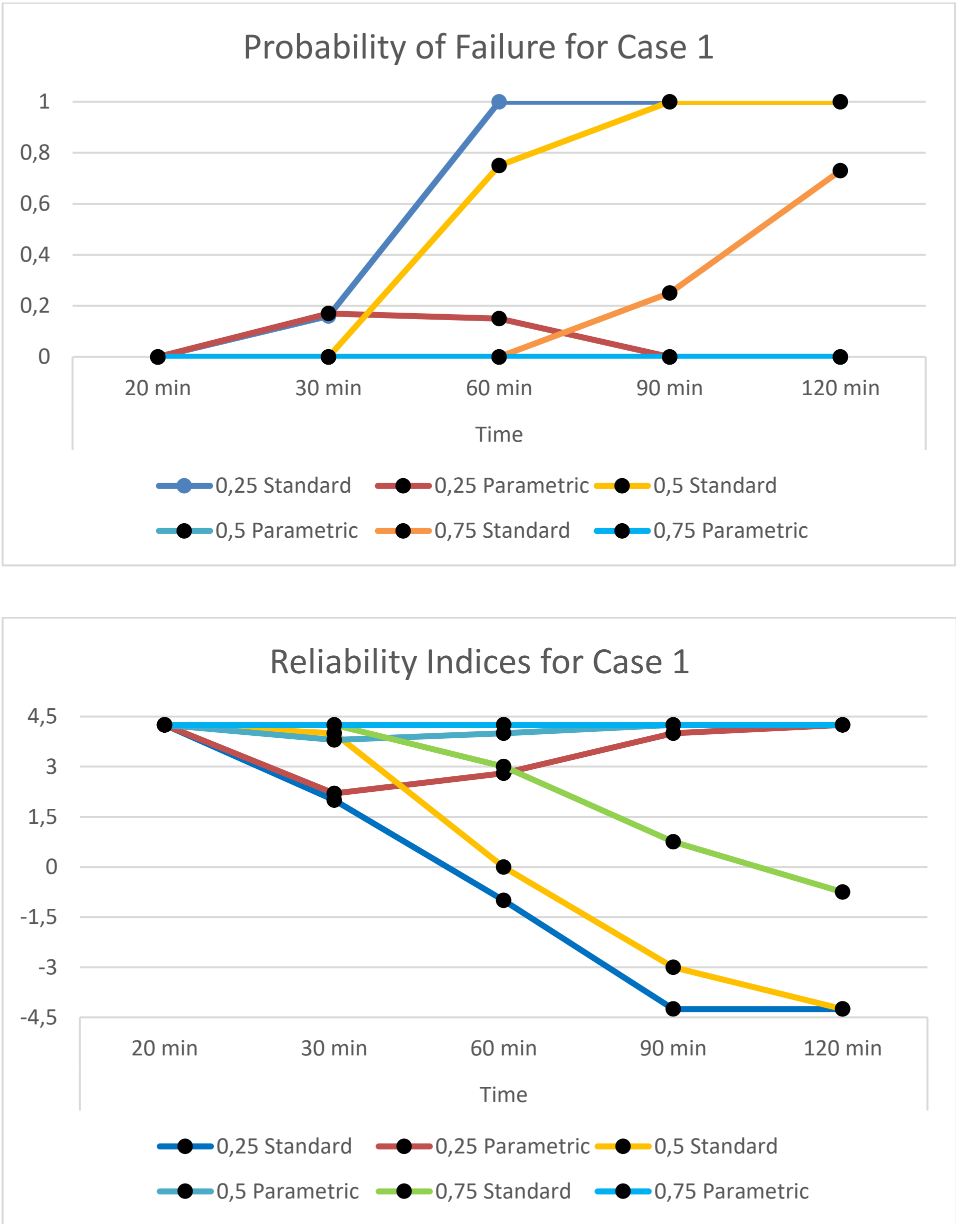

Figure 6.12: Reliability index and probability of failure for the beam with d' = 45 mm, 4 ϕ 10 mm, as a function of fire duration and type of fire (standard or parametric)

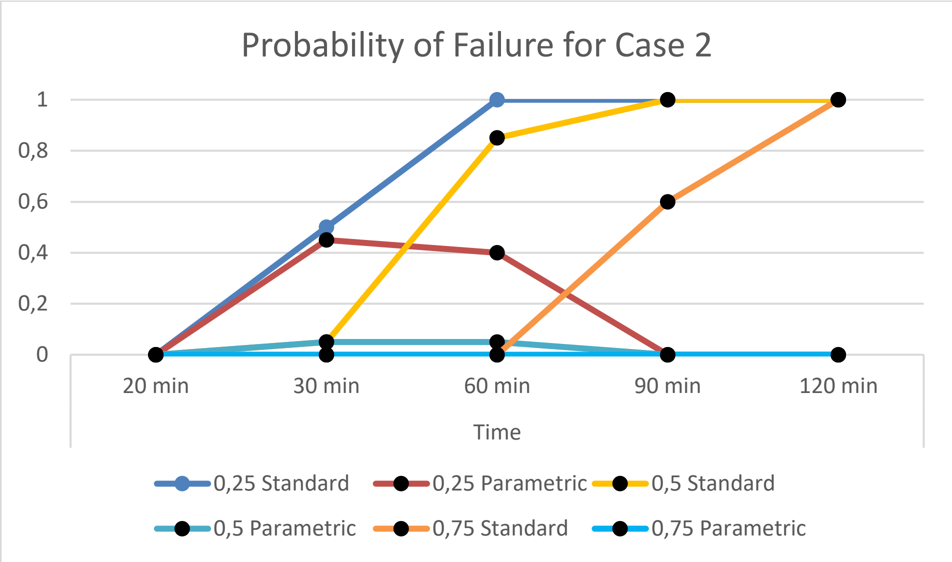

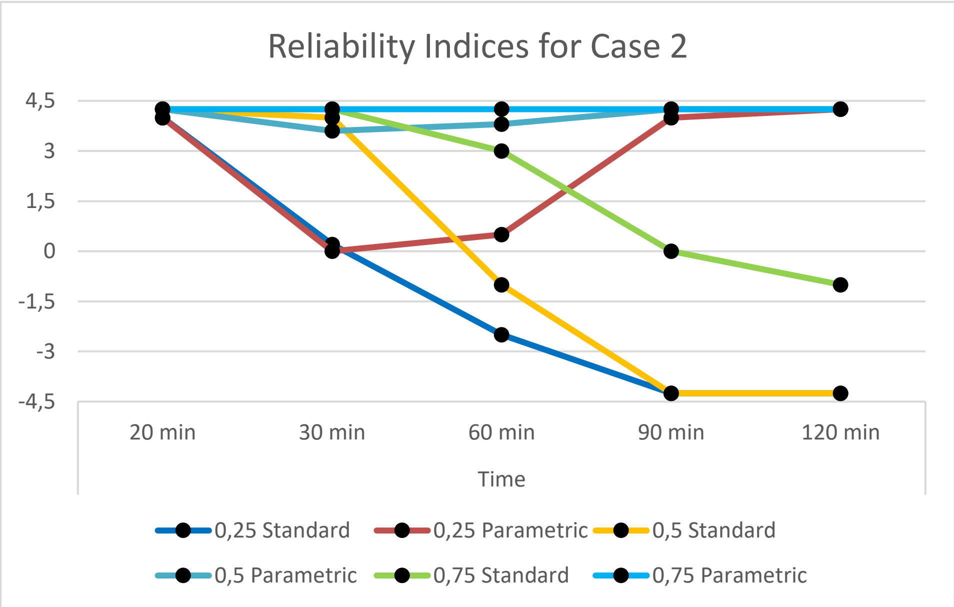

Figure 6.13: Reliability index and probability of failure for the beam with d' = 35 mm, 4 ϕ 10 mm, as a function of fire duration and type of fire (standard or parametric)

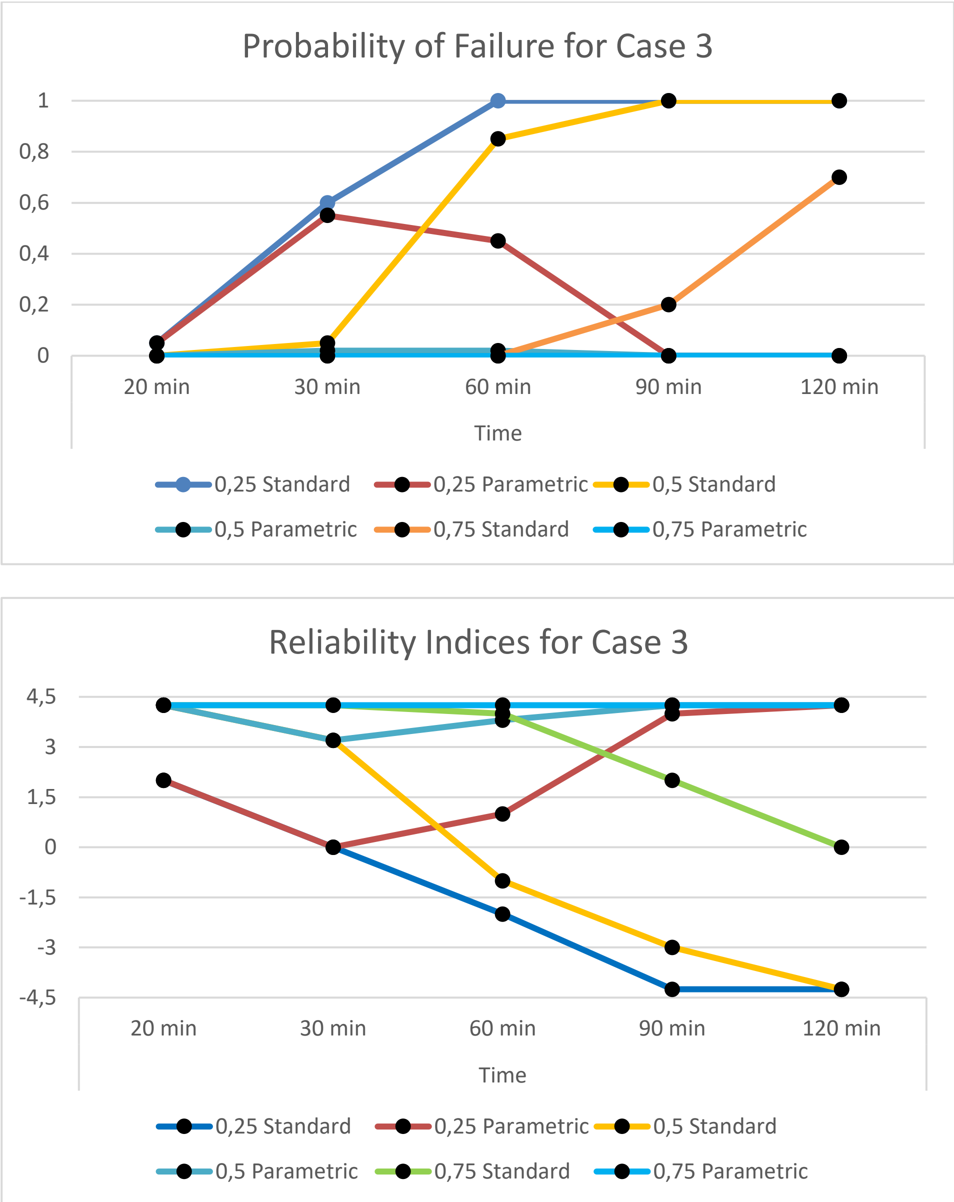

Figure 6.14: Reliability index and probability of failure for the beam with d' = 45 mm, 4 ϕ 12,5 mm, as a function of fire duration and type of fire (standard or parametric)

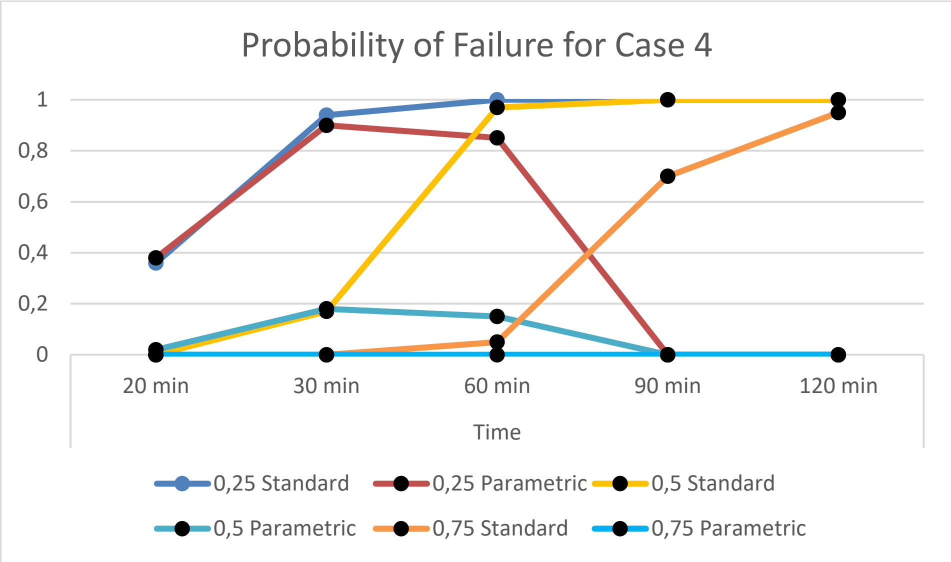

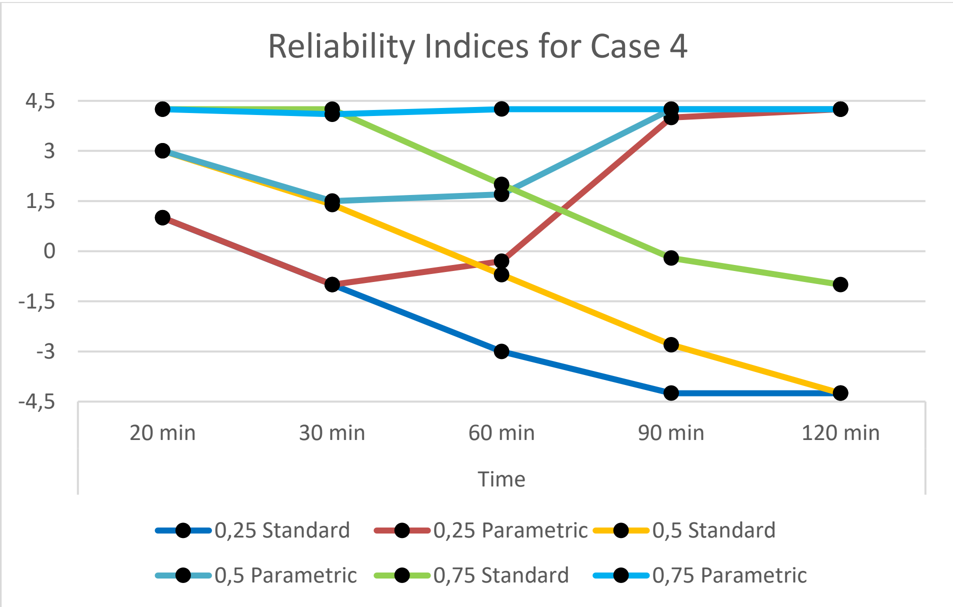

Figure 6.15: Reliability index and probability of failure for the beam with d' = 35 mm, 4 ϕ 12,5 mm, as a function of fire duration and type of fire (standard or parametric)

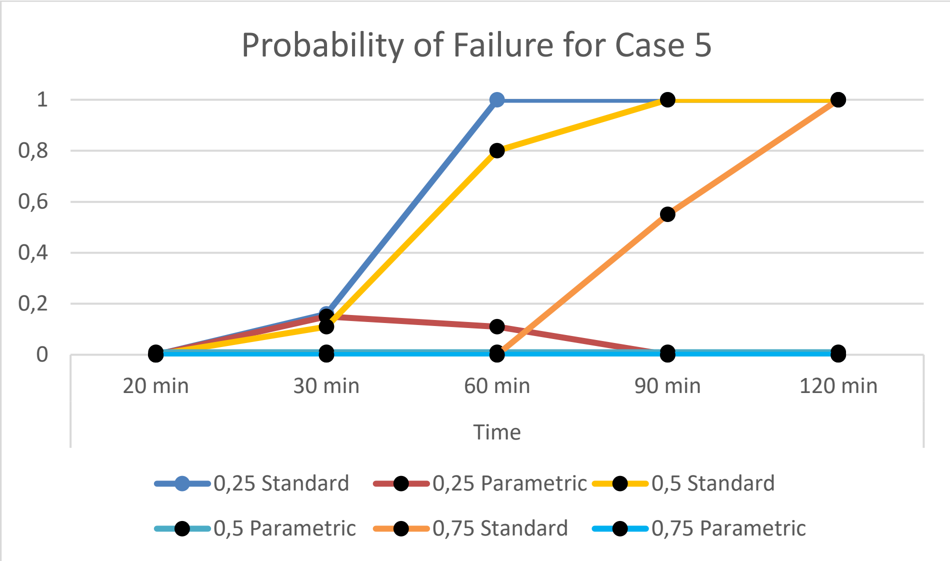

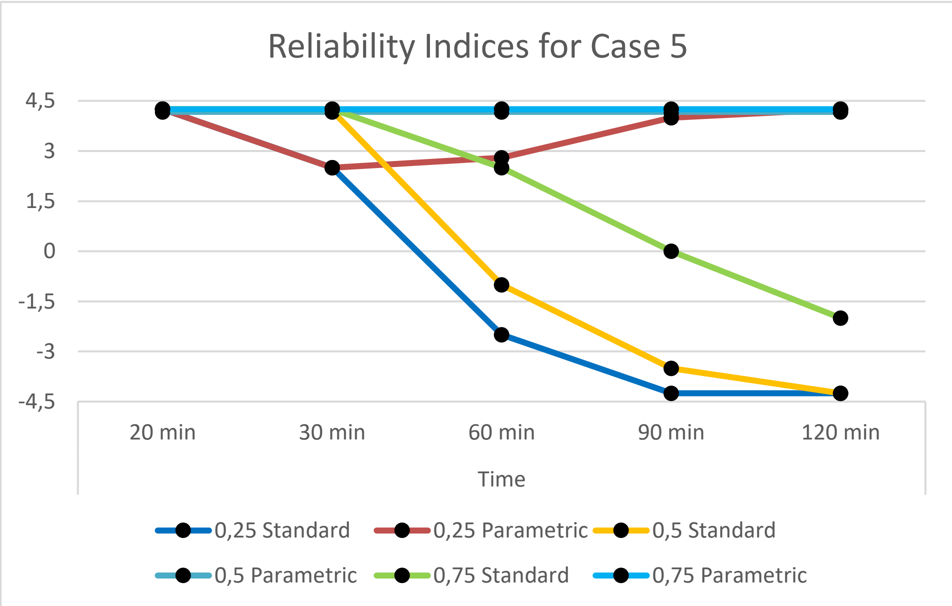

Figure 6.16: Reliability index and probability of failure for the beam with d' = 45 mm, 4 ϕ 16 mm, as a function of fire duration and type of fire (standard or parametric)

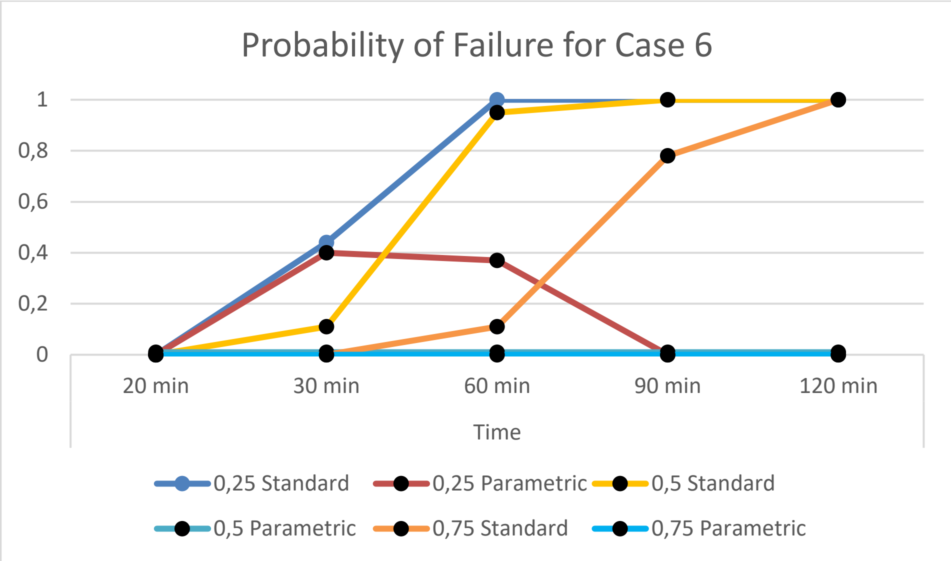

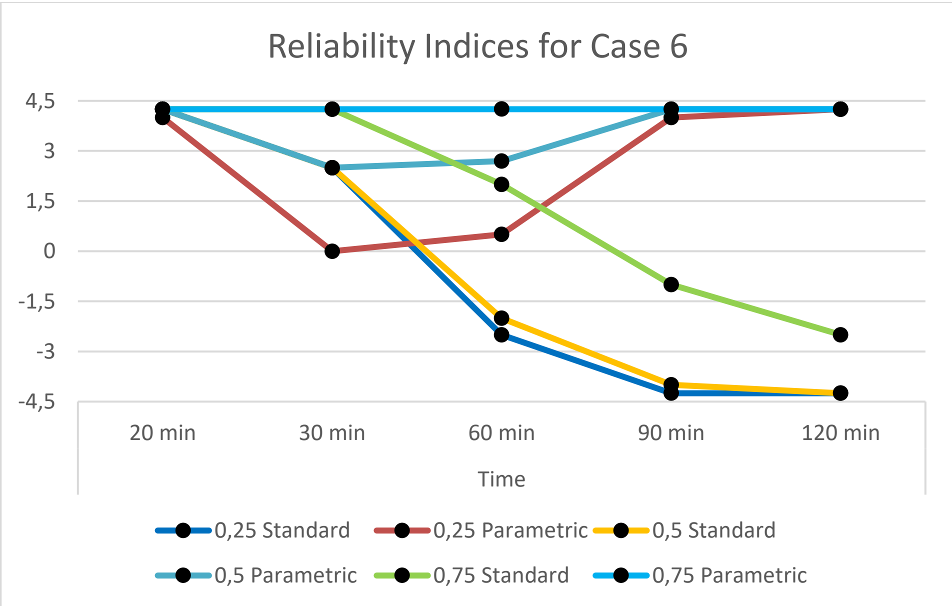

Figure 6.17: Reliability index and probability of failure for the beam with d' = 35 mm, 4 ϕ 16 mm, as a function of fire duration and type of fire (standard or parametric)

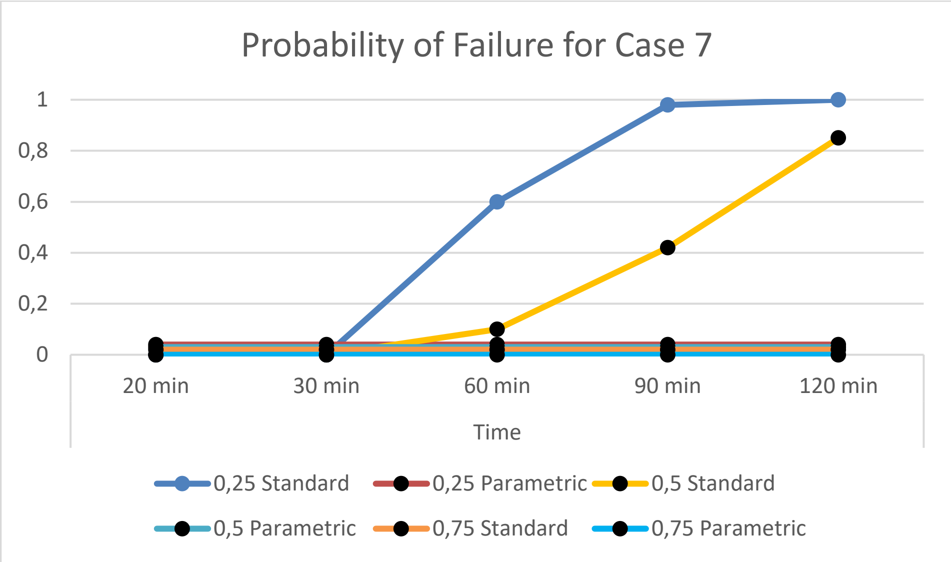

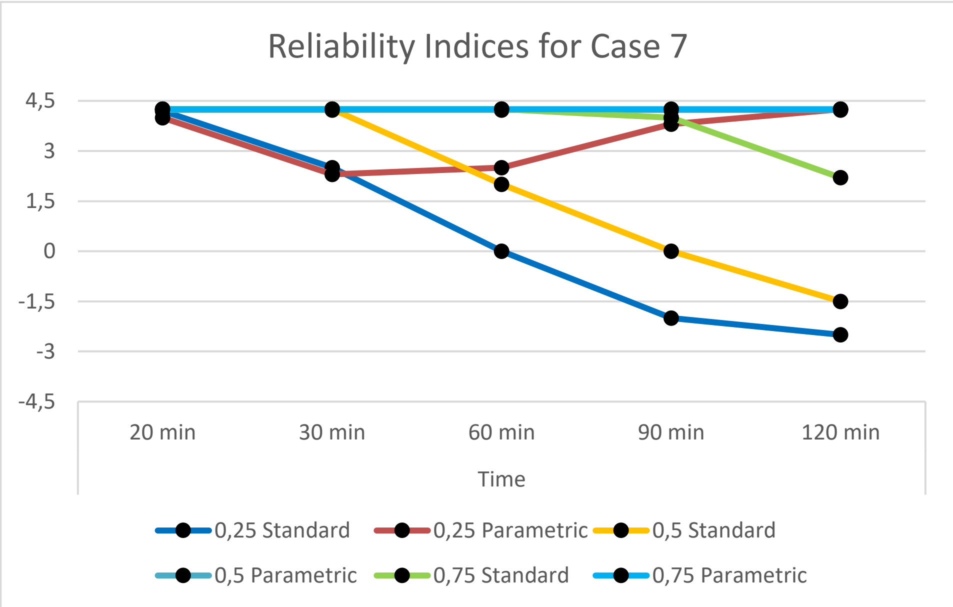

Figure 6.18: Reliability index and probability of failure for the beam with d' = 45 mm, 3 ϕ 20 mm, as a function of fire duration and type of fire (standard or parametric)

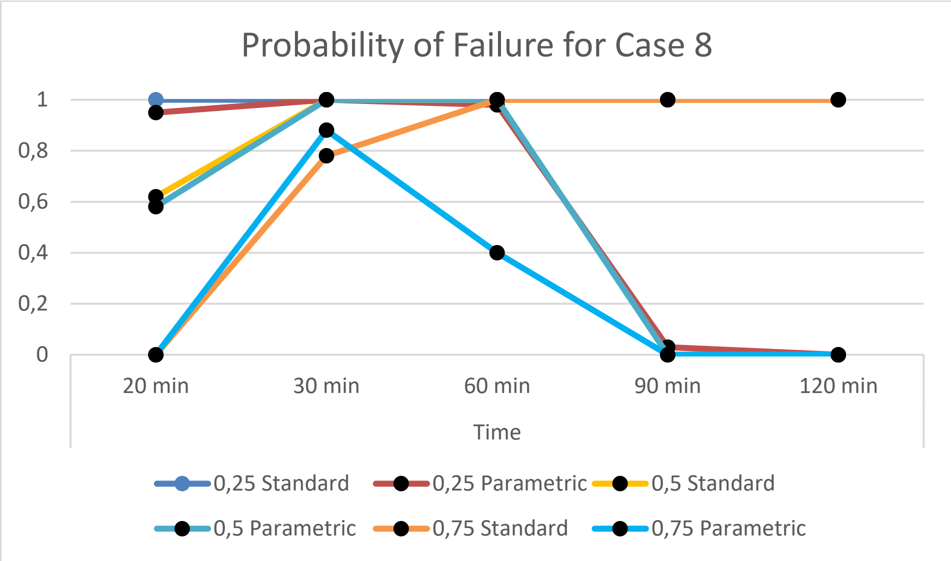

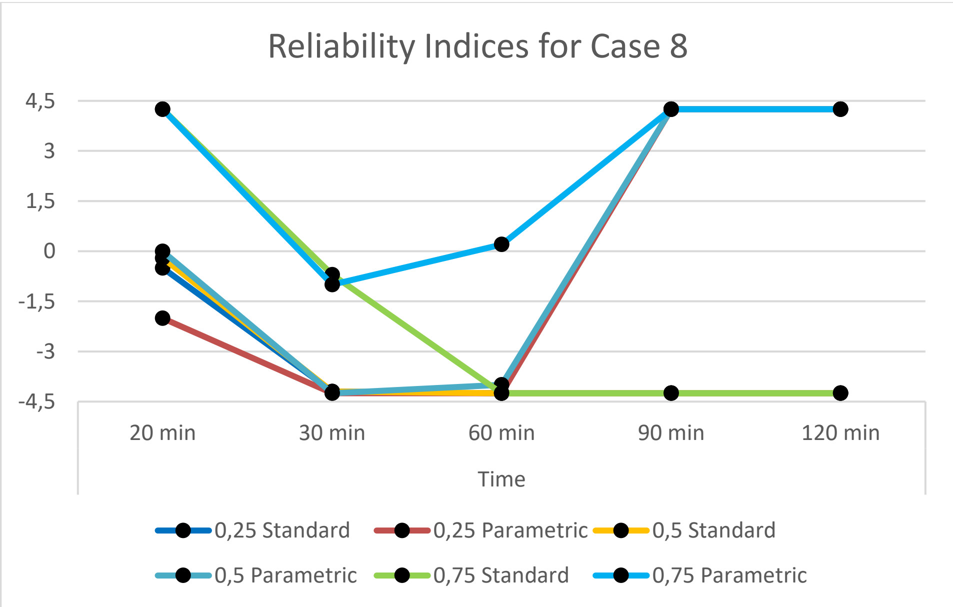

Figure 6.19: Reliability index and probability of failure for the beam with d' = 35 mm, 3 ϕ 20 mm, as a function of fire duration and type of fire (standard or parametric)

6.4.3 Discussion

In the analysis of the reliability levels associated with the selected RC beams under fire exposure, the effects of the following parameters have been investigated: beam dimensions, duration of fire exposure, and the nature of the fire itself.

The beams under consideration vary in their dimensions, particularly in the depth of the concrete cover and the size of the reinforcing bars. These variations are critical as they directly influence the thermal inertia of the beam. For instance, a larger concrete cover provides better insulation, delaying the heat transfer to the reinforcing steel, thereby enhancing the beam's fire resistance (e.g. beta of 2,75 for 30 min of fire for a load ratio of 0,25 and a parameterized fire - Figure 6.18 - versus a beta of – 4,25 for the same situation, with a 10 mm difference in cover – Figure 6.19). Similarly, larger reinforcing bars have a greater mass, taking longer to reach critical temperatures that compromise their structural integrity. Despite this, in the beam represented in Figure 6.19 (d' = 35 mm, 3 ϕ 20 mm) there is a great susceptibility of the element to fire damage. In this case the minimum concrete cover will be considerably smaller than the other selected beams. In this case, heat contact is greater with the steel, generating a lower reliability index for the 20-min duration of fire exposure.

The duration of fire exposure, herein assumed as 20, 30, 60, 90, and 120 minutes, has a significant impact on the resulting reliability levels. As the fire exposure duration increases, the temperature within the beam rises, leading to a reduction in the strength and stiffness of both the concrete and the steel reinforcement. This progressive degradation results in an increase in the probability of failure and a corresponding decrease in the reliability index over time (e.g., the lines in green, yellow, and dark blue in all reliability index graphs, where temperature increases from start to finish). The rate of degradation depends on the beam's characteristics; beams with larger concrete covers and reinforcing bars exhibit a slower rate of deterioration.

Note that in the specific case of the hotel under study, these beams would not achieve reliability indices compatible with a fire duration of 60 minutes. In such cases, several strategies can be considered to enhance fire resistance and maintain structural safety. These include increasing the concrete cover thickness to improve thermal insulation, using fire-resistant coatings or intumescent paints, optimizing the reinforcement layout to ensure better residual capacity, or incorporating active fire protection measures such as sprinklers to control fire development and reduce thermal exposure. Selecting the most appropriate solution depends on the design constraints, cost considerations, and the required level of fire safety

By examining these figures, it is observed the evolution of the resulting reliability levels as a function of time. For instance, beams with a smaller concrete cover and smaller reinforcing bars, as seen in Figures 6.12 versus 6.19, exhibit a faster reduction in the reliability index (and a higher probability of failure) compared to their counterparts with larger dimensions. This is attributable to the faster heat transfer to the reinforcing steel and the consequent rapid loss of structural integrity.

The analysis of the reliability index in relation to the duration of fire exposure and the type of fire (standard or parameterized) reveals significant insights, particularly when compared to the findings of Eamon and Jensen in their study "Reliability Analysis of RC Beams Exposed to Fire" (2013). As fire duration increases, a consistent trend is observed: reliability index values typically decrease, indicating a reduction in the structural reliability of RC beams under thermal stress. This decline is exacerbated in standard fire scenarios, where the temperature rise is abrupt and uniform. Eamon and Jensen found similar results in their research, indicating that as exposure time increased, the likelihood of structural failure also increased, leading to lower reliability index values.

The type of fire significantly impacts the resulting reliability levels. The standard fire model, while widely used in structural fire engineering, has notable limitations that can affect the accuracy of safety assessments. Primarily, it assumes a uniform temperature increase over time, often disregarding the specific material properties and geometry of a given structure. This oversimplification can lead to unrealistic thermal exposure scenarios that may not reflect actual fire conditions. Furthermore, the model lacks flexibility to account for ventilation effects, fuel load variations, and other factors that significantly influence fire development in real-life situations. These limitations suggest the need for more sophisticated, adaptable models that can better account for the complex dynamics of real fires.

In contrast, parameterized fire scenarios consider specific conditions of the compartment, such as ventilation and fire load, presenting a more realistic scenario. In these cases, the reliability index tends to exhibit a more gradual decline and, in some instances, recovery after certain exposure periods, such as around 60 minutes, as observed in the comparison of all Figures 6.12 – 6.19. Eamon and Jensen's findings support this notion, as their analysis indicated that tailored fire scenarios allowed for a better understanding of the material's response, providing a more resilient outlook on reliability than standard models.

The differentiation between standard and parameterized fires is crucial in understanding reliability index behavior. In standard fire models, rapid temperature escalation often leads to quicker degradation of structural integrity. As a result, reliability index values can become negative in relatively short exposure times, signaling an unacceptable probability of failure. This aligns with Eamon and Jensen's conclusions, which highlighted that RC beams exposed to standard fire conditions reached critical failure thresholds more quickly than those subjected to variable, real-world fire conditions.

In parameterized scenarios, the ability to model the thermal environment more closely to real-life situations can lead to different outcomes. In some cases, parameterized models showed resilience in reliability index values, allowing for recovery or stabilization after specific exposure times. Eamon and Jensen also noted the importance of considering fire dynamics and the effects of materials and geometries, suggesting that real-world conditions can prevent negative reliability index values, thereby indicating a structure's capability to withstand longer durations of thermal exposure without reaching critical failure.

The occurrence of negative reliability index values is particularly noteworthy, as it suggests that the probability of failure exceeds acceptable limits, posing serious implications for structural safety. In all the figures we can perceive scenarios where negative reliability index values emerged under standard fire conditions, emphasizing the critical nature of fire resistance in design. This research reinforces the understanding that reliance on standard fire models could lead to conservative predictions that do not align with actual performance, potentially compromising safety. In contrast, parameterized models may mitigate this issue by providing a more accurate representation of the conditions that structures face in real fires. The ability to model various fire scenarios, including peak temperatures and duration, allows for a more comprehensive reliability assessment. This approach can prevent structures from reaching negative reliability index values under certain conditions, highlighting the importance of advanced modeling in reliability analysis.

It is important to highlight that, from a standardization perspective, the design approach suggested in fire safety standards (e.g., ABNT NBR 15200) tends to be conservative, often leading to over-dimensioning of structures. This conservatism arises because standardized fire scenarios do not fully capture the complexity and variability of real fire conditions, as previously discussed. As a result, current design provisions may lead to unnecessary increases in construction costs and excessive material use, which is unsustainable in a context where resource efficiency is a priority.

However, as more experimental studies on fire-exposed beams become available, a more refined understanding of structural behavior under fire conditions is emerging. Comparisons between standardized models and test results indicate that some assumptions may be overly cautious, suggesting opportunities for more performance-based and reliability-driven approaches in future revisions of fire safety codes. The trend in structural fire engineering is moving toward incorporating advanced numerical modeling and probabilistic assessments, which will likely reduce excessive conservatism while ensuring adequate safety levels. This evolution highlights the importance of continuously updating design codes based on experimental and computational advancements, balancing safety with material efficiency and cost-effectiveness.

A discussion on the acceptable reliability levels of RC beams under fire, as given by the target reliability index, will be presented in the next Chapter.

6.5 Summary

In this chapter, a comprehensive analysis of the reliability of RC beams subjected to fire conditions is presented. The chapter begins with an introduction that outlines the objectives and importance of assessing structural integrity in fire scenarios. Following this, a model selection section discusses the criteria for choosing an appropriate resisting moment model for the RC beams, along with the validation and calibration processes that ensure its accuracy.

The selected beams section details the characteristics of the RC beams analyzed, including their dimensions and material properties. This foundation leads to a thorough statistical description of the basic variables, where the statistics related to both the resistance and load effects acting on the beams are derived.

The chapter continues with the establishment of the performance function of beams subjected to fire, which is critical for the subsequent reliability analysis. In the probabilistic calculation - MCS section, the methodology for conducting MCS is explained, focusing on the performance function and probabilistic parameters utilized in the analysis.

Finally, the discussion section synthesizes the results obtained from the reliability analysis, providing insights into the implications for the design and safety of RC beams exposed to fire.

7

LIFE-CYCLE COST ASSESSMENT OF RC BEAMS UNDER FIRE: A CASE STUDY

7.1 Introduction

Evaluating structural fire safety is crucial because fires pose significant risks to human life and the integrity of buildings. A fire can spread rapidly, compromising a structure's load-bearing capacity and potentially leading to collapse, failures, and serious harm to those inside or nearby. Consequently, structures must be designed and built with fire risk and appropriate protective measures in mind to reduce the impact of a potential fire. This includes using fire-resistant materials, implementing fire detection and alarm systems, installing fire suppression mechanisms, designing proper escape routes, and incorporating other fire safety provisions.

Assessing fire safety from a life cycle cost perspective allows for an informed analysis of costs, risks, and benefits over the lifespan of the structure. Structures built with fire protection measures in mind can better withstand fires, minimizing damage and loss. In the case study, failure probabilities of various beams under fire conditions were calculated, leading to considerations on what constitutes an acceptable failure probability and reliability index when factoring in risks, costs, and benefits.

A useful resource for calculating acceptable failure probabilities is the Design Guide - Structural Fire Safety by the International Council for Building (CIB, 1986), from which the methodology in this study adapts principles from Appendix 5 on Safety Factors and Differentiation Factors. Supporting studies in literature also reinforces this cost-based evaluation framework (Fisher, 2014; Van Coile et al., 2019B; Van Coile et al., 2018).

7.2 Acceptable Probability of Failure

The probability of reaching a specific limit state, such as when the failure condition M = R - S < 0 is met, was discussed in Chapter 4. Reliability methods like the First Order Reliability Method (FORM) and MCS, also covered in Chapter 4, are used to calculate failure probabilities. Here, $P_{f,a}$ and β_a represent the acceptable failure probability and target reliability index, respectively. Reliability verification ensures that these values meet established safety standards. As an example, target reliability indices can be introduced according to Szerszen and Nowak's (2003) calibration for various structural importance levels, helping define acceptable levels of risk and safety, summarized in the Table 7.1:

Table 7.1: Target Reliability index and failure probability according to Szerszen and Nowak (2003)

Structural Importance Level	**Target Reliability Index (β_a)**	**Target Failure Probability ($P_{f,a}$)**
Low-Risk Structures	2,5	6,2 x 10^{-3}
Moderate-Risk Structures	3,0	1,35 x 10^{-3}
High-Risk Structures	3,5	2,3 x 10^{-4}
Critical or Vital Structures	4,0	6,3 x 10^{-5}

Although Szerszen and Nowak provide reference values for general structural safety, determining an appropriate target reliability level for fire conditions requires a separate assessment. Fire scenarios introduce distinct challenges, including rapid temperature fluctuations, material degradation, and unpredictable fire dynamics. These factors may justify reliability targets that differ from those applied to conventional structural loads.

7.3 Application of the CIB Methodology

The acceptable failure probability for the (accidental) fire situation can be specified by Equation 7.1 (CIB, 1986):

$$P_{f,a} = \frac{p_l}{p_a} f(A) \tag{7.1}$$

where P_l is the acceptable probability of loss of life for a given reference period. Different values can be assigned to different safety classes - depending on the consequences of failure. Example values for acceptable loss of life (50 years) are listed in Table 7.2.

Table 7.2: Acceptable probability of loss of life (CEB, 1976, adapted)

Expected number of fatalities in case of fire	Economic losses		
	Low	Average	Great
Low	10^{-3}	10^{-4}	10^{-5}
Average	10^{-4}	10^{-5}	10^{-6}
Great	10^{-5}	10^{-6}	10^{-7}

P_a is the probability of occurrence of serious fires within the considered reference period. A simple estimate is obtained by Equation 7.2:

$$P_a = P(\text{fire}) P_1 P_2 ... \tag{7.2}$$

With P(fire) representing the probability of an (initial) fire outbreak, which depends on the occupancy and size of the compartment. In general, P(fire) can be modeled by Equation 7.3 (Rustein and Clarke, 1979):

$$P(\text{fire}) = pA^X \tag{7.3}$$

where p denotes the probability of occurrence per m²/year; A is the total area of fire compartments (m²); and X is an index with a value ≤ 1,0. For a calculation example it could be assumed as X = 1,0, therefore, we have a conservative value. The p values (per m²/year) are given in Table 7.3.

Table 7.3: Probability of occurrence of Fire (Rustein and Clarke, 1979, adapted)

Occupation	**Probability per m²/year**
Housing	10^{-5}
Offices	10^{-6}
Industrial buildings	10^{-6}

P_1,P_2, ... identify the decreasing probability of an initial fire turning into a major fire, depending on the various fire detection and firefighting provisions employed. Indicative values are shown in Table 7.4.

Table 7.4: Severe fire probability reduction factors (CIB, 1986, adapted)

Fire Safety Measures	P_i
Action of Fire Department	0,1
Properly maintained sprinkler system	0,02
Fire brigade	0,5 – 0,05
Properly maintained detection and alarm system	1 – 0,1

However, if multiple safety provisions are used, the product P_1P_2... should be linked to a lower bound to consider the interdependence of provisions in terms of their potential success.

A function f (A) can be introduced (Equation 7.4) to account an increased risk as the compartment size grow:

$$f(A) = \frac{A^*}{A} \tag{7.4}$$

with A* corresponding, for example, to the average compartment size for a certain type of occupancy.

7.3.1 Application to Case Study

7.3.1.1 Calculation of the Acceptable Probability of Failure

As a hypothetical scenario, it is assumed that the building under analysis is a hotel, with the case study focusing on one of its rooms. This hotel would have, for example, 4 floors, with each floor having 18 identical apartments as the one being studied (50 m² each), resulting in a total area of 3600 m², which is therefore the estimated area of the site.

7.3.1.2 Life and Economic Losses (Pf)

In this analysis, high economic losses and a moderate to high expected number of deaths will be considered. In this case, the acceptable annual probability of loss of life (P_f) is obtained from Table 7.2, by dividing the value of the life-cycle by 50, resulting in a value of $2\ x\ 10^{-8}$.

7.3.1.3 Probability of Occurrence of a Severe Fire (Pa)

From Table 7.3, the probability of fire occurrence per m²/year, denoted as p, is obtained, which is considered as 10^{-5} for residential buildings. The probability of an initial fire is then calculated accordingly.

P(fire) = $pA^X = 10^{-5}(3600)^1 = 0{,}036$

From Table 7.4 the following probability reduction factors will be adopted:

- Action of Fire Department → $P_1 = 0{,}1$
- Properly maintained sprinkler system → $P_2 = 0{,}02$
- The establishment does not have a fire brigade → $P_3 = 1$
- Properly maintained detection and alarm system → $P_4 = 0{,}1$

The annual probability of occurrence of a severe fire is then:

$P_a = P(fire)P_1P_2P_3 = (0{,}036)(0{,}1)(0{,}02)(0{,}1) = 7{,}2\ x\ 10^{-6}$

At this stage, it is also important to evaluate the outcomes in extreme situations, considering both the maximum and minimum levels of passive safety measures.

<u>Considering all passive measures:</u>

$P_a = P(fire)P_1P_2P_3 = (0{,}036)(0{,}1)(0{,}02)\ (0{,}5)(0{,}1) = 3{,}6\ x\ 10^{-6}$

<u>Not considering any passive measures:</u>

$P_a = P(fire)P_1P_2P_3 = 0{,}036$

7.3.1.4 Function f (A) Value

Since data about an "average fire compartment size" is not available, the function f (A) will be considered one, for this case study.

7.3.1.5 Acceptable Failure Probability and Reliability Index

Replacing the values of P_f and P_a calculated above in the Equation 7.1 and manipulating Equation 4.2, the following acceptable probability of failure and reliability index are obtained, respectively:

$$P_{f,a} = \frac{P_f}{P_a}\, f(A) = \frac{2\ x\ 10^{-8}}{7{,}2\ x\ 10^{-6}}\ 1 = \ 2{,}77\ x\ 10^{-3}$$

$P_{f,a} = \Phi(-\beta_a) \rightarrow \beta_a = -\Phi^{-1}\ (P_{f,a}) = \Phi^{-1}$ (0,9972)

Using the probability tables of the standard normal distribution, we obtain a $\beta_a = 2{,}77$.

<u>Considering all passive measures:</u>

$P_{f,a} = 5{,}56\ x\ 10^{-3}$

$\beta_a = 2{,}65$

<u>Not considering any passive measures:</u>

$P_{f,a} = 5{,}56\ x\ 10^{-7}$

$\beta_a = 3{,}72$

7.3.1.6 Case Study Reliability Assessment

In the case study, the reliability index, which represents the performance of the concrete beam, was calculated and presented in the Figures 6.12 to 6.19. A comparison of the values obtained with the target value calculated in this section is presented in Figures 7.1 to 7.4.

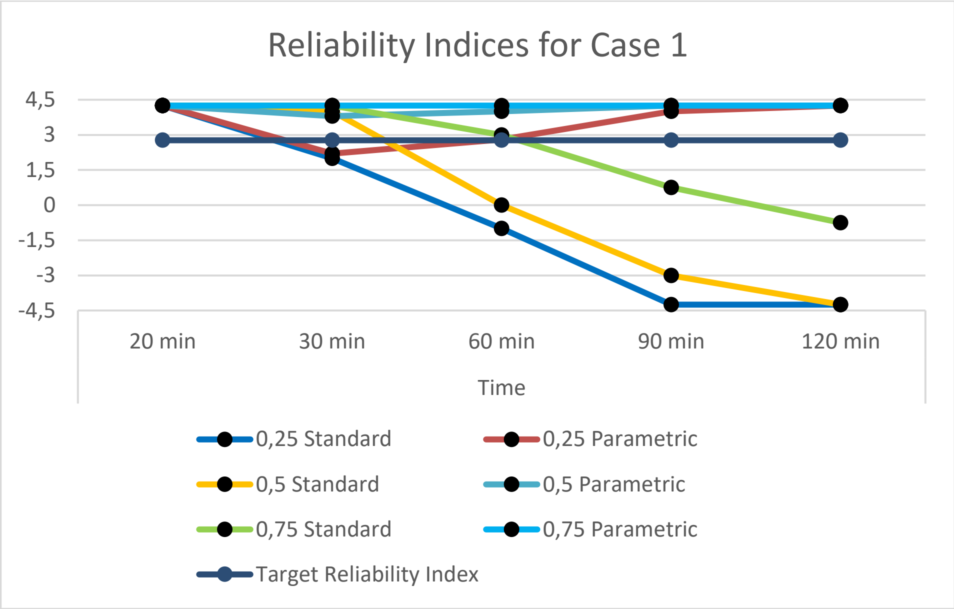

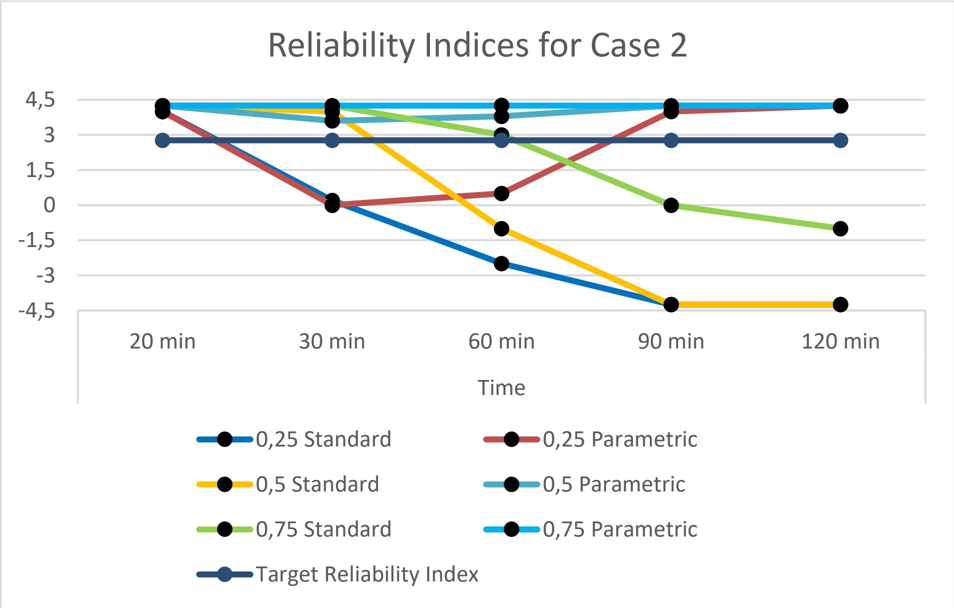

Figure 7.1: Representation of the target reliability index for cases 1 and 2

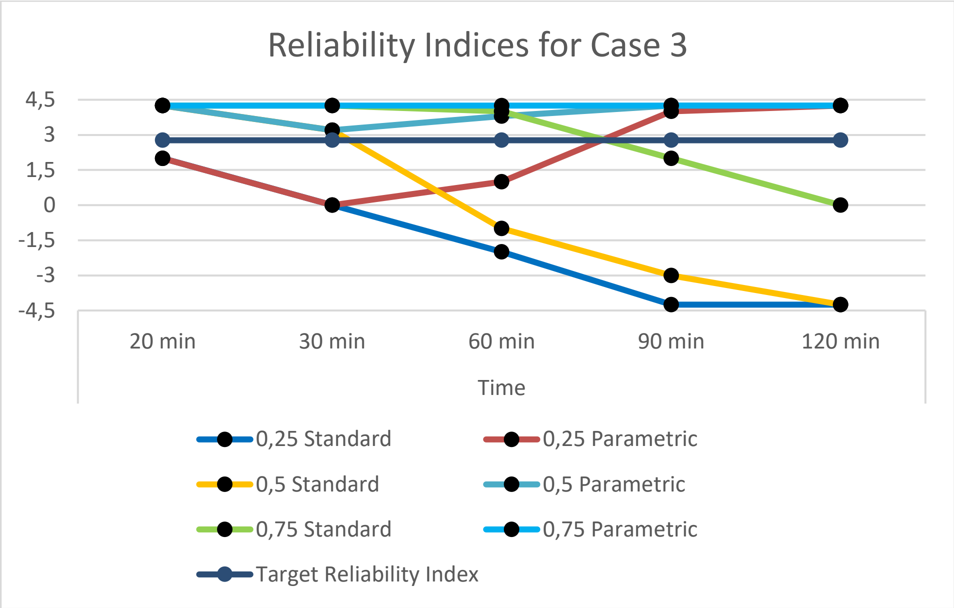

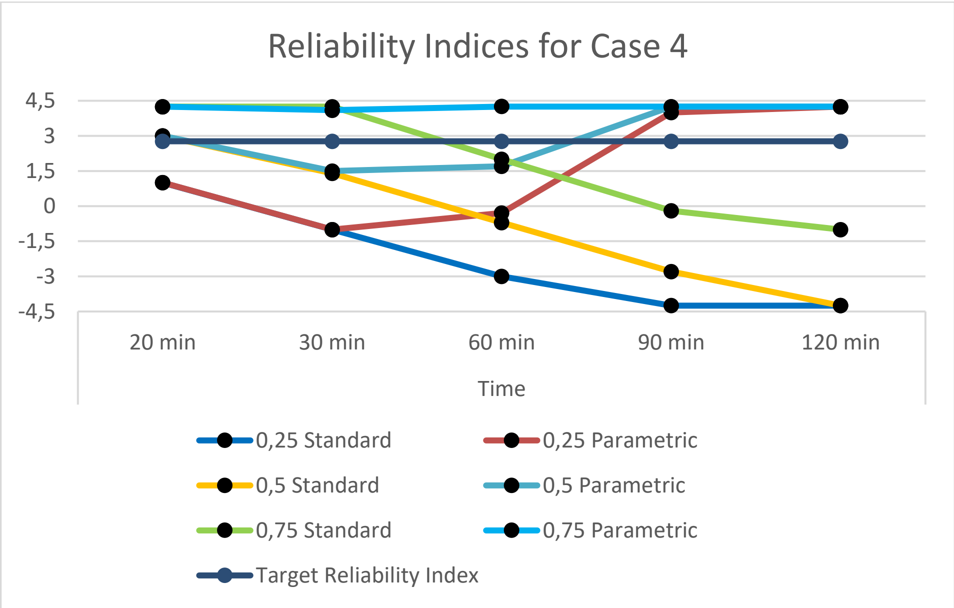

Figure 7.2: Representation of the target reliability index for cases 3 and 4

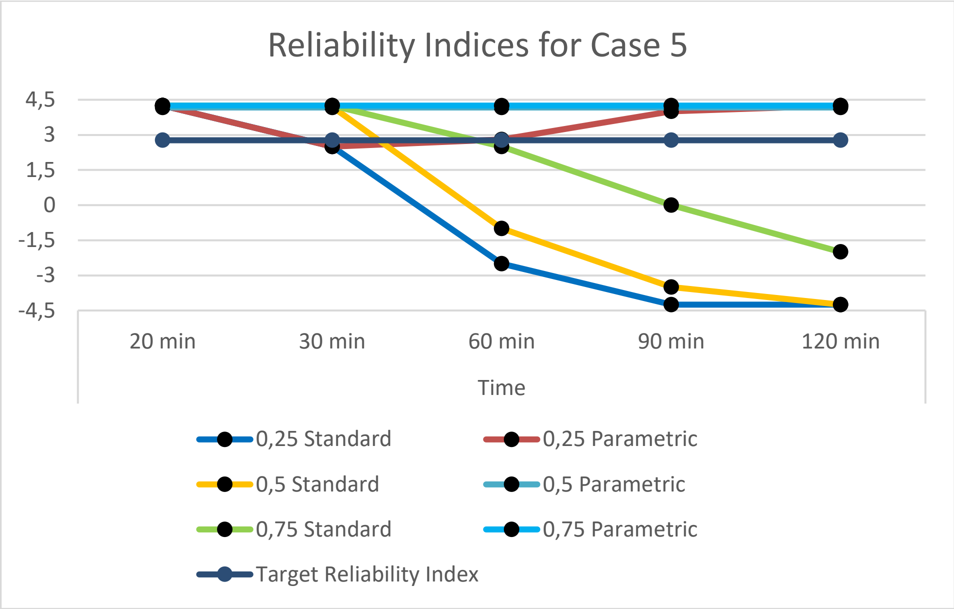

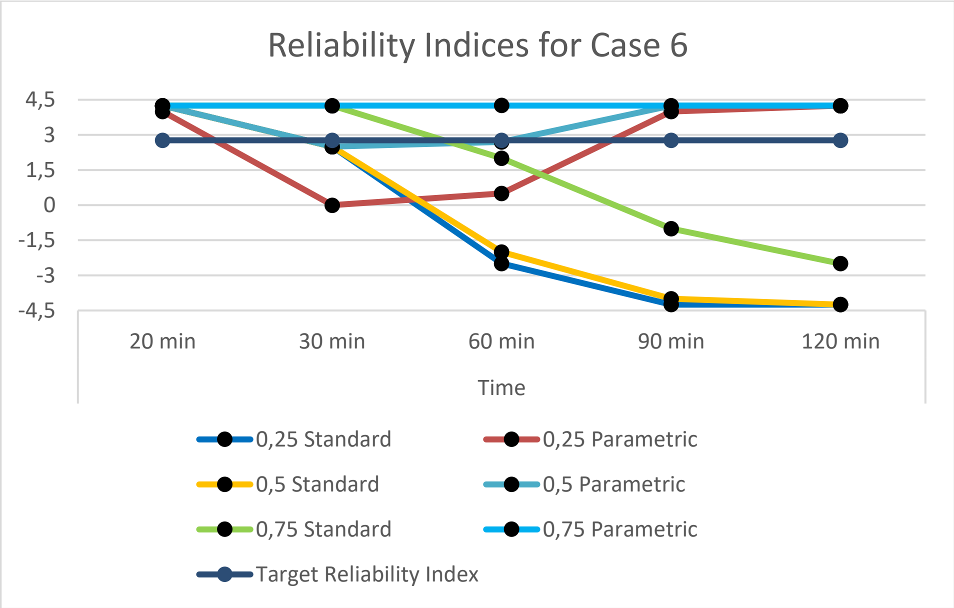

Figure 7.3: Representation of the target reliability index for cases 5 and 6

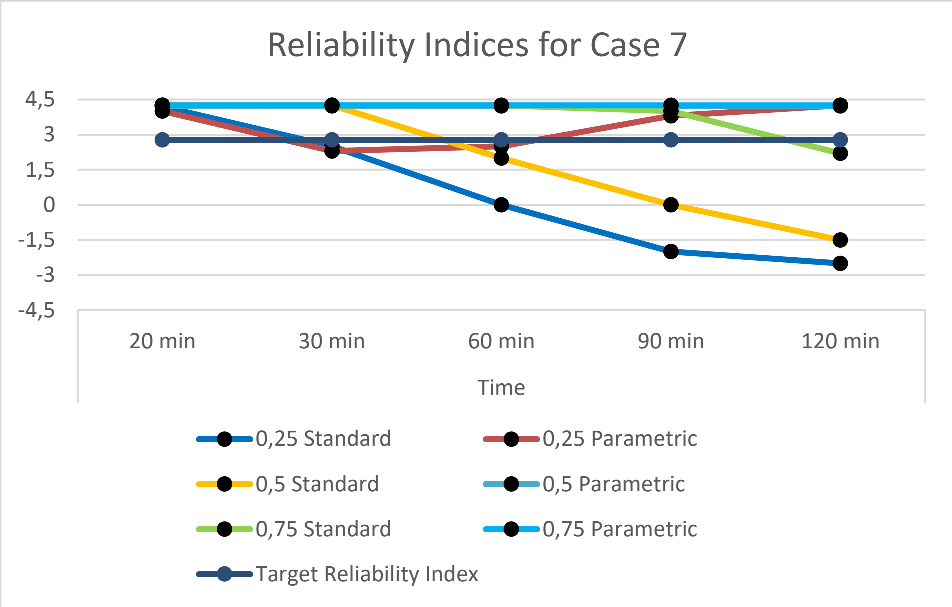

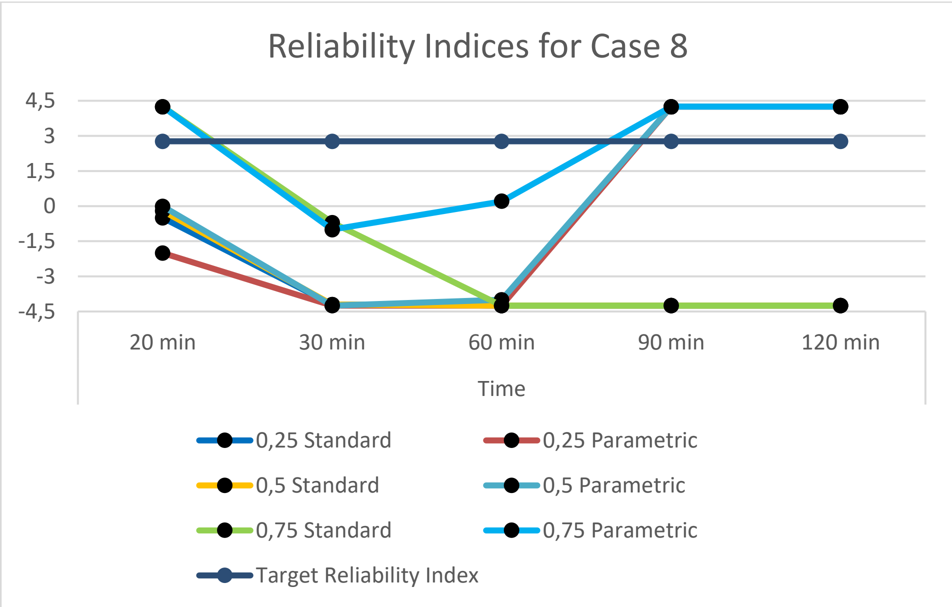

Figure 7.4: Representation of the target reliability index for cases 7 and 8

7.3.2 Methodology Discussion

From the Equations 7.1 and 7.2 presented, it can be seen how active protection measures can be considered, increasing the probability of acceptable failure by reducing the likelihood of fire development. This creates a trade-off between active and passive safety measures. For instance, in a scenario where a highly reliable fire suppression system limits the probability of a structurally significant fire to a very low level, it is understood that a substantial investment in active measures allows for a higher acceptable probability of failure. Consequently, a smaller investment in passive measures is anticipated, particularly when considering cost calculations related to structural safety. In this context, the maximum target reliability index found was 3,72 when no passive protection was considered, applicable in ambient temperature conditions for high-risk structures, critical or vital structures, according to Szerszen and Nowak (2003) – Table 7.1.

When all active safety measures are taken into account, the target reliability index decreases to 2,65. This reflects the enhanced robustness provided by these measures, which inherently reduce risk without relying solely on passive measures. In the case study, a target reliability index of 2,77 was observed, illustrating the nuanced balance between investments in active and passive safety measures. These findings emphasize the importance of integrating both types of protection to optimize overall safety while effectively managing costs.

This because, in real situations, resources are limited and spending on a certain security measure (active protection) leads to a reduction in resources to be applied to other measures (passive protection), that is, a trade-off is necessary (Hopkin et al., 2019).

Furthermore, as reported briefly, active measures are often interdependent (e.g. the fire brigade depends on fire extinguishers/ hydrant system to act), that is, one failure can lead to several others, which justifies the need, for example, of the establishment of a lower limit in the reduction of P(fire) - the case of multiplication P_1P_2... in Equation 7.2 - which cannot be zero.

Moreover, because they are active measures, they depend on human actions for activation. However, human error causes 20 to 90% of all major system failures or accidents, as discussed previously in section 4.2.2.7.

It is evident in this study that the failures indicated in the tables are not structural failures under fire conditions. These failures are more closely related to social factors, with human fatalities and economic losses being the main determinants.

It is important to emphasize that the consideration of these factors is relevant in this type of study, as it elevates the level of reliability analysis from a deterministic method to not only a probabilistic method but also a cost approach throughout the service life of the structure ($C_{lifetime}$). This could consider not only the cost associated with failure ($C_{failure\ associated}$) but also other costs such as those mentioned by Diniz (2006):

$$C_{lifetime} = C_{initial} + C_{inspection} + C_{repair} + C_{failure\ associated} + C_{demolition} + \dots$$

A weak point of this methodology is obtaining the statistical data presented in tables 7.1 to 7.3, which were used as an example. Each situation will vary depending on the technological development of the time and the applicable country. In this sense, research in this field should be developed, with the aim of maintaining constantly updated statistics on these parameters in order to correctly support the definition of an acceptable probability of failure, data that were not found in an updated form for the Brazilian reality.

Comparing the data observed in Figures 7.1 – 7.4 and considering the adopted methodology, several of the analyzed configurations would only be acceptable if the required fire resistance time (TRRF/FRR) for the structure—determined based on its occupancy type and building height—were 20 minutes. However, as shown in Figure 2.1, a 23-meter-high hotel (case under study) requires a fire resistance of at least 60 minutes. Under these conditions, many configurations would not meet the required safety levels, depending on the considered load ratio and fire type.

To address this issue, several measures could be implemented to enhance the fire resistance of the beams and ensure compliance with the required TRRF, as mentioned in last chapter. Possible solutions include increasing the concrete cover thickness to improve thermal insulation, using fire-resistant coatings or protective claddings, optimizing the reinforcement layout to ensure better residual capacity, or incorporating active fire protection systems such as sprinklers to reduce the severity of the fire exposure. Additionally, alternative design strategies, such as adjusting the structural load distribution or using higher-performance materials, could also be considered. The selection of the most suitable approach should be based on a cost-benefit analysis while ensuring that fire safety requirements are met.

It is important to note that technical standards are based solely on the standard fire. As can be seen in the Figures 7.1 – 7.4, many of the cases where the particularity of the case is evaluated, via parametrized fire, can lead to different understandings from the standardized ones. In general, many cases can be considered acceptable, since the fire temperature does not continue to increase indefinitely.

A methodology that considers several cost factors is discussed in the next section.

7.4 Application of the Life-Cycle Cost Methodology

In the realm of structural engineering and risk management, the concept of acceptable probability of failure and the associated cost methodology plays a vital role in optimizing structures and ensuring safety. The principle of ALARP (As Low As Reasonably Practicable) is central to these concepts, aiming to balance the cost of mitigating risks with the potential consequences of failure. Understanding these concepts and employing the appropriate methodologies is essential for effectively managing risks and making informed decisions in the design, construction, and maintenance of structures (Van Coile et al., 2019).

The evaluation methodology discussed here was adapted from Van Coile & Hopkin (2018), Van Coile et al. (2019) and Fisher (2014).

At this point it is worth rescuing Equation 4.15, where life-cycle cost (Y) is dependent of the (i) total building construction and maintenance cost (C), (ii) obsolescence cost (A), (iii) fire-induced material damages (D_M), (iv) fire-induced loss to human life and limb (D_L), and (v) reconstruction cost after fire-induced failure (D_R). The life-cycle cost function can then be described as follows (Van Coile and Hopkin, 2018):

$$Y(\theta) = C(\theta) + A(\theta) + D_M(\theta) + D_L(\theta) + D_R(\theta) \tag{7.5}$$

Each of the variables will be discussed in detail in the next sections.

7.4.1 Application to Case Study

7.4.1.1 Construction Cost (C)

Costs in beam construction can vary depending on several factors, including the type of beam, materials used, design requirements, labor costs, and project location. Here are some key cost considerations in beam construction (Dias, 2006):

1. **Material Costs:** The choice of materials significantly impacts on the overall cost of beam construction. Common materials for beams include steel, concrete, and wood. Each material has its own associated costs, which can vary based on availability, quality, and market conditions.
2. **Design Complexity:** The complexity of the beam design, such as the shape, span, and load-bearing requirements, can influence the construction costs. Complex designs may

require specialized fabrication techniques, additional supports, or customized components, which can increase material and labor expenses.

3. **Labor Costs:** The cost of skilled labor plays a significant role in beam construction. Labor costs can vary depending on factors such as the region, project timeline, labor availability, and specific skill requirements. Efficient construction planning and coordination can help optimize labor costs.
4. **Fabrication and Installation:** The fabrication and installation processes contribute to the overall cost. For concrete beams involve formwork, reinforcement placement, and concrete pouring.
5. **Equipment and Tools:** Beam construction may involve the use of specialized equipment and tools, such as cranes, lifting devices, formwork systems, and cutting tools. The cost of renting or purchasing these items should be considered.

The estimated cost for the study case was based on the author's experience and on the values established by SINAPI (National System of Prices and Indices for Civil Construction), considering the average values for May 2024 and are presented in Table 7.5.

Considering that the analysis of the entire research has been restricted to the beam, the cost assessment will also be restricted to this element, although it is known that the impact of failure on it can generate consequences for other structural components. In addition, the costs for maintenance of the beam will be neglected, considering that in the useful life of the structure, maintenance is hardly necessary in conventional situations.

Table 7.5: Beam construction cost

ITEN	SINAPI CODE	SERVICE DESCRIPTION	UNIT	QUANT.	UNIT. PRICE	TOTAL PRICE
1		**CONCRETE**				
	34483	PUMPABLE MACHINED CONCRETE, RESISTANCE CLASS C25, WITH GRAVEL 0 AND 1, SLUMP = 130 +/- 20 MM, EXCLUDES PUMPING SERVICE (ABNT NBR 8953)	m3	0,5	496,50	248,25
	88262	SHAPE CARPENTER WITH ADDITIONAL CHARGES	h	0,12	21,91	2,57
	88309	MASON WITH ADDITIONAL CHARGES	h	0,12	22,16	2,60
	88316	SERVANT WITH COMPLEMENTARY CHARGES	h	0,46	17,96	8,31
	90586	IMMERSION VIBRATOR, 45MM TIP DIAMETER, THREE-PHASE ELECTRIC MOTOR POWER OF 2 HP - CHP DAYTIME. AF_06/2015	chp	0,07	1,39	0,09
	90587	IMMERSION VIBRATOR, 45MM TIP DIAMETER, THREE-PHASE ELECTRIC MOTOR POWER OF 2 HP - CHP DAYTIME. AF_06/2015	chi	0,10	0,56	0,05
		SUB-TOTAL				261,87
2		**FORMWORK**				
	1345	PLASTIFIED PLYWOOD SHEET FOR CONCRETE SHAPE, 2.20 x 1.10 M, E = 18 MM	m²	2,15	91,58	196,90
	4491	STRIP *7.5 X 7.5* CM IN PINUS, MIXED OR REGIONAL EQUIVALENT - GROSS	m	2,18	7,92	17,27
	4517	BATH *2.5 X 7.5* CM IN PINUS, MIXED OR REGIONAL EQUIVALENT - GROSS	m	13,04	2,77	36,12
	5068	POLISHED STEEL NAIL WITH HEAD 17 X 21 (2 X 11)	Kg	0,39	25,43	9,92
	88239	CARPENTER'S ASSISTANT WITH ADDITIONAL CHARGES	h	0,47	18,89	8,86
	88262	SHAPE CARPENTER WITH ADDITIONAL CHARGES	h	2,34	21,91	51,30
	91692	BENCHMARKET CIRCULAR SAW WITH 5HP POWER ELECTRIC MOTOR, WITH 10" DISC COOKING - CHP DAYTIME. AF_08/2015	chp	0,12	25,63	3,03
	91693	BENCHMARKET CIRCULAR SAW WITH 5HP POWER ELECTRIC MOTOR, WITH 10" DISC COOKING - CHP DAYTIME. AF_08/2015	chi	0,35	24,42	8,52
		SUB-TOTAL				331,91
3		**REINFORCEMENT**				
	92803	CA-50 STEEL CUTTING AND BENDING, 10.0 MM DIAMETER	Kg	12,57	10,87	136,60
	92804	CA-50 STEEL CUTTING AND BENDING, 12.5 MM DIAMETER	Kg	15,71	9,35	146,87
	92805	CA-50 STEEL CUTTING AND BENDING, 16.0 MM DIAMETER	Kg	20,11	9,29	186,79
	92806	CA-50 STEEL CUTTING AND BENDING, 20.0 MM DIAMETER	Kg	18,85	10,96	206,59
	92791	CA-60 STEEL CUTTING AND BENDING, 6.3 MM DIAMETER	Kg	2,78	10,64	29,58
	43132	ANNEATED WIRE 16 BWG, D = 1.60 MM (0.016 KG/M) OR 18 BWG, D = 1.25 MM (0.01 KG/M)	Kg	0,015	24,75	0,37
	88245	OWNER WITH ADDITIONAL CHARGES	h	0,12	22,03	2,58
	88316	SERVANT WITH COMPLEMENTARY CHARGES	h	0,46	17,96	8,31
		SUB-TOTAL (excluding the reinforcement)				11,27
TOTAL 10,0 mm					**R$ 741,65**	**U$ 150,13**
TOTAL 12,5 mm					**R$ 751,93**	**U$ 152,21**
TOTAL 16,0 mm					**R$ 791,84**	**U$ 160,29**
TOTAL 20,0 mm					**R$ 811,65**	**U$ 164,30**

OBS: CHP - Productive Hourly Cost – considers the round-trip time of the transport (engine on), for the transport compositions; For the other compositions, it considers loading, unloading and maneuvering times; CHI - Unproductive Hourly Cost – considers waiting time and other working hours.

7.4.1.2 Obsolescence cost (A)

The obsolescence cost in the context of optimizing structures in fire situations refers to the economic impact associated with outdated or ineffective fire safety measures or technologies. It represents the cost incurred when existing fire protection systems, equipment, or strategies become obsolete or inadequate in the face of evolving fire hazards and standards (Fischer, 2014).

In the field of fire engineering, considering obsolescence costs is crucial for effective decision-making regarding the design, maintenance, and retrofitting of structures to enhance fire safety. By accounting for obsolescence costs, engineers can evaluate the long-term financial implications of implementing or neglecting necessary upgrades to fire protection systems.

This variable can be measured by (Van Coile & Hopkin, 2018):

$$A = C\ \frac{\omega}{\gamma} \tag{7.6}$$

where C is the initial cost, γ is the societal discount rate, that lies approximately between 2% and 5% (Fischer, 2014) and ω is the obsolescence rate, that could be approximated by $\frac{1}{expected\ life}$.

In this study, an average value of 3,5% is considered for societal discount rate (an average value). Considering the expected life for structures of 50 years, commonly used in studies, the obsolescence rate can be considered 0,02.

Important to note that the "societal discount rate" refers to a financial concept used in the optimization. It represents the rate at which future costs and benefits are discounted to their present value in order to make informed decisions about investments and resource allocation.

In the context of fire optimization, the societal discount rate is used to evaluate the economic viability of investing in fire prevention, mitigation, and response measures. It considers the long-term costs and benefits associated with different strategies and helps determine the optimal allocation of resources to minimize the overall impact of fires on society (Fischer, 2014).

The specific value of the societal discount rate can vary depending on factors such as the country, the specific project, and the time horizon being considered. It is often derived from a combination of economic, social, and environmental considerations. The rate typically reflects the opportunity cost of capital, inflation expectations, and the perceived value of future benefits compared to immediate costs (Fischer, 2014).

7.4.1.3 Fire-induced Material Damages (D_M)

The fire-induced material damage refers to the physical and structural harm caused to materials and components of a structure as a result of a fire. In the context of optimizing structures in fire situations, understanding and quantifying fire-induced material damages is crucial for evaluating the performance and resilience of the element, as well as for informing decisions regarding fire safety measures and structural design.

This variable can be measured by (Van Coile & Hopkin, 2018):

$$D_M = \mu_M \frac{\lambda_{fi} P_f}{\gamma} \tag{7.7}$$

where μ_M is the average failure cost, λ_{fi} is the rate of fully developed fire (Table 7.2) and P_f is the probability of failure.

λ_{fi}will have the same value as defined in section 7.3.1.3, that is 0,036.

To calculate the average failure cost of a beam belonging to a hotel, several factors need to be considered, including the consequences of failure, repair or replacement costs, and downtime or loss of revenue during the repair period.

1. **Consequences of Failure:**
    a. Cost of Property Damage: This includes the cost of repairing or replacing damaged components, such as walls, floors, or utilities affected by the beam failure.
    b. Business Interruption Costs: If the beam failure leads to the closure of the hotel or a section of it, the loss of revenue during the repair period needs to be considered.
2. **Repair or Replacement Costs:**

a. Cost of Beam Replacement: This involves the cost of removing the failed beam and installing a new one, including materials, labor, and associated construction expenses.

3. **Downtime and Loss of Revenue:**
   a. Loss of Revenue per Day: This is the average daily revenue generated by the hotel, which needs to be estimated based on factors like occupancy rate, room rates, and other income sources (e.g. restaurants, conference rooms).
   b. Repair Duration: The estimated time required for the repair or replacement of the beam.

One of the ways to consider these factors mathematically would be through the following formulas.

Average failure cost = cost of property damage + business interruption costs

- Cost of property damage = cost of beam replacement + cost of repairing other damaged components
- Business interruption costs = loss of revenue per day x repair duration

It will be considered, in this case, that the cost of beam replacement will be the same as the construction cost. The cost of repairing other damaged components will be considered a value of 20% of the construction cost as it is understood to be a reasonable value for correcting small, related damages.

Considering the limitation of the damage to a room and the average daily value for room rentals would be R$ 300,00 (U$ 60,00) and a correction time of 15 days, the business interruption cost could be considered R$ 4.500,00 (U$ 900,00).

It is important to note that the accuracy of these calculations depends on the quality of the data used and assumptions made. Gathering precise information regarding repair costs, revenue figures, and repair durations is crucial for obtaining reliable average failure cost estimates and may vary depending on the perception of the professional performing the analysis, the places where maintenance is conducted, the periods of the year, among others.

7.4.1.4 Fire-Induced Loss to Human Life (D_L)

Fire-induced loss to human life refers to the physical harm and potential loss of life caused by fires in structures. In the context of optimizing structures in fire situations, minimizing the risk of fire-induced loss to human life is a primary objective of fire protection and safety engineering.

This variable can be evaluated by (Van Coile & Hopkin, 2018):

$$D_L = \mu_L \frac{\lambda_{fi} P_f}{\gamma} \tag{7.8}$$

where μ_L is the LQI-based valuation of risk to human lives.

LQI-based valuation of risk to human lives refers to an approach for assessing and quantifying the level of risk to human lives based on the concept of "Life Quality Index" (LQI). It involves evaluating the potential impact of various hazards, such as fires, on the quality of life and well-being of individuals (Van Coile et al., 2019).

By employing the LQI-based valuation of risk to human lives, decision-makers can prioritize and allocate resources towards mitigating risks and implementing measures that aim to enhance the overall quality of life and well-being, particularly in situations involving hazards like fires (Van Coile et al., 2019).

It is worth noting that specific methodologies and approaches for LQI-based valuation may vary, and there may not be widely established standards or references available for this specific concept. However, it aligns with the broader field of risk assessment and risk management, where various frameworks and approaches exist to evaluate and quantify risks to human lives in different contexts (Fischer, 2014).

According to Van Coile et al (2019), LQI can be evaluated by:

$$LQI = g^q \, e \tag{7.9}$$

where g is the annual GDP per capita, e is the life expectancy and the exponent q define the trade-off between work and leisure.

The standard ISO 2394:2015 - *General Principles on Reliability of Structures* - states that q can, in general, be considered in the range of 0,18 - 0,20. For this study, an average value of 0,19 will be considered.

According to the world health organization GDP per capita for Brazil can be considered about R$ 43.978,36 (US$ 8.898) and the life expectancy of 75,9 years, considering the latest studies (2019).

In these terms, the LQI parameter can be considered $LQI = g^q\ e = \ 8.898^{0,19}\ 75,9 = 427,18$.

7.4.1.5 Reconstruction Cost after Fire-Induced Failure (D_R)

Reconstruction cost after fire-induced failure refers to the expenses associated with repairing or rebuilding a structure that has experienced structural failure due to a fire. In the context of optimizing structures in fire situations, understanding and estimating the reconstruction cost after fire-induced failure is important for evaluating the economic impact of fires and informing decisions regarding fire safety measures, structural design, and risk management.

This variable can be measured by (Van Coile & Hopkin, 2018):

$$D_R = C\ \frac{\lambda_{fi}\, P_f}{\gamma} \tag{7.10}$$

7.4.1.6 Acceptable Failure Probability and Reliability Index

A compilation of all the costs previously presented is summarized in Table 7.6, in terms of reals and dollars.

Finally, the total costs (Y) can be represented by the equations 7.11 to 7.14 respectively for φ10, φ 12,5, φ 16, φ 20 mm, in terms of dollars.

$$Y(P_f) = 235,92 + 1704,82\ P_f \tag{7.11}$$

$$Y(P_f) = 239,19 + 1709,53\ P_f \tag{7.12}$$

$$Y(P_f) = 251{,}88 + 1727{,}81\ P_f \tag{7.13}$$

$$Y(P_f) = 258{,}19 + 1736{,}89\ P_f \tag{7.14}$$

Table 7.6: Total costs

Initial Costs (C)	**R$**	**U$**
10,0 MM	741,65	150,13
12,5 MM	751,93	152,21
16,0 MM	791,84	160,29
20,0 MM	811,65	164,3
Obsolescence cost (A)	**R$**	**U$**
10,0 MM	423,80	85,79
12,5 MM	429,67	86,98
16,0 MM	452,48	91,59
20,0 MM	463,80	93,89
Fire-induced material damages (D_M)	**R$**	**U$**
10,0 mm	5543,98. P_f	1111,02. P_f
12,5 mm	5556,67. P_f	1113,58. P_f
16,0 mm	5605,93. P_f	1123,56. P_f
20,0 mm	5630,38. P_f	1128,51. P_f
Fire-induced loss to human life (D_L)	**R$**	**U$**
All cases	595,23. P_f	439,39. P_f
Rec. cost after fire-induced failure (D_R)	**R$**	**U$**
10,0 mm	762,84. P_f	154,42. P_f
12,5 mm	773,41. P_f	156,56. P_f
16,0 mm	814,46. P_f	164,87. P_f
20,0 mm	834,84. P_f	168,99. P_f

The values assumed by the functions and, consequently, the establishment of a target reliability index are dependent on the failure probability of the structure.

By plotting the cost as a function of the probability of failure in a range from 0 to 1, it is possible to visualize the behavior of the growth of functions and the low variability between them.

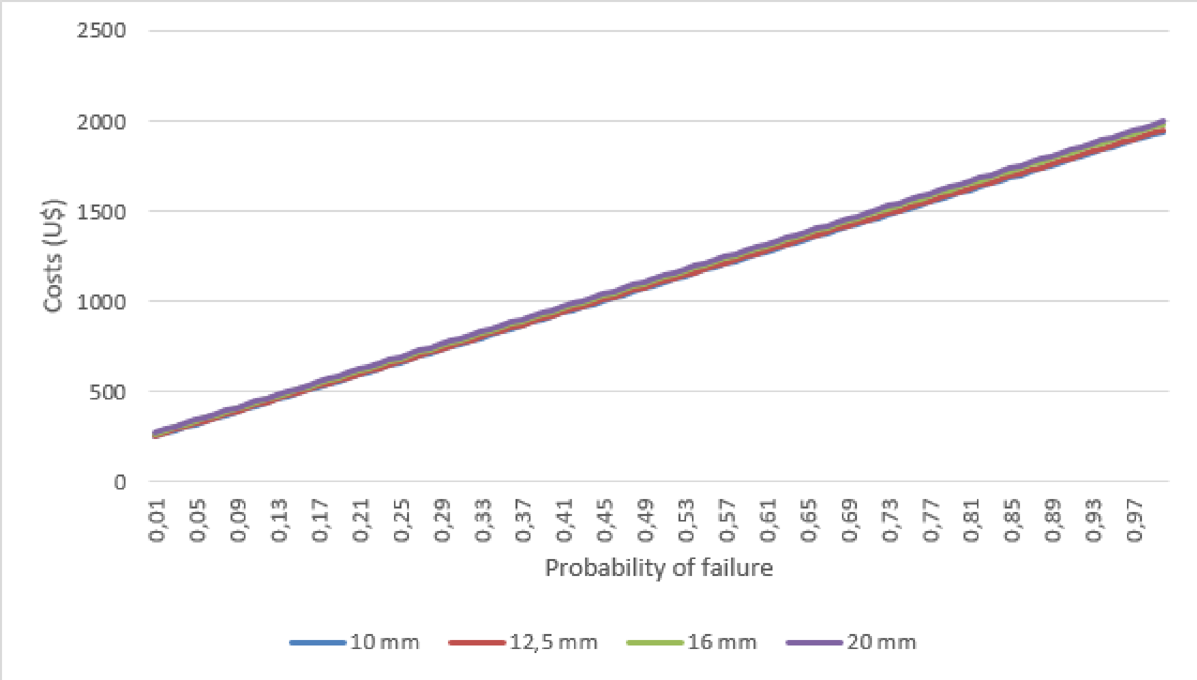

Figure 7.5: Costs as a function of the probability of failure

For this specific case, considering the acceptable failure probability defined in 7.3.1.5 as 0,00277, the acceptable cost for each case would be US$ 240,64 (φ10 mm), US$ 243,93 (φ 12,5), US$ 256,67 (φ 16 mm), US$ 263,00 (φ 20 mm).

7.4.2 Methodology Discussion

The life-cycle costs methodology, which incorporates the costs associated with the ALARP (As Low As Reasonably Practicable) concept and acceptable failure probability, necessitates a systematic approach to managing risks throughout the life-cycle of a system or structure. This methodology integrates economic considerations with the goal of minimizing risks to an acceptable level while optimizing costs over the system's operational life cycle (Van Coile et al., 2019).

Key aspects of this methodology, as observed in the case study, include risk identification and assessment. This initial phase involves a comprehensive evaluation of potential risks that the system or structure may encounter throughout its life-cycle. It requires analyzing various hazards, assessing their probabilities of occurrence, and evaluating the consequences of failure. The assessment takes into account both tangible and intangible costs associated with these potential failures.

The ALARP principle plays a crucial role in guiding decision-making within the risk management process. It emphasizes the importance of balancing the costs and benefits of risk reduction measures, aiming to lower risks to a level that is "As Low As Reasonably Practicable." This principle acknowledges that complete risk elimination may not be feasible or cost-effective, but it underscores the necessity of striving to reduce risks to an acceptable level.

A thorough cost-benefit analysis is also conducted to evaluate the economic implications of various risk reduction measures. This analysis compares the costs of implementing these measures with the potential benefits in terms of risk reduction and associated costs. The objective is to identify cost-effective strategies that align with the acceptable failure probability and deliver the greatest risk reduction for the investment made.

Furthermore, life cycle cost considerations are integral to the methodology. It encompasses not only the initial investment, but also the costs associated with maintenance, repair, and potential failures throughout the operational life-cycle of the system or structure. This long-term perspective allows decision-makers to assess the overall cost-effectiveness of different risk mitigation strategies.

Finally, the methodology emphasizes continuous monitoring and improvement. It highlights the importance of regularly reassessing risks and associated costs, recognizing that these factors may evolve over time. Adjustments may be necessary to ensure that risk mitigation measures remain effective and economically viable.

By adopting this methodology, engineers can make informed decisions that optimize life-cycle costs while managing risks to an acceptable level. This approach fosters an initiative-taking and systematic attitude toward risk management, balancing the need for safety with the economic feasibility of risk reduction measures.

It is important to note that in the case under study, costs remain low when considering just one beam. However, should the analysis be expanded to encompass the entire compartment or an entire structure, the costs would significantly increase. Moreover, the data obtained provides a framework for establishing parameters for each of the costs involved in the structure, allowing for an evaluation of the optimal value to be pursued concerning the expenses incurred.

7.5 Summary

This chapter provides a comprehensive assessment of life-cycle costs and the determination of an acceptable failure probability for RC beams subjected to fire conditions. It begins with an introduction to the significance of evaluating these factors in ensuring structural safety. The chapter then explores the CIB methodology, which integrates life and economic losses with the probability of a severe fire to establish an acceptable failure probability and reliability index. This is further illustrated through a case study that aids in understanding the practical implications of the methodology.

Following this, the chapter discusses the application of the life-cycle cost methodology, which encompasses various aspects such as construction costs, obsolescence costs, fire-induced material damages, loss of human life, and reconstruction costs. By analyzing these elements, the methodology seeks to determine optimal costs associated with the maintenance and safety of RC structures in fire scenarios.

The comparative analysis of the two methodologies highlights their respective strengths and applications, emphasizing their importance in enhancing the design and safety of RC structures under fire conditions. The insights gained from this chapter are intended to inform future research and practical applications within the field of structural engineering, ultimately contributing to improved safety standards and cost-effectiveness in high-risk environments.

8

Summary, Conclusions and Suggestions for Future Research

8.1 Summary

The present study introduced a comprehensive framework for assessing the reliability of RC beams in fire scenarios. This research underscored the disparities in partial safety factors among various standards, including ABNT NBR 8681, ACI 216.1, and ASCE 7. It highlighted a significant gap in systematic and probabilistically calibrated approaches for integrating fire effects into current design standards for RC structures. Unlike steel beams, which have established reliability analyses in both national and international contexts, RC beams are notably underrepresented in this regard.

While concrete is inherently non-combustible and offers insulation due to its low thermal conductivity, the findings highlight the need for further investigation. Various uncertainties related to key parameters—such as the steel's yield strength, the concrete's compressive strength, and their degradation at elevated temperatures—warrant a more detailed analysis. Although concrete generally performs well under extreme conditions, certain scenarios require a deeper understanding of its behavior when exposed to fire.

The design criteria for RC beams at ambient temperatures are based on limit states determined through probabilistic analyses. However, the existing standards for designing RC structures in fire scenarios predominantly rely on prescriptive methods, such as those outlined in ABNT NBR 15200:2024. Consequently, there is a clear need for further research to update these standards, aligning them with the philosophical underpinnings of ABNT NBR 6118:2023.

This research commenced with an exploration of fire engineering principles, emphasizing the significance of this topic in light of historical fire incidents in Brazil, such as the fires at the Joelma and Andraus buildings in São Paulo. It presented essential concepts including fire severity, fire resistance, and the ABNT NBR 15200:2024 standard for RC structures in fire situations. Subsequently, the design methods proposed by this standard were elucidated, and the model chosen for calculating the beam's resistance was validated and calibrated through Finite Element Method (FEM) analysis using the SAFIR software.

Additionally, the study introduced structural reliability concepts, addressing the inherent uncertainties in engineering design and various reliability analysis methods. The Monte Carlo Simulation (MCS) method was chosen for its practicality in handling complex probabilistic evaluations, with a total of 1.000.000 simulations performed across all cases.

To systematically assess fire performance, four distinct configurations of RC beams were analyzed under fire exposure durations of 20, 30, 60, 90, and 120 minutes, considering both standard and parametric fire conditions. For each beam configuration and fire duration, simulations were conducted while varying the load ratios (r = 0,25, 0,50, and 0,75) and concrete cover thickness. This resulted in a total of forty-eight unique scenarios, with the large sample size ensuring statistical robustness in the reliability assessment.

In conclusion, this research presented and applied a comprehensive methodology for evaluating the likelihood of acceptable failure through a life-cycle cost analysis. These methodologies not only offer valuable insights into risk management but also facilitate informed decision-making across diverse scenarios. By implementing these approaches, organizations can enhance their risk management strategies, optimize costs, and improve overall performance, leading to more effective and sustainable outcomes.

8.2 Conclusions

Fire represents one of the most prevalent hazards that RC structures encounter, capable of inflicting substantial damage and leading to structural failures. Therefore, evaluating the reliability of RC beams under fire exposure is critical to ensuring their safe and continued operation. Furthermore, the financial implications associated with the maintenance and repair of fire-damaged structures can be considerable, making the analysis of life-cycle costs for RC beams essential.

This study shifted from a deterministic evaluation of RC beam performance to a reliability-based approach, accounting for the variability of design factors and incorporating both random (inherent) and epistemic uncertainties. The research highlighted the challenges in selecting a reliable model for assessing the performance of RC beams under elevated temperatures, especially considering the limited body of research in the field of structural reliability for fire conditions.

Building on the findings from the methodology discussions, this research highlights the significant impact of fire suppression systems on the decision-making process related to structural reliability. When active protection measures are effectively implemented, the acceptable probability of failure increases, allowing for reduced investments in passive measures. For example, the maximum target reliability index of 3,72, observed without passive protection in the case study, illustrates the delicate balance between safety investments. On the other hand, with comprehensive active safety measures in place, the reliability index drops to 2,65, emphasizing the importance of an integrated approach that optimizes both safety and cost.

However, in the context of fire scenarios, the reliability index should always be greater than or equal to its value under ambient temperature conditions (e.g., $\beta = 2{,}8$ for beams in ambient temperature). With comprehensive active fire protection measures in place, the reliability index drops to 2,65, indicating the importance of maintaining an adequate level of reliability even under fire conditions. This reflects the necessity of a well-integrated safety approach that balances both safety and cost, ensuring that the reliability index does not fall below the baseline established for normal conditions, whether or not fire suppression measures are employed.

The analysis also emphasized the need to account for substantial variability in material properties under fire conditions, such as carbonization and the reduction of cross-sectional area. This variability introduces uncertainties that can adversely affect the performance of RC structures. By conducting a reliability assessment, the study identified potential deficiencies in design, thereby providing a basis for reevaluating structural performance to meet expected standards.

Moreover, the study confronted challenges in obtaining reliable data regarding acceptable probabilities of loss of life, the probability of fire occurrence, and factors influencing severe fire probabilities, which are critical for effective risk management. The emphasis on obtaining contextually relevant data for the Brazilian reality is paramount, as it supports more accurate risk assessments and informs better decision-making.

The methodology discussion also highlighted the life-cycle costs associated with the ALARP (As Low As Reasonably Practicable) principle, underscoring the necessity for a systematic approach to risk management. This approach includes conducting thorough cost-benefit analyses to evaluate the economic implications of various risk reduction measures, ensuring that costs associated with maintenance, repair, and potential failures are adequately integrated into the decision-making process.

Furthermore, the evaluation of parameterized fires indicated that bending resistance stabilizes after 30 minutes of exposure, suggesting a departure from excessively conservative designs based on standard fire scenarios. This realization reinforces the potential for optimizing designs through nuanced analyses that consider the characteristics of the specific compartment, potentially leading to cost reductions while maintaining safety.

In conclusion, this research provides a theoretical foundation for advancing ABNT NBR 15200:2024 towards a probabilistic framework that enables performance-based evaluations rather than strictly prescriptive assessments. The proposed methodology offers a reliability and cost-effective design framework for RC beams subjected to fire exposure, considering uncertainties related to material properties, structural parameters, and fire conditions. By integrating considerations of life-cycle costs, risk management principles, and the interplay between active and passive safety measures, this approach not only serves as a basis for optimization of life-cycle costs, but also ensures the reliability of the structure. This research delivers valuable insights for engineers and designers in the construction industry, fostering the development of safe and economically viable RC structures capable of withstanding the challenges posed by fire hazards.

8.3 Suggestions for Future Research

Building on the insights gained from the conducted study, as well as recognizing the gaps identified in the literature and the limited existing research on this important theme, several valuable avenues for future research are suggested:

- **Development of Models:** The current study utilized simplified models to address uncertainties in the interaction between fire and RC beams, but the complex behavior exhibited by these structures under fire conditions presents significant modeling challenges. To better capture this interaction, future research could focus on developing more sophisticated probabilistic models that integrate Finite Element Modeling (FEM) with fire dynamics. By incorporating statistical distributions and stochastic processes, these advanced models can enhance the representation of how fire affects structural integrity, accounting for factors such as temperature gradients and material degradation. This approach aims to improve predictive accuracy and supports the development of innovative design strategies that enhance fire safety and resilience in structural engineering.

- **Spalling:** The prediction and modeling of spalling behavior in RC structures exposed to fire present significant complexities and uncertainties, which were outside the scope of the current research but could have a substantial impact on the results. Future studies should prioritize the investigation of spalling mechanisms and the various factors influencing this phenomenon, such as concrete composition, moisture content, and heating rates. Given the variability of these factors, developing accurate predictive models for spalling is essential for a comprehensive understanding of how RC behaves under fire conditions. By incorporating spalling into future analyses, researchers can enhance the reliability of their predictions and improve the overall assessment of structural performance in fire scenarios, leading to safer and more resilient design practices.
- **Boundary Conditions:** The current study focused solely on simply supported beams, which provided a foundational understanding of the behavior of RC structures under fire conditions. However, this limitation highlights the potential for future research to explore a broader range of boundary conditions. Investigating different support configurations, such as columns and slabs, could yield valuable insights into how various boundary conditions influence the fire performance and structural integrity of RC beams. By expanding the scope to include these alternative conditions, future studies can enhance the applicability of the findings and contribute to a more comprehensive understanding of the behavior of structures subjected to fire, leading to improved design methodologies and safety standards.
- **Failure Mode:** The current study primarily focused on the flexural behavior of RC beams under fire conditions, providing valuable insights into their performance. However, this focus on flexural behaviour limits the understanding of the full structural response. Future research could benefit from investigating the effects of fire on shear behavior in RC beams. By examining how shear forces interact with fire conditions, researchers can gain a more comprehensive understanding of the structural performance

under extreme conditions. This is particularly important since shear failure, which can lead to sudden and brittle rupture, is a critical concern under fire conditions. Expanding the scope to include shear effects will not only enhance the reliability of predictive models but also contribute to the development of more robust design guidelines, ensuring the safety and resilience of structures exposed to fire.

- **Statistics of Random Variables:** The inherent variability in concrete properties, such as strength and thermal conductivity, poses significant challenges for accurately predicting structural performance. Future research should focus on developing advanced statistical models that capture the uncertainty and variability of these random variables more effectively. This could involve utilizing probabilistic methods that incorporate comprehensive data sets, including material tests and environmental factors, to better characterize the stochastic nature of concrete behavior under fire. By enhancing the statistical treatment of these variables, future studies can improve the reliability of performance predictions and contribute to more resilient structural designs in fire scenarios.
- **Experimental Validation:** Specifically, it is crucial to investigate cases that were not covered in the current studies, such as varying fire scenarios, different beam geometries, and alternative material compositions. Additionally, a more in-depth examination of the mean values, standard deviations, and distribution types of the random variables considered will enhance the robustness of the findings. By conducting experiments that encompass a wider range of conditions and uncertainties, future studies can provide a more comprehensive understanding of RC beam performance under fire, leading to improved design practices and safety standards.
- **System vs. Component Reliability Analysis:** The current study focused exclusively on the reliability of a single structural component, specifically an RC beam, under fire conditions. While this approach provides valuable insights into the behavior of individual components, it does not fully capture the complexities of system-level reliability, especially when multiple failure modes, such as bending and shear, can occur within a single component. Future research should expand the analysis to explore the interactions and dependencies between various structural elements in a complete system. By examining how components like beams, columns, and connections interact under fire exposure, researchers can develop a more comprehensive understanding of overall system reliability. This expanded approach could also address potential failure

modes that arise from the interactions of multiple components, ultimately leading to more effective design strategies and improved safety in fire scenarios.

- **Optimization Techniques:** The current study employed a standard methodology to determine the target reliability index for different assumptions regarding the performance of RC beams under fire conditions. However, this approach has room for enhancement. Future research should focus on exploring advanced optimization techniques that can refine design strategies, making them more efficient and cost-effective. Additionally, investigating how different design variables interact within the context of fire exposure could lead to more robust and innovative solutions.
- **Economic Analysis:** While the current study provided a foundational economic analysis of RC beams under fire conditions, it primarily focused on initial costs without delving deeply into the complexities of long-term economic factors, such as discount rates. Future research should place greater emphasis on exploring the implications of discount rates in economic evaluations, as they significantly impact the perceived cost-effectiveness of various design strategies over time. By incorporating realistic discount rates, researchers can more accurately assess construction costs, maintenance expenses, and potential revenue losses during periods of downtime. Comprehensive analyses that consider the time value of money will enhance understanding of the long-term financial implications of different design approaches, guiding stakeholders toward more cost-optimal solutions for RC beams exposed to fire.
- **Risk Tolerability and Valuation of Human Life:** Determining an acceptable level of risk in the context of RC structures exposed to fire is inherently subjective and varies significantly depending on stakeholders' perspectives, regulatory requirements, and societal norms, as evidenced in the case studies. Additionally, the ethical complexities surrounding the valuation of human life further complicate this assessment. Assigning a monetary value to human life can be controversial and may not adequately reflect the emotional and social impacts of potential fatalities or injuries. Future research should explore these intertwined issues by examining how risk tolerability frameworks can be developed to incorporate ethical considerations and the societal implications of risk assessment. This approach will contribute to a more nuanced understanding of risk management strategies that prioritize both safety and the human experience in fire scenarios.

- **Human Error:** The current study acknowledged the influence of human error on the performance and safety of RC beams under fire conditions, but this aspect was not thoroughly examined. Future research should focus on systematically analyzing the role of human error in design, construction, and maintenance processes related to fire safety. By investigating how factors such as decision-making, communication, and operational practices contribute to human error, researchers can identify critical areas for improvement. Incorporating methodologies such as Human Factors Engineering and Failure Mode and Effects Analysis (FMEA) could provide valuable insights into minimizing human errors in fire-related scenarios. A deeper understanding of human error can lead to the development of more effective training programs, guidelines, and design strategies that enhance the safety and reliability of RC structures under fire exposure.

REFERENCES

ACI 216.1-07. “Code Requirements for Determining Fire Resistance of Concrete and Masonry Construction Assemblies”. American Concrete Institute, Farmington Hills, MI, 2007.

ACHENBACH, M., GERNAY, T., MORGENTHAL, G. “Quantification of model uncertainties for reinforced concrete columns subjected to fire”. Fire Safety Journal, 108, 102832, 2019.

FORRESTER A. I. J., SÓBESTER A., KEANE A. J., “Engineering Design via Surrogate Modelling: A Practical Guide”, 2008.

ANEESHA BALAJI, M.; AATHIRA, T.; MADHAVAN PILLAI, M. AND NAGARAJAN, P. “Reliability studies on RC beams exposed to fire based on IS456:2000 design methods.” Structural Engineering and Mechanics Journal, 2016.

ANG, A. H-S., TANG, W. H. “Probability Concepts in Engineering Planning and Design. Volume II: Decision, Risk, and Reliability”. John Wiley & Sons. Pg 206 -216, 1990.

ANG, A. H-S., TANG, W. H. “Probability Concepts in Engineering Planning and Design. Volume I: Basic Principles”. John Wiley & Sons. Pg 82, 1975.

ASCE/SEI 7-10. “Minimum Design Loads for Buildings and Other Structures”. American Society of Civil Engineers, Reston, VA, 2010.

BACARJI, E. “Building structures analysis: column design”. Master's Dissertation, São Carlos School of Engineering, University of São Paulo, 1993.

BAI, L.; WANG, Z.; HAN, Y., ZHU, D. “Analysis of residual load-carrying capacity and reliability of RC beams after exposure to fire”. Journal of Harbin Engineering University, 42(2), 126-138, 2007.

BAI, L.; WANG, Z.; SU J.; QIAO M. “Bending reliability of RC beam after fire exposure”. Journal of Harbin Engineering University, 47(3), 226-238, 2009.

BAILEY, C.G. AND KHOURY, G. “Performance of concrete structures in fire”. MPA The Concrete Centre, United Kingdom, 2011.

BRAZILIAN ASSOCIATION OF TECHNICAL STANDARDS. "ABNT NBR 8681: Actions and Safety in Structures - Procedure". Rio de Janeiro, 2004.

BRAZILIAN ASSOCIATION OF TECHNICAL STANDARDS. "ABNT NBR 15200: Design of concrete structures in a fire situation - Procedure". Rio de Janeiro, 2024.

BRAZILIAN ASSOCIATION OF TECHNICAL STANDARDS. “ABNT NBR 14432: Fire resistance requirements for building construction elements - Procedure”. Rio de Janeiro. 2001.

BRAZILIAN ASSOCIATION OF TECHNICAL STANDARDS. “ABNT NBR 6118: Design of concrete structures – Procedure”. Rio de Janeiro, 2023.

BRAZILIAN ASSOCIATION OF TECHNICAL STANDARDS “ABNT NBR 6120: Loads for the calculation of building structures”. Rio de Janeiro, 2019.

BSI. “Fire Tests on Building Materials and Structures”. BS 476-20. British Standards Institution, London, 1987.

CAI, B.; FENG, F. “A new reliability analysis approach for the flexural capacity of postfire reinforced concrete beams retrofitted with CFRPs”. ICE Proceedings Structures and Buildings, 2019.

CIB 1986. Design Guide for Structural Fire Safety. Fire Safety Journal, vol 10, Fire Commission of the Conseil International du Batiment, 1986.

CEB 1976. Common Unified Rules for Different Types of Material and Construction; Report nº 116, Joint Committee for Structural Safety, 1976.

COELHO, T. A. P. “Reliability Assessment of Reinforced Concrete Beam Sections in a Fire Situation”. Master’s dissertation. Federal University of Minas Gerais, 2018.

COELHO, T. A. P.; DINIZ, S. M. C.; RODRIGUES, F. C. “Estimating the elastic modulus of concrete under moderately elevated temperatures via impulse excitation technique”. Journal of Structural Fire Engineering. , v.15, p.603 - 618, 2024.

COSTA, C. N. “Design of reinforced concrete elements in a fire situation”. PhD Thesis, University de São Paulo, 2008.

COSTA, C. N.; SILVA, V. P. “Design of reinforced concrete structures in a fire situation. Tabular methods presented in international standards”. V EPUSP Symposium on concrete structures, 2003.

COSTA, C. N; RITA, I. A. et al. “Principles of the "500 ºC method" applied in the design of reinforced concrete columns in a fire situation, based on the requirements of ABNT NBR 6118 (2003) for design at room temperature”. IBRACON - 46th Brazilian Concrete Congress, 2004.

CROCE, P.A. GROSSHANDLER, W.L.; BUKOWSKI, R.W.; GRITZO, L.A. “A position paper on performance-based design for fire code applications.” Fire Safety Journal, 43(3), 234- 236, 2008.

DEFALCO, F. D. “Investigation of the compressive response of modern structural steels at fire load temperatures”. Ph.D Thesis, University of Connecticut, 1974.

DIAS, P. R. V. Cost Engineering: A Budgeting Methodology for Civil Works. 6. ed. Rio de Janeiro: Hoffmann, 215 p, 2006.

DINIZ, S.M.C. “Structural Reliability: Rational Tools for Design Code Development”, 2008 Structures Congress: Crossing Borders, 2008.

DINIZ, S. M. C. A "Structural Reliability and the Evolution of Technical Standards". VI EPUSP Symposium on Concrete Structures, April 2006.

DITLEVSEN, O.; MADSEN, H. O. "Structural reliability methods". 1. ed. Wiley, 1996.

EAMON, C; JENSEN, E. "Reliability analysis of prestressed concrete beams exposed to fire". Journal of Structural Engineering, 43(1), 69-77, 2012.

EAMON, C; JENSEN, E. "Reliability Analysis of RC Beams Exposed to Fire". Research Publications - Wayne State University, 2013.

ELLINGWOOD, B.R.; SHAVER, J.R. "Reliability of RC Beams Subjected to Fire." ASCE Journal of the Structural Division. 103(ST5), 1047-1059, 1977.

EUROCODE 1. "Design of Concrete Structures. ENV 1992, Actions on structures - Part 1-2: General actions - Actions on structures exposed to fire". Brussels: European Committee for Standardization, 2002.

EUROCODE 2. "Design of Concrete Structures. ENV 1992, Part 1-2: General Rules- Structural Fire Design". Brussels: European Committee for Standardization, 2002.

FABER M. H.; SORENSEN J. D., "Indicators for inspection and maintenance planning of concrete structures," Structural Safety, vol. 24, no. 2–4, pp. 377–396, 2002.

FÉDERATION INTERNATIONALE DU BÉTON – CEB-FIP. "MC 2010: Model code 2010". Lausanne, 2011.

FISCHER, K. "Societal decision-making for optimal fire safety". ETH Zurich, 2014.

FITZGERALD R.W. "Structural Integrity during Fire". Fire Protection Handbook. 18ª Edition. National Fire Protection Association. Quincy, Massachusetts, 1997.

FRANGOPOL, D.M; ESTES, A.C. "Life-Cycle Cost Design of Deteriorating Structures", Journal Structural Engineering, ASCE, Vol.123, No.10, pp.1390-1401, 1997.

GERNAY, T. "Thermal Response of Structures". Lecture notes. Johns Hopkins University, 2018.

GERNAY, T. "Fire resistance and burnout resistance of reinforced concrete columns". Fire safety journal. 104, 67-78, 2019.

GERNAY, T.; KODUR, V., NASER, M.Z., IMANI, R., BISBY, L. Concrete Structures. In: International Handbook of Structural Fire Engineering (Eds.: LaMalva, K. and Hopkin, D.). Springer, Cham, 2021.

GREEN MF, BENICHOU N, KODUR V, BISBY LA. "Design Guidelines for Fire Resistance of FRP-Strengthened Concrete Structures"; Eighth International Conference on FRP in Reinforced Concrete Structures FRPRCS-8, 2007.

GUEDES SOARES, C. Quantification of model uncertainty in structural reliability. In: Guedes Soares, C. Probabilistic Methods for Structural Design v. 56, 1997.

HALDAR, A.; MAHADEVAN, S. "Probability, Reliability, and Statistical Methods in Engineering Design", Wiley, 304 p., 2000.

HARMATHY, T. Z., "Thermal Properties of Concrete at Elevated Temperatures," J. of Materials 5, 47–74, 1970.

HART G. C. "Uncertainty Analysis, Loads, and Safety in Structural Engineering". Prentice-Hall, Englewood Cliffs, Nova Jersey, 1982.

HERTZ, K. "Analyses of prestressed concrete structures exposed to fire". Technical University of Denmark, Lyngby, 1985.

HIBBELER, R. C. Strength of materials. 7.ed. São Paulo: Pearson Prentice Hall, 637 . p. ISBN: 8576053736, 2015.

HOPKIN, D.; SPEARPOINT, M.; ARNOTT, M.; VAN COILE, R. "Cost-benefit analysis of residential sprinklers— Application of a judgement value method". Fire Saf. J. 106, 61–71, 2019.

HOPKIN, D., FU, I., and VAN COILE, R. "Adequate fire safety for structural steel elements based upon life-time cost optimization". Fire Safety Journal, 103095, 2020.

HOPKIN, D., VAN COILE, R., LANGE, D. "Certain uncertainty - demonstrating safety in fire engineering design and the need for safety targets". SFPE Europe, 7, 2017.

HOSSER, D., DORN, T., & RICHTER, E. "Brandschutztechnische Bemessung von Bauteilen nach Eurocode 2-5: Vergleichsrechnungen zur Untersuchung des Sicherheitsniveaus bei unterschiedlichen Bauarten; Abschlußbericht". Institut für Baustoffe, Massivbau und Brandschutz, 1995.

HOSSER, D., WEILERT, A., KLINZMANN, C., SCHNETGÖKE, R., & ALBRECHT, C. "Erarbeitung eines Sicherheitskonzeptes für die brandschutztechnische Bemessung unter Anwendung von Ingenieurmethoden gemäß Eurocode 1 Teil 1-2 (Sicherheitskonzept zur Brandschutzbemessung)". Abschlussbericht zum DIBt-Vorhaben ZP, 52-5, 2008.

INACIO, P. J. "Evolution of ambient temperature in buildings subject to fire". Master's dissertation. Universidad Nova de Lisboa, 2011.

IS 456, "Plain and reinforced concrete - Code of Practice", Fourth revision, Bureau of Indian Standards, New Delhi, 2000.

ISO 2394:2015. "General principles on reliability of structures". International Standard, 2015.

JCSS. "Probabilistic Model Code". The Joint Committee on Structural Safety. Available online at https://www.jcss-lc.org/jcss-probabilistic-model-code/, 2002.

JENSEN, E, J. VAN HORN, C. EAMON. "Variability of Fire and Concrete Temperatures and the Associated Uncertainty in Structural Behavior". Proceedings, 6th Intl Conference on Structures in Fire, Lansing, MI, 959-966, 2010.

JOVANOVIĆ, B., VAN COILE, R., HOPKIN, D., ELHAMI KHORASANI, N., LANGE, D., & GERNAY, T. “Review of current practice in probabilistic structural fire engineering: permanent and live load modelling”. Fire Technology, 2020.

KODUR, V. “Properties of Concrete at Elevated Temperatures”. Hindawi Publishing Corporation. ISRN Civil Engineering. Volume 2014, Article ID 468510, 2014.

KRISHNA, A., PRIYADARSINI, R.S., & NARAYANAN, N. “Effect of Elevated Temperatures on the Mechanical Properties of Concrete”. In Proceedings of the 2nd International Conference on Structural Integrity and Exhibition 2018. Paper presented at the conference, College of Engineering, Thiruvananthapuram, Kerala, India, 2018.

LAW, M. “Prediction of Fire Resistance”, Paper in Symposium No. 5, Fire Resistance Requirement of Buildings, A New Approach. Department of the Environment and Fire Offices Committee Joint Fire Research Organization. HMSO. London, 1973.

LI, Y., TANG, Y. “Experiment Study and Function Reliability Analysis on RC Continuous Beam Subject to High Temperature and Strengthened with CFRP Sheets”. Journal of Harbin Engineering University, 2005.

LIND, N. C., NATHWANI, J. S., & SIDDALL, E. “Managing risks in the public interest”. Waterloo: Institute of Risk Research. University of Waterloo Press, 1992.

LIND, N. C.; DAVENPORT, A. G. “Calibration of design codes”. Journal of the Structural Division, ASCE, v. 98, n. ST7, p. 1639–1654, 1972.

LUCHERINI, A. “Experimental study of the behavior of steel structures protected by different intumescent coatings and exposed to various fire scenarios” Thesis for: M.Sc. in Civil Engineering. Technical University of Denmark, 2016.

MA, Q., R. GUO, Z. ZHAO, Z. LIN, and K. HE. “Mechanical properties of concrete at high temperature—A review.” Constr. Build. Mater. 93 (Sep): 371–383, 2015.

MADSEN, H.O., KRENK, S., E LIND, N.C., “Methods of Structural Safety”, Prentice Hall, New Jersey, p. 403, 1986.

MALHOTRA, H. L. “In Situ/Nondestructive Testing of concrete – A Global Review“, In Situ/Nondestructive Testing of Concrete, ACI Special Publication SP-82, American Concrete Institute, Detroit, 1984.

MALIK, M., BHATTACHARYYA, S.K., & BARAI, S.V. “Thermal and mechanical properties of concrete and its constituents at elevated temperatures: A review”. Construction and Building Materials, 270, 121398, 2021.

MARAEAS, C; FASOULAKIS, Z; TSAVDARIDIS, K. “Post-fire assessment and reinstatement of steel structures”. Journal of Structural Fire Engineering, Vol 8 No. 2, 2017.

MATHWORKS. “Reliability Analysis Tools”. Retrieved February 22, 2024, from https://www.mathworks.com/help/stats/reliability-analysis.html , 2024.

MEHTA, P.K.; MONTEIRO, P.J.M. “Concrete: structure, properties and materials”. São Paulo: PINI, 573p, 1994.

MELCHERS, R. E., BECK, A. T. "Structural Reliability Analysis and Prediction". 3a. ed. Hoboken: John Willey & Sons, 506 p, 2018.

MELCHERS, R. E. "Structural Reliability: Analysis and Prediction". Ellis Horwood Ltd., Chichester. Pg 52-62, 1999.

NEGRISOLO, W. "Architecting fire safety". Graduate Program in Architecture and Urbanism at the University of São Paulo. São Paulo, 2011.

NISTIR 7563. "Best Practice Guidelines for Structural Fire Resistance Design of Concrete and Steel Buildings". National Institute of Standard and Technology, 2009.

NOWAK A.S., SZERSZEN M. "Calibration of design code for buildings (ACI 318): Part 1—statistical models for resistance". ACI Struct J 2003;100(3):377–82, 2003.

NOWAK, A. S.; COLLINS, K. R. "Reliability of structures". 2. ed. CRC Press, 2013.

O'CONNOR, M. "Performance based design of buildings in fire". Technical Lecture Series 2019 of the Institution of Structural Engineers. Available in https://www.youtube.com/watch?v=PDj2pbBwAVk, 2019.

PURKISS, J.A. "Fire Safety Engineering". Elsevier, 2007.

QUINTIERE, J. G. "Principles of Fire Behavior". Delmar Publishers, New York. Pg 2-3, 1998.

QURESHI R., NI, S., KHORASANI, N.E., VAN COILE, R., GERNAY, T. "Probabilistic models for temperature-dependent strength of steel and concrete". Journal of Structural Engineering, 146(6), 2020.

RACKWITZ, R. "Optimization the basis of code-making and reliability verification". Struct Saf 2000;22:27-60, 2000.

REIS, A. S. "Determination of fire scenarios in buildings". Dissertation (master's in civil engineering). Aveiro University. Portugal. 2011.

RIGBERTH, J. "Simplified Design of Fire Exposed Concrete Beams and Columns", Report No.5063, Department of Fire Safety Engineering, Lund University, Sweden, 2000.

ROBERT, F.; DAVENNE, L; STOIAN, L. "Fire resistance assessment of concrete structures". Workshop 'Structural Fire Design of Buildings according to the Eurocodes' – Brussels, 2012.

RUSTEIN, R.; CLARKE. M. B. "The Probability of Fire in Different Sectors of Industry", Fire Surveyor, 1979.

SEITO, A. I., GILL, A.A., ONO, F.D.P, SILVA, S.B., CARLO, U.D., SILVA, V.P. "Fire Safety in Brazil". São Paulo: Project Editor. 2008.

SHOOMAN, M.L. "Probabilistic reliability: an engineering approach". New York: McGraw-Hill, 1968.

SILVA, V. P. "Steel Structures in Fire Situation". São Paulo, 2001.

SPINARDI, G., BISBY, L. & TORERO, J. “A Review of Sociological Issues in Fire Safety Regulation”. Fire Technology, 53, 1011-1037, 2017.

STEWART, M. G., MELCHERS, R.E. “Probability Risk Assessment of Engineering – Systems”. Chapman & Hall, London. Pg 186-201, 1997.

SZERSZEN, M.M., NOWAK, A.S. “Calibration of design codes for buildings (ACI 318): Part 2 - Reliability analysis and resistance factors”. ACI Structural Journal, V. 100, n. 3, 383-391. New York. 2003

SZOKE, S. “PBD: A Component in the Future of Structural Engineering”. Structure Magazine, 2015.

TANG, Y. “Experiment Study and Reliability Analysis on RC Continuous Beam under High Temperature Function Strengthened with CFRP Sheets”. Journal of Harbin Engineering University, 38(3), 05-20, 2006.

THOFT-CHRISTENSEN, P., BAKER, M. J. “Structural Reliability Theory and Its Applications”. Spriner-Verlag, Berlin. Pg 4-7, 1982.

VAN COILE, R.; CASPEELE, R. AND TAERWE, L. “Full-Probabilistic Analysis of Concrete Beams During Fire”. Journal of Structural Fire Engineering, 2011.

VAN COILE, R., CASPEELE, R., AND TAERWE, L. “Lifetime cost optimization for the structural fire resistance of concrete slabs”. Fire technology, 50(5), 1201-1227, 2014.

VAN COILE, R. ”Reliability-based decision making for concrete elements exposed to fire”. Doctoral dissertation. Ghent University, 2015.

VAN COILE, R.; CASPEELE, R. AND TAERWE, L. “Towards reliability-based structural fire safety: development and probabilistic applications of a direct stiffness method for concrete frames exposed to fire”. Master’s Dissertation, 2016.

VAN COILE, R., HOPKIN, D. “Target safety levels for insulated steel beams exposed to fire, based on lifetime cost optimization”. Proceedings of IALCEE 2018, 2018.

VAN COILE, R., HOPKIN, D., LANGE, D., JOMAAS, G., & BISBY, L. “The need for hierarchies of acceptance criteria for probabilistic risk assessments in fire engineering”. Fire technology, 55(4), 1111-1146, 2019A.

VAN COILE, R.; JOMAAS, G.; BISBY, L. “Defining ALARP for fire safety engineering design via the Life Quality Index”. Fire Saf. J, 107, 1–14, 2019B.

VROUWENVELDER, T. “Developments towards full probabilistic design codes”. Structural Safety 24, 417-432, 2002.

WANG, Z.; QIAO, M.; ZHU, D. AND HAN, Y. “The Reliability Analysis of Reinforced Concrete Beams under High Temperature”. Proceedings, 2010 Third International Joint Conference on Computational Science and Optimization, 327-330, 2010.

WANG, Z.; XUE, Z.; AND QIAO, M. "Analysis on fire resistance of reinforced concrete beams base on the failure probability". Key Engineering Materials Vols. 452-453, pp 197-200, 2011.

WICKSTROM, U. "A very simple method for estimating temperature in fire exposed concrete Structures". Fire Technology Technical Report SP-RAPP 1986: 46. Swedish National Testing Institute, 1986.

YANG, X. P. "The effect of fire conditions on reliability of steel beam". China, 2011.

ZEHFUSS, J. and HOSSER, D. "A parametric natural fire model for the structural fire design of multi-store buildings". Fire Safety Journal, 42, Issue 115-126, 2007.

ZEIML, M., LACKNER, R., and MANG, H.A., "Experimental insight into spalling behavior of concrete tunnel linings under fire loading". Acta Geotechnical. 3(4): p. 295-308, 2008.

ANNEX A – RELIABILITY ANALYSIS: APPLICATION IN ONE OF THE BEAM CONFIGURATIONS

A1. Objective

The objective of this appendix is to describe in detail the procedure conducted in the reliability analysis of RC beams in a fire situation for the bending limit state. For this purpose, the evolution of the probability of failure is evaluated for different temperatures ranging from 20 to 120 min of fire exposure. As an example, the detailed analysis of one of the configurations established in Chapter 6 is presented.

A2. Geometric Characteristics and Mechanical Properties of Materials

The beam with reinforcement of 4 ϕ 12,5 mm will be used to illustrate the procedure adopted in the reliability analysis. The characteristics of this beam are:

Tabel A.1: Characteristics of the Beam Under Study

Characteristics Related to Resistance	Characteristics Related to load effects
• f_{ck} = 25 MPa = 2,5 kN/cm² • f_{yk} = 500 MPa = 50 kN/cm² • b = 20 cm • h = 50 cm • γ_g = 1,4 • γ_q = 1,4 • A_s = 5,0 cm² • ρ (%) = 0,50 • d' = 4,5 cm • s = 3,5 cm	• r = 0,25 • L = 5 m • Uniformly distributed load • 120 min of fire exposure • Standard fire

A3. Calculation of the resisting moment and load effects

a) Determining Resisting Moments

The deterministic resisting moment can be calculated using Equation 3.7, which for 120 min of fire exposure is:

$M_R\ (T) = \left(A'_s . f_y(T_r)\right) . (d - d') + \ (A_s - A'_s). f_y(T_r). \left(d - \frac{a(T_c)}{2}\right)$ = 13,53 KN.m

Where:

$f_y(T_r) = f_y . r$ = 60,38 MPa

- $n_x = n_y = \ 0{,}18 \ln\left(\frac{\alpha_r t}{s^2}\right) - 0{,}81 = 0{,}391$

  - $\alpha_r$obtained via calibration with FEM results = 0,75;

  - t = 120 min /60 min = 2 hours;

  - s = 0,035 m

- $n_w = 1 - 0{,}0616 t^{-0{,}88}$ = 0,967

- $T_r = \left(n_w . \left(n_x + n_y - 2. n_x . n_y\right) + \left(n_x . n_y\right)\right) T$ = 643,24 °C

  - T = 1.049 °C

- $r = \frac{720-(T_r+20)}{470} = \ 0{,}121;\ 0 \le r \le 1;$

$a(T_c) = \frac{(A_s - A'_s).f_y(T_r)}{0{,}85.f_c.b(T_c)} = 0{,}00985$ m

- $x_{500} = \sqrt{\frac{\alpha_r t}{\exp\left(4{,}5 + \frac{480}{0{,}18 n_w T}\right)}} = 0{,}0292$ m

- b (T_c) = b – 2.x_{500} = 0,1415 m

The deterministic equation for the generation of the statistics of the resisting moment is given by Equation 6.1. Using the MCS code that uses the statistics of the basic variables related to the resisting moment (see Table 6.2) it is found, for the case of 120 min of fire exposure (performing the MCS with 100,000 sample size), that the resisting moment has a mean of 15,96 kNm, minimum value of 11,11 kNm and maximum value of 22,50 kNm. The corresponding histogram is presented in Figure A1.

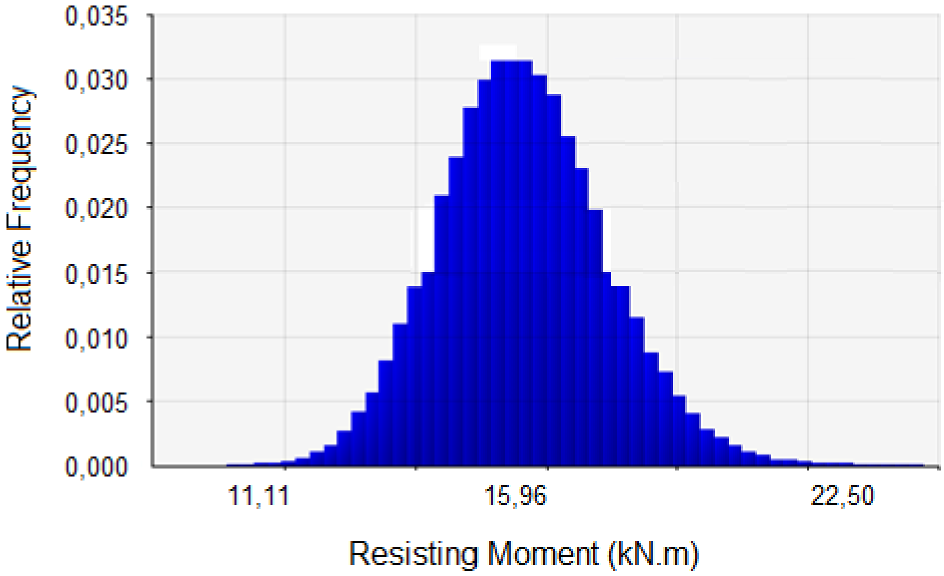

Figure A.1: Histogram of the Resisting Moment

a) Determining the Bending Moment

Before proceeding with the evaluation of the applied moment, it is necessary to define the mean values of the permanent and accidental loads. This calculation can be performed using Equations 6.11 and 6.12, considering that the applied moment can be taken as equivalent to the resisting moment (limit situation), as explained in the previous chapters.

$\mu_{\mathrm{LL}} = \frac{8}{L^2} \cdot \frac{M_{Sd}}{\left(\frac{5.(1-r)}{\mathrm{r}}.\gamma_g + \frac{\gamma q}{0,2}\right)} = 1,21$ kN

- $M_{Sd} = M_n\ (T) = 13,53\ \mathrm{KN.m}$

$\mu_{\mathrm{PL}} = \mu_{\mathrm{LL}}.\frac{5.(1-r)}{\mathrm{r}} = 18,19$ kN

The equation for evaluating the statistics of the bending moment is presented in Equation 6.2, thus resulting in the following equation:

$M_{S,fi} = \boldsymbol{\theta}_{\mathbf{S}}.(M_{PL} + M_{LL}) = \theta_S.\left[\left(\frac{L^2}{8}.PL\right) + \left(\frac{L^2}{8}.LL\right)\right]$

$\mu_{\mathrm{PL}} = PL$

$\mu_{\mathrm{LL}} = LL$

Using the MATLAB code to develop a MCS and the statistics for the bending moment defined in Table 6.11 it is found (performing the MCS with a sample size of 100.000) that the bending moment has a mean of 57,60 kNm, minimum value of 53,95 kNm and maximum value of 64,81 kNm. The corresponding histogram is presented in Figure A2.

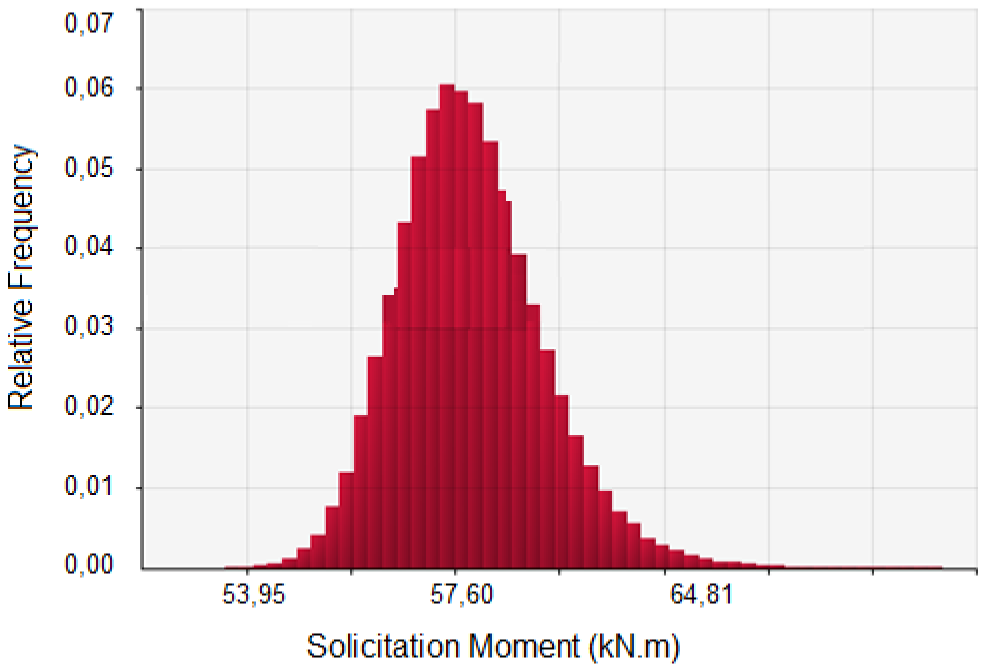

Figure A.2: Histogram of the Bending Moment

A4. Calculation of the Failure Probability

Using the code, once again, and the same number of iterations already used in the other analyses, the probability density curves are obtained as presented in Fig. A3.

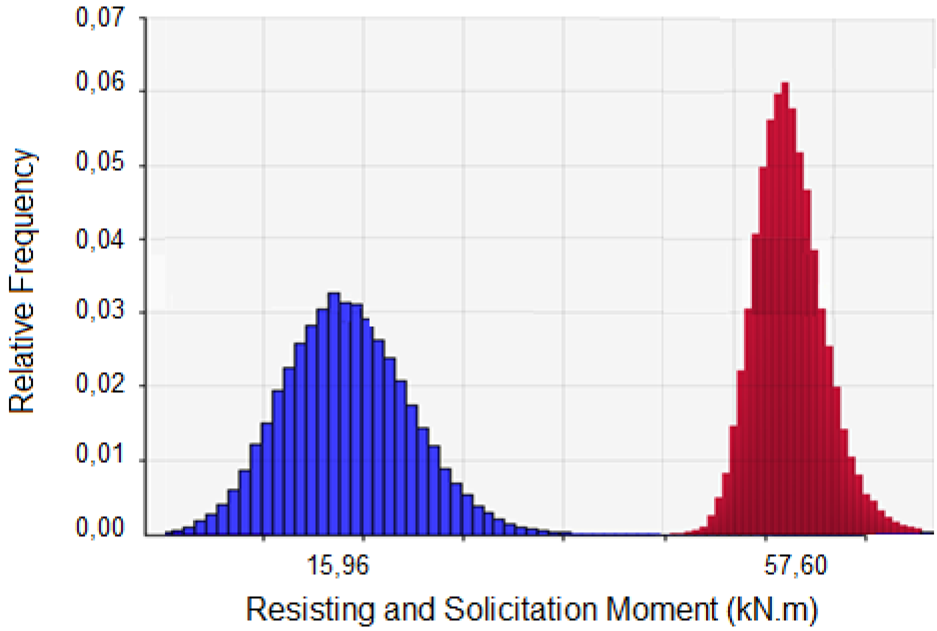

Figure A.3: Histograms of the Bending Moment (red) and Resisting Moment (blue)

Figure A.3 illustrates the supply (resistance) vs. demand (bending moment) problem, related to the beam under analysis at a temperature of 120 min of fire exposure. In the evaluation of the structural reliability of the RC beam in fire conditions, the output of interest is the probability of failure (e.g. the probability that the safety margin assumes values less than or equal to zero).

For this case, it is clear that the probability of failure is maximal, at practically 100% (see Figure 6.3), a result expected for exposure to fire for 120 min.

From the obtained probability of failure, the corresponding reliability index is given by Equation 4.2:

$$\beta = \Phi^{-1}\,(1 - 0{,}99999) =\approx -4{,}25$$

A5. Calculation of Error Associated with Sample Size

As demonstrated in Equation 4.14, the error associated with the sample size can be defined as follows.

$$\%error = 200\sqrt{\frac{1-P_f}{n\,.P_f}} = 0{,}00065\%$$

In other words, the estimated failure probability has a margin of error of ± 0,00065%.

ANNEX B – MATLAB CODE FOR RELIABILITY ANALYSIS

```
% MCS for Reliability of Reinforced Concrete Beam in Fire Situation

% Close all open figures
close all;

% Define constants and parameters
b = 0.2; % Width of the beam (m)
h = 0.5; % Height of the beam (m)
L = 5; % Length of the beam (m)
fc = 25000; % Compressive strength of concrete (kN/m²)
fy = 500000; % Yield strength of steel (kN/m²)

% Load ratios
rc = [0.25, 0.5, 0.75];

% Time of exposure to fire (minutes)
time_exposure = [20, 30, 60, 90, 120];

% Number of MCS
num_simulations = 1000000;

% Progress bar setup
f = waitbar(0, 'Simulation Progress');
tic; % Start timer

% Define cases (As, A's, s, d')
cases = [0.00032, 0, 0.045, 0.040;
         0.00032, 0, 0.035, 0.030;
         0.00050, 0, 0.045, 0.039;
         0.00050, 0, 0.035, 0.029;
         0.00080, 0, 0.045, 0.037;
         0.00080, 0, 0.035, 0.027;
         0.000945, 0, 0.045, 0.035;
         0.000945, 0, 0.035, 0.025];

% Standard and parametrized fire temperatures (considering compartment
characteristics)
standard_fire_temperatures = [781.35, 841.8, 945.34, 1006, 1049];
parametrized_fire_temperatures = [787.69, 840.98, 643.18, 345.37, 47.57];

% Alpha values for standard and parametrized fires (via calibration with SAFIR
results - Range: 0.75 - 1.5)
alpha_standard = [1.48, 1.30, 1.10, 0.98, 0.78;
                  1.35, 1.22, 1.03, 0.95, 0.81;
                  1.30, 1.21, 1.05, 0.92, 0.75;
                  1.34, 1.18, 1.07, 0.97, 0.77;
                  1.25, 1.16, 1.02, 0.90, 0.86;
                  1.27, 1.15, 1.11, 0.99, 0.72;
                  1.32, 1.19, 1.12, 0.95, 0.71;
                  1.45, 1.22, 1.08, 0.96, 0.79];
```

```
alpha_parametrized = [1.48, 1.32, 1.50, 1.50, 1.50;
                      1.35, 1.25, 1.50, 1.50, 1.50;
                      1.30, 1.33, 1.50, 1.50, 1.50;
                      1.34, 1.31, 1.50, 1.50, 1.50;
                      1.25, 1.28, 1.50, 1.50, 1.50;
                      1.27, 1.27, 1.50, 1.50, 1.50;
                      1.32, 1.33, 1.50, 1.50, 1.50;
                      1.45, 1.37, 1.50, 1.50, 1.50];

% PL and LL values for each case and load ratio
PL_LL_values = [11.89, 0.79, 7.93, 1.59, 3.96, 2.38;
                12.16, 0.81, 8.11, 1.62, 4.05, 2.43;
                18.19, 1.21, 12.13, 2.43, 6.06, 3.64;
                18.61, 1.24, 12.41, 2.48, 6.20, 3.72;
                28.66, 1.91, 19.10, 3.82, 9.55, 5.73;
                29.35, 1.96, 19.56, 3.91, 9.78, 5.87;
                33.09, 2.21, 22.06, 4.41, 11.03, 6.62;
                33.89, 2.26, 22.60, 4.52, 11.30, 6.78];


% Initialize arrays to store reliability indices and failure probabilities
reliability_indices  =  zeros(length(cases),  length(rc),  length(time_exposure),
2); % 2 for standard and parametrized fire
failure_probabilities = zeros(length(cases), length(rc), length(time_exposure),
2);

% Initialize arrays to store Mn_T values and statistics
Mn_T_values = zeros(size(cases, 1), length(time_exposure), 2, num_simulations);
% 2 for standard and parametrized fire
Mn_T_stats = zeros(size(cases, 1), length(time_exposure), 2, 4); % 4 for min,
mean, max, cov
random_theta_R_values   =   zeros(size(cases,   1),   length(time_exposure),   2,
num_simulations); % 2 for standard and parametrized fire


% Loop over each case
for case_num = 1:size(cases, 1)
    As = cases(case_num, 1);
    A_s = cases(case_num, 2);
    s = cases(case_num, 3);
    d_prime = cases(case_num, 4);
    d = h - d_prime;

    % Loop over load ratios
    for rc_idx = 1:length(rc)

        % Get PL and LL values for the current case and load ratio
        PL = PL_LL_values(case_num, rc_idx * 2 - 1);
        LL = PL_LL_values(case_num, rc_idx * 2);

        % Loop over time of exposure to fire
        for time_idx = 1:length(time_exposure)

            % Loop over fire types (1 = standard, 2 = parametrized)
            for fire_type = 1:2

                   % Initialize counter for number of failures
                   num_failures = 0;
```

```
                    % Set different seeds for each fire type and simulation cycle
                    rng(case_num + time_idx + fire_type); % Seed based on case
number, time index, and fire type


                    % Perform MCS
                    for sim = 1:num_simulations

                        % Generate random variables for the simulation
                        random_As = normrnd(As, 0.02 * As);
                        random_fy = lognrnd(log((1.16 * fy)^2 / sqrt((0.07 * 1.16
* fy)^2 + (1.16 * fy)^2)), sqrt(log(1 + (0.07 * 1.16 * fy)^2 / ((1.16 * fy)^2))));
                        random_h = normrnd(h, 0.04 * h);
                        random_fc = lognrnd(log((1.23 * fc)^2 / sqrt((0.15 * 1.23
* fc)^2 + (1.23 * fc)^2)), sqrt(log(1 + (0.15 * 1.23 * fc)^2 / ((1.23 * fc)^2))));
                        random_b = normrnd(b, 0.04 * b);
                        random_d_prime = lognrnd(log(d_prime^2 / sqrt((d_prime *
0.1)^2 + d_prime^2)), sqrt(log(1 + (d_prime * 0.1)^2 / d_prime^2)));
                        random_theta_R = lognrnd(log(1.1^2 / sqrt((1.1*0.1)^2 +
1.1^2)), sqrt(log(1 + (1.1*0.1)^2 / 1.1^2)));
                        random_theta_R_values(case_num, time_idx, fire_type,
sim) = random_theta_R;
                        random_theta_S = lognrnd(log(1^2 / sqrt(0.1^2 + 1^2)),
sqrt(log(1 + 0.1^2 / 1^2)));
                        random_MPL = normrnd((PL * L^2) / 8, 0.1 * ((PL * L^2) /
8));
                        random_MLL = gamrnd(0.04, (LL * L^2) / 200);

                        % Calculate temperature-dependent properties
                        if fire_type == 1
                            Tr = standard_fire_temperatures(time_idx);
                            alpha_r = alpha_standard(case_num, time_idx);
                        else
                            Tr = parametrized_fire_temperatures(time_idx);
                            alpha_r = alpha_parametrized(case_num, time_idx);
                        end

                        t = time_exposure(time_idx) / 60; % Convert time to hours
                        nw = 1 - (0.0616 * t^(-0.88));
                        nx = (0.18 * log(alpha_r * t / s^2)) - 0.81;
                        ny = nx; % Assuming nx = ny
                        Tc = (nw * ((nx + ny) - (2 * nx * ny)) + (nx * ny)) * Tr;
                        r = (720 - (Tc + 20)) / 470;
                        r = max(min(r, 1), 0); % Ensure 0 <= r <= 1
                        fyTr = random_fy * r;
                        x_500 = sqrt((alpha_r * t) / exp(4.5 + (480 / (0.18 * nw
* Tr))));
                        b_Tc = random_b - 2 * x_500;

                        % Calculate resistant moment (Mn_T) and load effects
(MS_fi) based on random variables
                        a_Tc = (random_As * fyTr) / (0.85 * random_fc * b_Tc);
                        Mn_T = random_theta_R * ((A_s * fyTr)*(random_As * fyTr
* (random_h - 2 * random_d_prime)) + ((random_As - A_s) * fyTr * ((random_h -
random_d_prime) - (a_Tc / 2))));
                        MS_fi = random_theta_S * (random_MPL + random_MLL);

                        % Store Mn_T value
                        Mn_T_values(case_num, time_idx, fire_type, sim) = Mn_T;
```

```
                        % Check if the beam fails
                        if Mn_T < MS_fi
                            num_failures = num_failures + 1;

                        % Update progress bar
                        elapsed_time = toc; % Time elapsed since the start of the
loop
                        total_iterations = size(cases, 1) * length(rc) *
length(time_exposure) * 2 * num_simulations;
                        current_iteration = ((case_num - 1) * length(rc) *
length(time_exposure) * 2 * num_simulations) + ...
                                            ((rc_idx - 1) * length(time_exposure)
* 2 * num_simulations) + ...
                                            ((time_idx - 1) * 2 *
num_simulations) + ...
                                            (fire_type - 1) * num_simulations +
...
                                            sim;
                        progress_percentage = (current_iteration /
total_iterations) * 100;
                        estimated_time_remaining = (elapsed_time /
current_iteration) * (total_iterations - current_iteration) / 60; % Convert
seconds to minutes

                        if estimated_time_remaining > 60
                            hours = floor(estimated_time_remaining / 60);
                            minutes = mod(estimated_time_remaining, 60);
                            time_remaining_str = sprintf('Estimated time
remaining: %d hours and %.2f minutes', hours, minutes);
                        else
                            time_remaining_str = sprintf('Estimated time
remaining: %.2f minutes', estimated_time_remaining);
                        end

                        waitbar(progress_percentage / 100, f, sprintf('Simulation
Progress: %.2f%%\n%s', progress_percentage, time_remaining_str));

                        end
                    end

                    % Calculate and store statistics for Mn_T
                    Mn_T_case = squeeze(Mn_T_values(case_num, time_idx,
fire_type, :));
                    theta_R_case = squeeze(random_theta_R_values(case_num,
time_idx, fire_type, :));
                    Mn_T_case = Mn_T_case ./ theta_R_case; % Divide by
random_theta_R
                    Mn_T_stats(case_num, time_idx, fire_type, 1) = min(Mn_T_case,
[], 'all');
                    Mn_T_stats(case_num, time_idx, fire_type, 2) =
mean(Mn_T_case, 'all');
                    Mn_T_stats(case_num, time_idx, fire_type, 3) = max(Mn_T_case,
[], 'all');
                    Mn_T_stats(case_num, time_idx, fire_type, 4) = var(Mn_T_case,
0, 'all') / mean(Mn_T_case, 'all')^2;

                    % Calculate reliability index and failure probability
                    failure_probability = num_failures / num_simulations;
```

```
                    failure_probability = min(max(failure_probability, eps), 1-
eps); % Ensure the probability is within the bounds of 0 and 1
                    reliability_index = -norminv(failure_probability);
                    reliability_indices(case_num, rc_idx, time_idx, fire_type) =
reliability_index;
                    failure_probabilities(case_num, rc_idx, time_idx, fire_type)
= failure_probability;

                end
            end
        end

        % Update progress bar
        waitbar(case_num / size(cases, 1), f, sprintf('Simulation Progress: Case
%d/%d', case_num, size(cases, 1)));


        % Plot reliability indices and failure probabilities
        figure;
        subplot(2, 1, 1);
        hold on;
        for rc_idx = 1:length(rc)
            for fire_type = 1:2
                if fire_type == 1
                    temp_label = 'Standard';
                else
                    temp_label = 'Parametrized';
                end
                jitter_amount = 1;
                jittered_time_exposure     =     time_exposure     +     (rand(1,
length(time_exposure)) - 0.5) * jitter_amount;
                plot(jittered_time_exposure,
squeeze(reliability_indices(case_num, rc_idx, :, fire_type)), '-o', 'LineWidth',
2, 'DisplayName', sprintf('rc = %.2f, Temp = %s', rc(rc_idx), temp_label));
            end
        end
        xlabel('Time of Exposure to Fire (minutes)');
        ylabel('Reliability Index');
        title(sprintf('Reliability Indices for Case %d', case_num));
        legend('show');
        grid on;
        hold off;

        subplot(2, 1, 2);
        hold on;
        for rc_idx = 1:length(rc)
            for fire_type = 1:2
                if fire_type == 1
                    temp_label = 'Standard';
                else
                    temp_label = 'Parametrized';
                end
                jitter_amount = 1;
                jittered_time_exposure     =     time_exposure     +     (rand(1,
length(time_exposure)) - 0.5) * jitter_amount;
                plot(jittered_time_exposure,
squeeze(failure_probabilities(case_num,    rc_idx,    :,    fire_type)),    '-o',
'LineWidth',  2,  'DisplayName',  sprintf('rc  =  %.2f,  Temp  =  %s',  rc(rc_idx),
temp_label));
```

```
            end
        end
        xlabel('Time of Exposure to Fire (minutes)');
        ylabel('Failure Probability');
        title(sprintf('Failure Probabilities for Case %d', case_num));
        legend('show');
        grid on;
        hold off;
    end

    % Create figures for Mn_T statistics
    for case_num = 1:size(cases, 1)

        % Create figure for current case
        figure('Name', sprintf('Case %d', case_num), 'NumberTitle', 'off');

        % Plot table for standard fire
        data_standard = squeeze(Mn_T_stats(case_num, :, 1, :));
        if isvector(data_standard)
            data_standard = reshape(data_standard, [size(data_standard, 2), 1]);
        end
        t_standard = uitable('Data', data_standard, 'ColumnName', {'Min -
Standard', 'Mean - Standard', 'Max - Standard', 'COV - Standard'}, 'RowName',
{'20 min', '30 min', '60 min', '90 min', '120 min'});

        % Adjust the dimensions of the figure and table
        fig_width = 500;
        fig_height = 450;
        table_width = 560;
        table_height = 200;

        % Center the table in the figure
        t_standard.Position = [(fig_width - table_width) / 2, (fig_height -
table_height) / 2 - 110, table_width, table_height];

        % Plot table for parametric fire
        data_parametric = squeeze(Mn_T_stats(case_num, :, 2, :));
        if isvector(data_parametric)
            data_parametric = reshape(data_parametric, [size(data_parametric, 2),
1]);
        end
        t_parametric = uitable('Data', data_parametric, 'ColumnName', {'Min -
Parametric', 'Mean - Parametric', 'Max - Parametric', 'COV - Parametric'},
'RowName', {'20 min', '30 min', '60 min', '90 min', '120 min'});

        % Center the table in the figure
        t_parametric.Position = [(fig_width - table_width) / 2, (fig_height -
table_height) / 2 + 110, table_width, table_height];
    end
```

ANNEX C - LIST OF PUBLICATIONS

This chapter presents the list of publications in congresses and journals, directly and indirectly related to the topic of this thesis, which has been developed by the author since the beginning of this research in master's dissertation, started in 2016.

- ✓ COELHO, T. A. P.; DINIZ, S. M. C. *Reliability Study of Reinforced Concrete Slabs in Fire Situation via Monte Carlo Simulation*. In: XXXVIII Ibero-Latin American Congress on Computational Methods in Engineering, 2017, Florianópolis, SC, 2017.
- ✓ COELHO, T. A. P.; DINIZ, S. M. C. *Evaluation of the Reliability of Reinforced Concrete Slabs in a Fire Situation.* In: 59 Brazilian Congress of Concrete, 2017, Bento Gonçalves, RS, 2017.
- ✓ COELHO, T. A. P. *Evaluation of Concrete Modulus of Elasticity Variation at Different Temperatures.* In: 59 Brazilian Concrete Congress, 2017, Bento Gonçalves, RS, 2017.
- ✓ COELHO, T. A. P.; DINIZ, S. M. C. *Reliability Study of Reinforced Concrete Beam Sections in Fire Situation*. In: 60th Brazilian Concrete Congress, 2018, Foz do Iguaçu, PR, 2018.
- ✓ COELHO, T. A. P.; DINIZ, S. M. C.; RODRIGUES, F. C.; VAN COILE, R. *Reliability Evaluation of Concrete Beams Exposed to Fire*. In: Applications of Structural Fire Engineering - ASFE'21, 2021, Ljubljana. Proceedings of Applications of Structural Fire Engineering - ASFE'21, 2021.
- ✓ COELHO, T. A. P.; DINIZ, S. M. C. ;RODRIGUES, F. C.; VAN COILE, R. *Experimental Investigation of the Elastic Modulus of High Strength Concrete at Elevated Temperatures*. In: Applications of Structural Fire Engineering - ASFE'21, 2021, Ljubljana. Proceedings of Applications of Structural Fire Engineering - ASFE'21, 2021.
- ✓ COELHO, T. A. P.; DINIZ, S. M. C. ;RODRIGUES, F. C.; VAN COILE, R. *State-of-the-art review of the reliability evaluation of concrete beams exposed to fire.* Journal of Structural Fire Engineering, 2022.
- ✓ COELHO, T. A. P.; DINIZ, S. M. C. ;RODRIGUES, F. C.; *Estimating the elastic modulus of concrete under moderately elevated temperatures via impulse excitation technique.* Journal of Structural Fire Engineering, 2024.
- ✓ QUADROS, P. A.; CALIXTO, J. M. F.; VIEIRA, R. N. C.; COELHO, T. A. P.; DINIZ, S. M. C. *Análise estatística da relação entre o módulo de deformação secante e a resistência à compressão do concreto*. CADERNO PEDAGÓGICO (LAJEADO. ONLINE), v. 21, p. e7733, 2024.